Monitoring of Tool Wear and Surface Roughness Using ANFIS Method During CNC Turning of CFRP Composite

Md Mofakkirul Islam
The University of Texas Rio Grande Valley

PREDICTION OF TOOL WEAR AND SURFACE FINISH USING ANFIS MODELING DURING CNC TURNING OF CFRP COMPOSITES

A Thesis

by

MD MOFAKKIRUL ISLAM

Submitted in Partial Fulfillment of the

Requirements for the Degree of

MASTER OF SCIENCE IN ENGINEERING

Major Subject: Manufacturing Engineering

The University of Texas Rio Grande Valley

May 2022

PREDICTION OF TOOL WEAR AND SURFACE FINISH USING ANFIS MODELING DURING CNC TURNING OF CFRP COMPOSITES

A Thesis
by
MD MOFAKKIRUL ISLAM

COMMITTEE MEMBERS

Dr. Alley Butler
Chair of Committee

Dr. Anil Srivastava
Co-chair of Committee

Dr. Douglas Timmer
Committee Member

May 2022

ABSTRACT

Islam, Md Mofakkirul, Prediction of Tool Wear and Surface Finish using ANFIS modeling during CNC turning of CFRP composites Master of Science in Engineering (MSE). May, 2022, 95 pp, 58 figures, 9 tables, references, 72 titles.

Carbon fiber-reinforced plastic (CFRP) is gaining wide acceptance in areas including sports, aerospace and automobile industry . Because of its superior mechanical qualities and lower weight than metals, it needs effective and efficient machining methods. In this study, the relationship between the cutting parameters (Speed, Feed, Depth of Cut) and response parameters (Vibration, Surface Finish, Cutting Force and Tool Wear) are investigated for CFRP composite. For machining of CFRP, CNC turning operation with coated carbide tool is used. An ANFIS model with two MISO system has been developed to predict the tool wear and surface finish. Speed, feed, depth of cut, vibration and cutting force have been used as input parameters and tool wear and surface finish have been used as output parameter. Three sets of cutting parameter have been used to gather the data points for continuous turning of CFRP composite. The model merged fuzzy inference modeling with artificial neural network learning abilities, and a set of rules is constructed directly from experimental data. However, Design of Experiments (DOE) confirmation of this experiment fails because of multi-collinearity problem in the dataset and insufficient experimental data points to predict the tool wear and surface roughness effectively using ANFIS methodology. Therefore, the result of this experiment do not provide a proper representation, and result in a failure to conform to a correct DOE approach.

DEDICATION

I dedicate my work to my mother, Most Mohsin Ara Begum; my late father, Abdul Aziz; my wife Fahmida Nasrin Priti; and my son Mozaienul Islam Prottay. Thanks to the almighty for helping me and guiding me through the difficult times. Without the constant support and help of my supervisor, family and friends, my journey here at UTRGV would not have been possible.

ACKNOWLEDGMENT

I would like to acknowledge my supervisor, Dr. Alley Butler, for his outstanding guidance and support. His knowledge, expertise and his ongoing mentorship have helped me overcome all the difficulties I faced during this master's program. I am delighted that I got the opportunity to work in the Advanced Machining Lab under Dr. Anil Srivastava's supervision. I am greatful to Manufacturing and Industrial Engineering Deparement funding me throughout my graduate studies. Besides, I am very thankful to my colleague S M Abdur Rob and Md Shahriar Forhad. I would specially mention S M Abdur Rob as his industriousness motivated me a lot. I have learned a lot from S M Abdur Rob, as he has excellent experience in CNC machining.

TABLE OF CONTENTS

LIST OF TABLES

LIST OF FIGURES

CHAPTER I

INTRODUCTION

The manufacturing industry is regularly striving to reduce its cutting costs and increase the quality of the machined parts. The need for high tolerance manufactured goods is quickly increasing. The growing needs to boost productivity, to machine more complicated parts and to improve quality in high volume by the industry which are the driving force behind the development of cutting tool materials (Yoshio et al., 2007). The direct contact between cutting tool, work piece specimen, and the chips during machining operation impose thermal and mechanical stresses on the cutting tool. As a result, changes to the geometry, volume loss, and sharpness of the cutting tool can occur either gradually or abruptly. This change, which is known as tool wear, normally takes place at the rates dependent upon machining conditions, work piece material, as well as the cutting tool material and tool geometry. According to the standard ISO 3685:1993 for wear measurements, the major cutting edge is considered to be divided into four regions, as shown in Figure 1.1:

- Region C is the curved part of the cutting edge at the tool corner.
- Region B is the remaining straight part of the cutting edge in zone C.
- Region A is the quarter of the worn cutting-edge length b farthest away from the tool corner
- Region N is notch type wear. It is the extended area between the mutual contact between the tool and work piece along the major cutting edge.

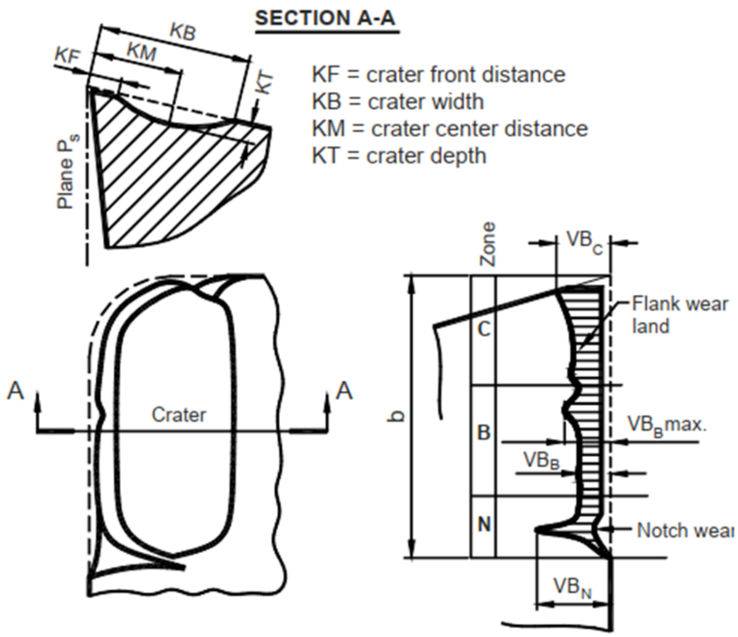

Fig. 1.1 Tool Wear According to Standard ISO 3685:1993

Tool wear detection is an important topic for tool condition monitoring (TCM). The maximization of useful tool life is usually associated with the optimization of machining processes. The key issue is to search for a suitable trade-off between tool wear and productivity, considering the tool's cost, its replacement cost, the cost of writing off the machine's idle time, and so forth. Avoiding damage from excessive tool wear is another significant factor. The tool can be replaced after it breaks but it means increased costs since the post-breakage stage is one of the deceptive, most unpredictable times, aside from the harm that may be done to the part and, not unusually, to the whole machine itself (Gajate et al., 2012).

Surface finish is the finer irregularities of surface texture which generally includes those irregularities that come out from inherent action of the production system. The average surface finish (Ra) quantifies the component's of surface quality. The average finish can be defined as the average value of the departures from its centerline which is taken over a sampling length of the surface (Dweiri et al., 2003). The finished product's quality is determined by its dimensional and surface quality. Surface finish and texture are used to describe and identify the surface quality. Surface finish is one of the most common indexes for determining the quality of surface (Chen and Savage, 2001). Manufacturing processes fail to achieve theoretical surface finish owing to flaws on machined surfaces caused by process inadequacies and imbalances. Measuring techniques are required to establish the true state of surfaces and manufacture components with greater precision. It is important to use theoretical models that allow for prediction of surface finish based on response characteristics (Sivaro et al., 2000).

Carbon fiber manufacturing and processing are now driven by the civil aircraft sector, which benefits from the material's low weight, high strength, and corrosion resistance (Robarts, 2007). Carbon fiber reinforced plastic (CFRP) contributes roughly 50 wt% of the weight of modern aircraft like the Boeing 787 and the Airbus A350 (Sheikh-Ahmad, 2009). Two or more elements are commonly found in fiber reinforced materials. They are matrix and fiber, in order to take advantage of their greatest qualities while avoiding their flaws. In general, the matrix is ductile, and the fiber is brittle. The matrix works as a load conveying medium in fiber reinforced composite materials, while the fibers act as a load carrying medium (Mohan et. al., 2005). Machining of CFRP components is critical for commencing serial manufacturing of high precision CFRP components. CFRP materials are difficult to machine due to their anisotropic and non-homogeneous structure, and also due to the abrasive action by the reinforcing carbon fibers on the edge of the cutting tool when being machined (Chen, 1997). Metal machining processes like milling and drilling are also used frequently for the machining of CFRP parts.

Tool Wear in Turning Process

Out of different forms of machining operations, boring, turning, milling, broaching, grinding, honing, and lapping are the key value-adding metal cutting processes required for the production of assembly components and final products. During turning process, the tool is subjected to tremendous mechanical stress, high temperatures, and corrosion from cutting fluids. Thus, edges gradually wear down, leading to premature catastrophic collapse. Plastic deformation, material fluency at high temperatures, fatigue, and brittle fracture due to coupled loads and low tool tenacity are key reasons of tool breakage (Sharma et al., 2008b). Cutting tools undergo several wear mechanisms during machining, namely abrasion, adhesion, diffusion, fatigue, and chemical wear (Altintas, 2000). Typical tool wear situations usually involve more than one of these kinds of wear. However, it is well understood that mechanical abrasion on the flank face of the cutting tool characterizes the primary tool wear mechanism. It is mainly observed on the flank face of the primary cutting edge of the tool and thus is one of the primary reasons for the majority of the flank wear. Abrasion wear occurs because of hard particles interacting at the tool-work piece interface. For instance, when some part of the chips gets locked onto the work piece-tool interface and the machining operation is still continued, these particles get dragged. This causes abrasion wear on the tool surface. Abrasion wear exists for all the machining conditions. It cannot be avoided and can only be minimized. Abrasion wear prevails for all the conditions due to machining at high speed (Jie Gua et al., 1999). Abrasion wear causes the carbide elements in the tool to protrude out of the flank face and hence disturb the geometry of the flank face. Abrasion wear is undesirable because it can not only wear the tool quickly but also adversely impact the surface finish on the work piece. A typical graph of wear vs. cutting time or cutting distance includes three regions. The first region (region I in Figure 1.2) is the area of primary or initial wear. The comparatively elevated wear rate (an increase of tool wear per unit time or length of the cutting path) in this region is described by accelerated wear of the tool layers damaged during manufacturing or re-sharpening. The second region (region II in Figure 1.2) is the region of steady-state wear. This is the normal operating region for the cutting tool. The third region (region III in Figure 1.2) is known as the tertiary or accelerated wear region. Accelerated tool wear in this area is generally associated with high cutting forces, temperatures, and severe tool vibrations. Normally, the cutting tool should not be used in this region. The cutting tool life is either the cutting time/distance at the limit of the low wear rate region or the time to reach a given wear land value based on the material being cut (Shaw, 2005). Tool wear is a time-dependent stochastic process, so the time to reach the failure region can fluctuate greatly from tool to tool.

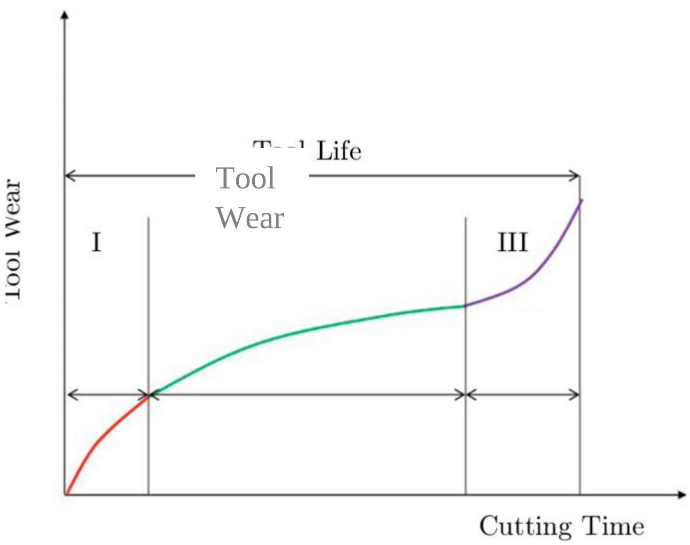

Fig. 1.2 Tool Wear Vs Cutting Time Curve (Umaras et al., 2019)

Tool Wear Measurement Approaches

For turning operation, continuous monitoring of the tool wear is imperative for the determination of a suitable time for tool replacement or reconditioning in order to alleviate any adverse effects of the worn tool on the machined surface. In general, the condition of the cutting tool can be determined through two possible methods, namely direct and indirect methods. Broadly speaking, (1) direct, where the actual tool wear is measured in-situ; (2) indirect, where a parameter correlated with tool wear is measured (Dan and Matthew, 1990). Direct measurement using optical devices has been extensively and effectively employed in studying the extent of tool wear as well as to understand its mechanisms. The optical measurement of tool flank wear has also been proven to be useful in estimating the tool's useful life by employing the classical Taylor's tool life equation. However, the drawbacks of this method are: (1) it is time consuming, and (2) the machining operation must be interrupted in order to determine the extent of tool wear. Taylor presented the following equation (Cook et al., 1989):

$$V_c T^n = C \tag{1}$$

where Vc is the cutting speed (m/min), T is the tool life (min) taken to generate certain flank wear (VB_B), n is an exponent that relies on the cutting parameters and C is a constant. The parameters n and C depend on cutting speed, work material, tool material, etc. The constant C has units of fpm and is the speed at which the tool life continues 1 min. According to the basic Taylor tool life formula, the cutting speed is the only parameter that adversely affects the tool life. This is because this formula was obtained using high-carbon and high-speed steels as tool materials. With the further development of carbides and other tool materials, it was found that parameters like the cutting feed and the depth of cut (DOC) are also significant. As a result, Taylor's tool life formula was rewritten to accommodate these changes as:

$$V_c\ T_n\ f^a\ d^b = C \qquad (2)$$

where *d* is the depth of cut (mm) and *f* is the feed rate(mm/rev). The exponents *a* and *b* are to be determined experimentally for each combination of the cutting conditions.

Unlike direct measurement approaches are established by correlating suitable sensor signals to tool wear states. The tool condition is estimated from the measurable signal feature. Researchers have used measurement data of forces (Altintas, 1988; Altintas and Yellowley, 1989; Du et al., 1995; Byrne et al., 1995; Saglam and Unuvar, 2003; Nouri et al., 2012) vibrations (El-Wardany et al., 1996; Berger et al., 1998; Dilma and Lister, 2012; Srinivasa et al., 2002) acoustic emission spindle motor and feed currents to estimate tool wear state. Several comprehensive surveys of these works have been published. Traditional models like statistical regression and response surface methodology approaches have been used previously by some researchers in modeling the cutting process. But these methods cannot overcome the nonlinearity of relationships between cutting conditions and the output response. On the other hand, soft computing, as the name suggests, refers to a collection of computational techniques developed from computer science research. The major aims are to model and analyze complex, nonlinear, and imprecise phenomena that may exist in the process variables. The techniques are usually robust and capable of yielding complete, accurate, and reliable solutions (Azmi, 2015). AI-based models are developed using non-conventional approaches such as Artificial Neural Network (ANN), Fuzzy Logic (FL), and Genetic Algorithm (GA) (Dweiri et al., 2003; Brezocnik et al., 2004; Cus & Zuperl, 2006). Recently, AI-based models have become the preferred trend, and these are applied by most researchers to develop a model for near-optimal conditions in machining. It is also considered as a successful approach to modeling the machining process for predicting performance measures through the development of an expert system. An expert system is an interactive intelligence program with an expert-like performance in solving a particular type of problem using the knowledge base, inference engine, and user interface. A model based on ANN is able to learn, adapt to changes and mimic the human thought process with little human interaction. The FL model deals with linguistic variables rather than calculation based crisp values. The GA model, meanwhile, involves the coding of solution states in chromosomes as a series of binary elements zero and one. Similar to the conventional approaches which consist of various numbers of alternative techniques, AI also provides alternative techniques in modeling as mentioned above. Different techniques may be suitable for particular modeling problems in the machining process and may not be suitable for other ones (Zain et al., 2010).

Surface Finish Measurement Approaches

Machinability is about cutting the material with maximum removal rate, shortest time, maximum tool life, and best surface finish. In globally competitive market, high quality surface finish is a crucial factor. A lot of analytical methods were developed and used for predicting surface finish and an empirical model was also used for the prediction of surface finish during turning operation (Hadi and Ahmed, 2006). The empirical model is developed using nonlinear regression analysis and logarithmic data transformation. Experiments with metal cutting and statistical tests show that the model created in this study causes fewer errors and achieves a satisfactory result. In precision turning with a diamond cutting tool, mathematical models were utilized to model and analyze vibration and surface finish (Chen et al., 2011). Some preliminary studies in applying the fundamental artificial intelligence technique to model machining processes have recently been published in the literature, concluding that the modeling of surface quality in machining processes has primarily relied on Artificial Neural Networks and fuzzy set theory (Chaudhary et al., 2005). The impact of machining parameter combinations on achieving a good surface finish in turning and utilizing fuzzy modeling to anticipate surface finish values is also presented (Rajasekaran et al., 2011). It is also worth noting that the neural network utilized in the study enabled the resolution of a difficult-to-define and mathematically described problem. This may be seen in the study where the neural network is used based on data from face milling machining processes, with the goal of producing a link between cutting force and instantaneous angle φ (Savković et al., 2013).

Neuro-Fuzzy System

A human operator can often anticipate the condition of the tool by auditing the machining conditions and by taking advantage of his sensory perceptions. However, in automated manufacturing, the relationship between process characteristics and tool wear state is difficult to capture. This is at least partly due to the relative obscurity of the relationship between tool wear and process characteristics, and partly due to lack of reliable means of sensing these characteristics via direct or even indirect sensing mechanisms. On the other hand, the capacity of artificial neural networks to capture complex nonlinear relationships in a relatively efficient manner has motivated several researchers to pursue the use of these networks in developing diagnostic models of tool wear and surface finish. The relative effectiveness of neural network-based models of tool wear and surface finish is, however at least partly, offset by their lack of transparency. In other words, the nonlinear interrelation between sensor readings and tool wear state embedded in a neural network remains hidden as connection weights, and unavailable to the user. In this work, the researchers attempt to remedy this situation by using the knowledge embedded in a pre-trained neural network to construct a fuzzy logic-based model of tool wear.

Neuro-fuzzy inference techniques associate the paradigms of fuzzy logic and neural networks to benefit from both techniques, achieving the simplicity of modeling (neural networks), while providing knowledge available in a set of if-then rules. Neuro-fuzzy systems have been broadly used in modeling, identification, and monitoring of complex systems. Since its origin in the early nineties, neuro-fuzzy systems have gone through various changes over the years, giving rise to various directions in research. For example, depending on the type of inference that the neuro-fuzzy system uses, or according to the structure of the neuro-fuzzy system, the neuro-fuzzy system can be differentiated into various sub-groups within the neuro-fuzzy approaches. Figure 1.3 provides some perspectives.

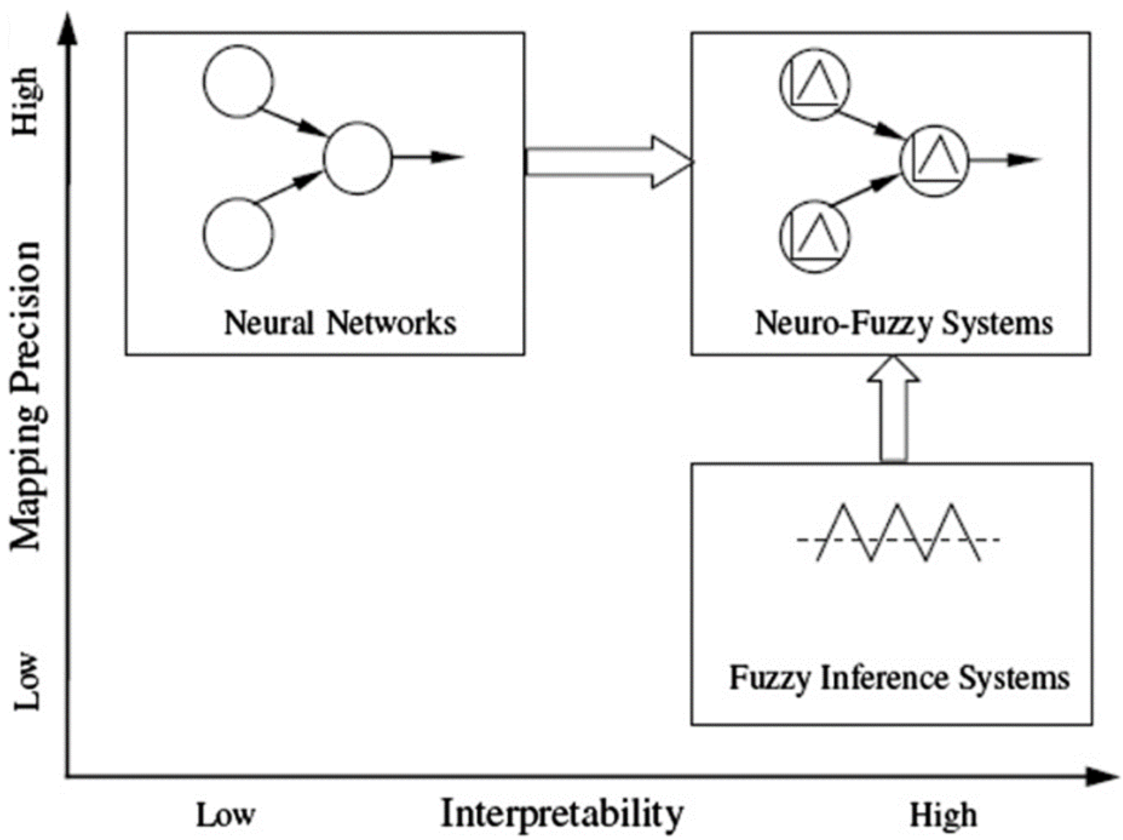

Fig. 1.3 Nero-fuzzy Spectrum (Gill et al., 2012)

The adaptive-network-based fuzzy inference system (ANFIS) is one of the first neuro-fuzzy systems to be developed (Jang, 1993). Its principle is founded on extracting fuzzy rules in each level of a neural network. Once the rules have been obtained, they provide the requisite information on the global behavior of the system. ANFIS executes the Takagi-Sugeno model. ANFIS architecture is comprised of five layers, as shown in Fig. 1.4. The nodes illustrate with squares are nodes with adjustable parameters, whereas the nodes represented by circles are fixed nodes. The first layer represents fuzzy membership functions. The second and the third layer comprise nodes that form the antecedent parts in each rule. The fourth layer calculates the first-order Takagi-Sugeno rules for each fuzzy rule. The fifth layer (output layer) calculates the weighted global output of the system. ANFIS uses error backpropagation as the learning strategy to obtain the antecedent parameters of the rules. The consequent parameters of each rule are decided using the least-squares method. A step in the learning procedure has two passes: in the first or forward pass, the input patterns are propagated, and the optimal consequent parameters are estimated by an iterative least mean square method, while the premise parameters are assumed to be fixed for the current cycle through the training set. In the second or backward pass, the patterns are propagated again, and in this epoch, backpropagation is used to adjust the premise parameters, while the consequent parameters remain fixed. This procedure is then iterated until the error criterion is satisfied (Denai et al. 2007).

In this study, the cutting force (F), vibration (a), cutting speed (V), feed (f) and depth of cut (DC) are selected as input parameters because quite often the tool wear phenomenon is reflected by time-domain and frequency domain analysis of these variables. Cutting tool vibrations are caused by rubbing at the work-piece tool flank interface, the creation of a built-up edge, and the waviness of the work surface during machining. Acceleration is best measure of vibrations when they are occurring at high frequencies. Cutting force is an important variable that is relatively easy to be measured in real-time. Though numerous factors influence surface finish, including cutting tool and work piece qualities, tool geometry, and machine tool stiffness, machining

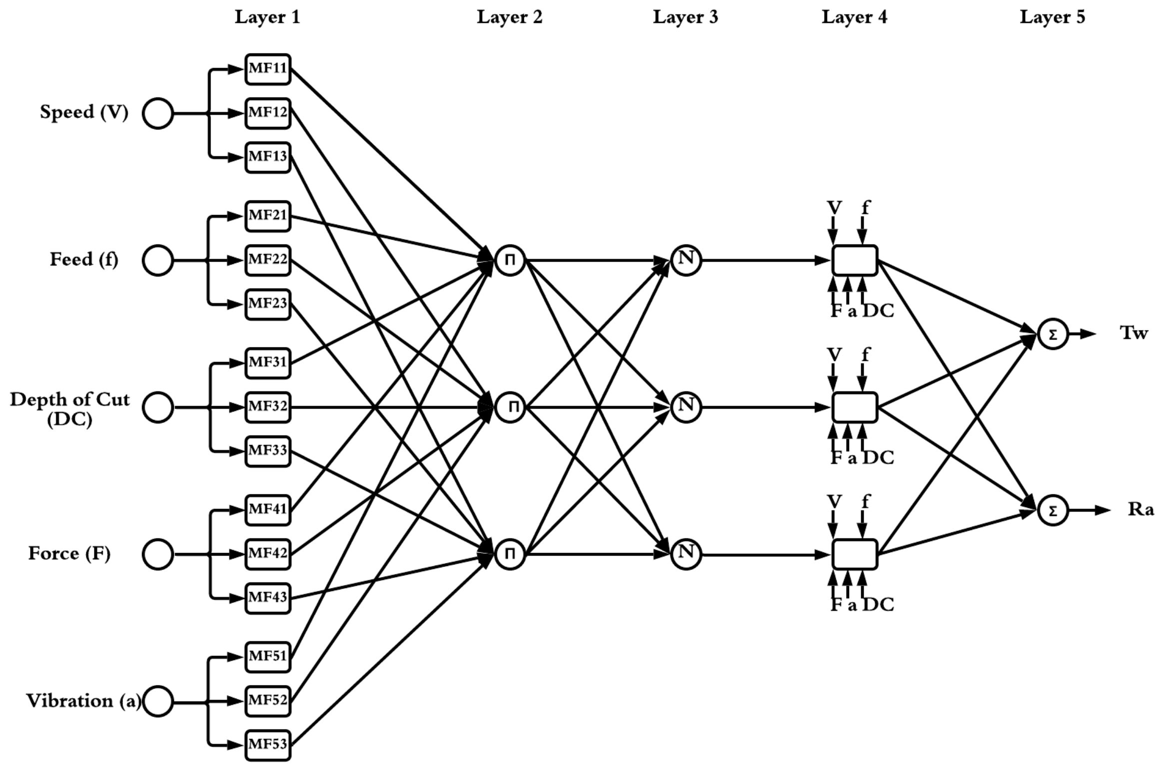

Fig. 1.4 ANFIS Structure

parameters such as cutting speed, feed, and depth of cut are regarded the most important (Palanikumar, 2007).

The objective of this study is to predict the tool wear and surface finish (Ra) and study the relationship between the cutting parameters (speed, feed rate and depth of cut) and the response parameters (vibration, surface finish, cutting force and tool wear) during the turning of CFRP composite. The research is focused on:

- Analyze the relationship between cutting parameters and response parameters for continuous turning of CFRP composite.
- Prediction of wear and surface finish with minimal error percentage using ANFIS method

This thesis first supplies a literature review as chapter II. Chapter III then provides the methodology, and chapter IV covers the result and discussion. Chapter V provides the conclusions, recommendations, and future work.

CHAPTER II

LITERATURE REVIEW

The study of intelligent systems to predict tool wear in machining has been the subject of investigation for several decades. Reviews of the literature include work by Byrne at al. (1995), Sick (2002) and Rehorn et al. (2005) and Al-Zubaidi et al. (2011). Although these review papers are more exhaustive in their coverage of the literature, this thesis provides a more compact and focused discussion of prior work.

Many of the applications have used artificial neural networks, fuzzy sets/logic, or combined neural networks and fuzzy sets/logic. For example, Haber and Alique (2003) used a back propagation ANN to predict output for the milling of a slot. In contrast, Ming et al. (1999) used fuzzy inference where the rules were trained by a genetic algorithm (GA). Their process also used a time series autoregressive (AR) model of the feed directional acceleration to predict tool flank wear. Other work by Sasanto and Chen (2003) used fuzzy logic with center of gravity defuzzication. Their paper, however, does not explain how the rules are achieved or optimized. Iqbal et al. (2007) used fuzzy logic as a reasoning mechanism for a metal milling process. They employed simulated annealing to optimize the fuzzy reasoning process. Fu and Hope (2006) reported artificial intelligence techniques used for milling operations with fuzzy membership functions represented by B-splines. The load, force, acoustic emissions, and vibration were provided to a feature extraction system, which then ported information to a membership function calculation, followed by fuzzy calculations, and an artificial neural network. Figure 2.1 is taken from their paper. In related work Mesina and Langari (2001) captured the acoustic emissions (AE), force, motor current and a CPI to train a ANN to produce a measure of tool wear. They then created a fuzzy linguistic mechanism to allow transparency for input and output relationships. Figure 2.2 represents their system. Similar work for end milling is described by Uros et al. (2009). Each of these reported systems has involved milling processes on metal. Other efforts have reported on work with turning processes

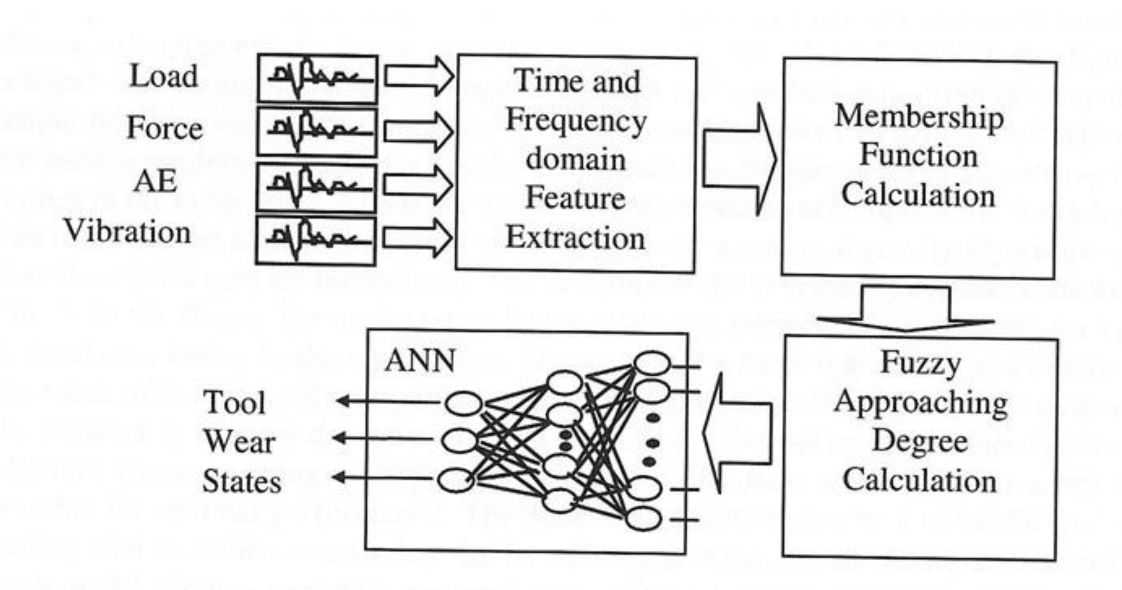

Figure 2.1 Fuzzy Neuro Tool Wear Monitoring System (Fu and Hope, 2006)

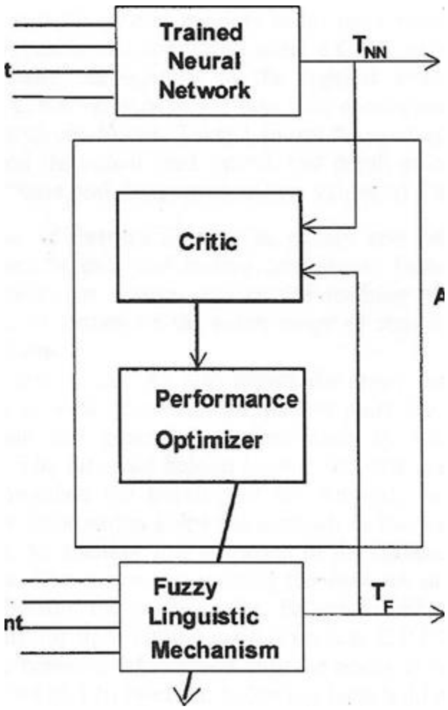

Figure 2.2 Neuro and Fuzzy Tool Wear Monitoring System (Mesina and Langari, 2001)

In addition to work done in milling operations, some investigations have involved turning operations. Similar intelligent system architectures have been used with turning, fuzzy systems, artificial neural networks, and neuro-fuzzy approaches. For example, Fang (1995) developed a fuzzy expert system from a "well established machining reference database, expert intelligence on logic reasoning and experimental results." In similar work, Achiche et al. (2002) developed a system for tool wear monitoring using fuzzy logic which is optimized by a genetic algorithm. In contrast, Ko and Cho (1994) employed fuzzy pattern recognition with time series AR modeling to predict tool wear on a diamond tool edge for copier drum turning. Others have used artificial neural networks or have used fuzzy neural approaches for estimating tool wear or other parameters in metal turning operations.

Examples of the use of artificial neural networks are plentiful for turning operations. To predict flank wear in turning, Rangwala and Dornfeld (1990) describe using a feed forward ANN that predicts flank wear in turning at the 95% level. In another example, Wang et al. (2008) employed an extended Kalman filter for input signals and compared this to ANN and analytical approaches. In another paper, Purushothaman (2010) also used an extended Kalman filter and an ANN to predict tool wear in turning. Further, Rahman et al. (1995) used a neural network based online fault diagnosis scheme to monitor the level of tool wear, chatter vibration and chip breakage in turning operations. For turning ANSI 4340 steel, Masory (1991) used an ANN with back-propagation training to determine tool wear, and Pal et al. (2011) used wavelet transforms and principal component analysis to predict flank wear on a hand lathe. Niu et al. (1998) used an adaptive resonance theory (ART) neural network for feature recognition with wavelets. This system was used in turning to extract fresh and worn states of a tool. Warnecke and Kluge (1998) used an ANN for focusing on tolerances in a turning operation rather than tool wear. In a different approach, Choudhury et al. (1999) added an optical sensor, as input to an artificial neural network to measure flank wear in turning. See Figure 2.3. Other approaches involved neuro-fuzzy systems.

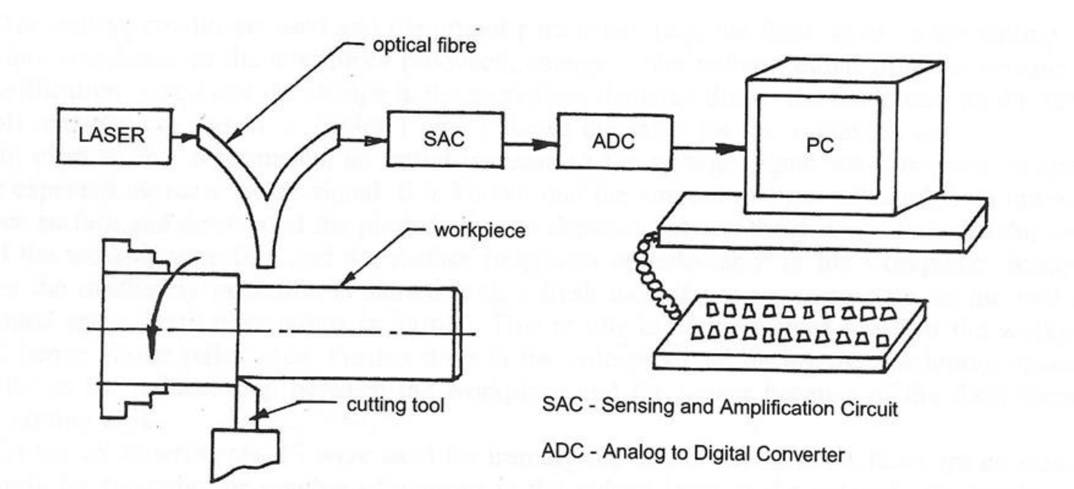

Figure 2.3 Schematic Diagram of Experimental Apparatus (Choudhury et al., 1999)

With most neuro fuzzy systems, the artificial neural network provides the ability to model numerical data sets from training sets, and the fuzzy inference provides the transparency of having human understandable rules. So, neuro-fuzzy systems provide a significant advantage. Neuro-fuzzy systems were employed by Kuo (2000) who used fuzzy neural networks with Kohonen learning for feature mapping and error back propagation for determining premise and consequent parameters in turning. In other work, Balizinki et al. (2002) provided a competitive study in which three fuzzy neuro systems were compared for turning: a feed forward back propagation neural network, a fuzzy decision support system, and a neural network based fuzzy inference system. Others have adopted the ANNFIS architecture, shown in Figure 2.4, to study flank wear in the turning of metals (Gill et al., 2012 and Gajate et al., 2009). In fact, Gajate et al. state "the hybridization of fuzzy logic with neural networks is the most well established and best-known method."

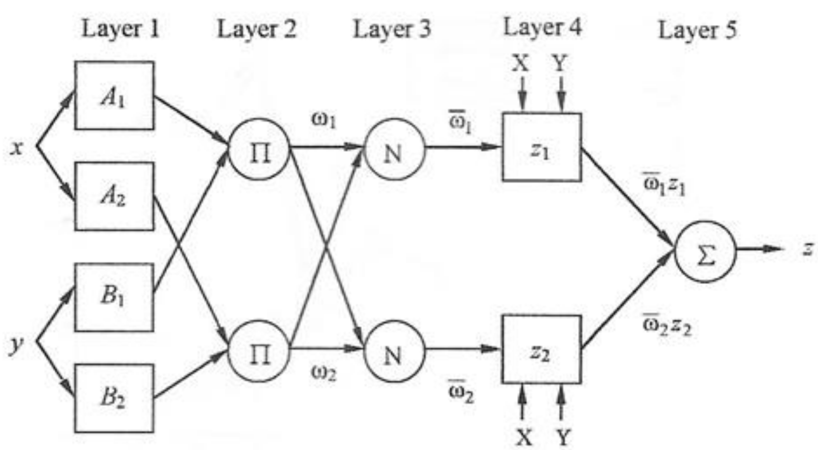

Figure 2.4 ANFIS Architecture (Bodi, 2011)

This review has discussed milling and turning of metals; however, there are examples of work with drilling operations. For example, Sokolowiski (2004) used a Mamdani method fuzzy logic and feed forward neural network to model tool wear. Others have also modeled metal drilling operations to predict the tool wear.

Apparently, from a diligent search by the author, the study of tool wear modeling using intelligent system techniques in milling, turning, and drilling predominantly focuses on the machining of metals. However, there are examples in the literature of the machining of non-metals. For example, Azmi (2015) focused on tool wear prediction for glass fiber reinforced polymer composites (GFRP) using neuro-fuzzy modeling approaches. He reports success with ANNFIS modeling for end milling. In other work by Azmi and his collaborators (Azmi et al., 2013) multiple regression analysis is compared to artificial neural network fuzzy inference systems for GFRP. The neuro-fuzzy approach was found to be superior for modeling an end milling process. Although there are other published studies of machining of non-metals, the limited number of papers found in this literature survey motivates additional research in this area, such as the present study.

Although this literature survey is by force of constraints limited, the author argues that it is a fair summary and representative of the existing published work on soft computing (fuzzy, neuro, and fuzzy neuro) and the modeling of tool wear and related factors for machining operations. Further, it is argued that the work contained in this thesis is a valuable contribution to existing knowledge for this subject.

CHAPTER III

METHODOLOGY

ANFIS Methodology

The core concept behind neuro-adaptive learning approaches is straightforward. These methods allow the fuzzy modeling procedure to learn knowledge about a data set in order to compute the membership function parameters that best allow the associated fuzzy inference system to track the input-output data. ANFIS creates an input-output mapping based on simulated input-output data pairs and human knowledge (in the form of fuzzy if-then rules). It is used to create a set of fuzzy if-then rules with appropriate membership functions to generate the input-output pairs. Figure 3.1 illustrates the neural network structure.

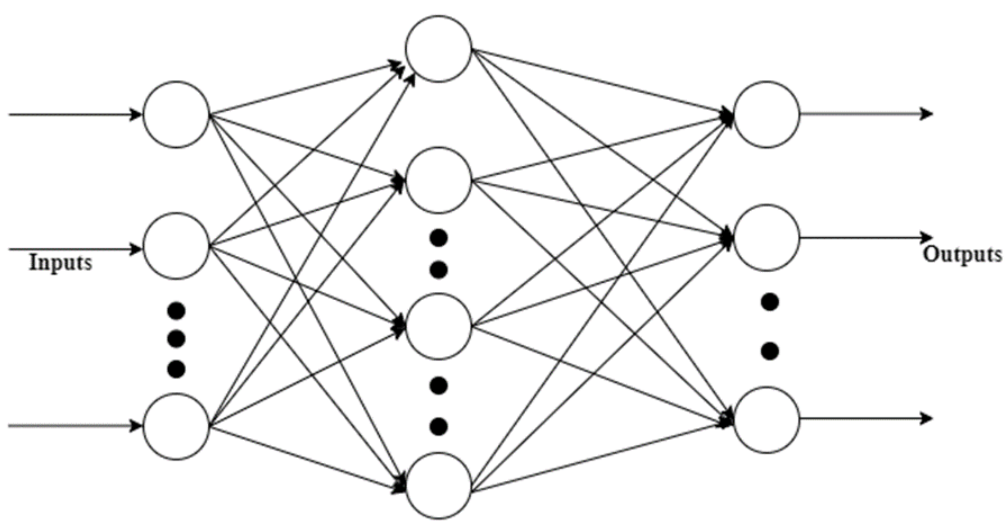

Fig.3.1 Basic Structure of Neural Network

Neural Network

In biological neurons, dendrites and axons work as input and output. Synaptic connections are formed when axons of neurons connect to dendrites of other neurons (synapses). The dendritic tree's input signals are weighted and added in the cell body before being produced in the axon, which generates the output signal. Different mathematical models of neuron were proposed in agreement with the biological model. A set of input signals x_1, x_2, x_3………, x_n (vector x) is received by neuron which are usually output signals of other neurons. Every input signal is multiplied by a connection weight, w, which is an analog of synapse efficiency. The summation module corresponding to the cell body receives weighted input signals and performs algebraic summing and the excitement level of neuron is determined; as shown in Figure 3.2.

$$I = \sum_{i=1}^{n} x_i w_i \quad (3.1)$$

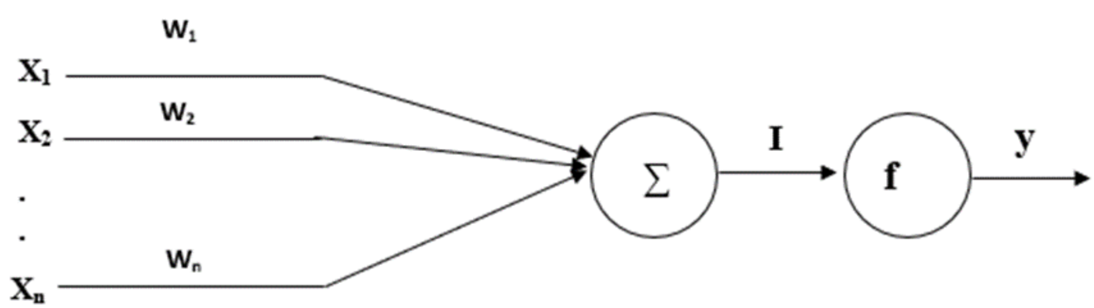

Fig.3.2 Mathematical Neuron

The output signal of a neuron is determined by conducting the excitement level through the function activation function, f as in equation 3.2

$$y = f(I) \quad (3.2)$$

The network receives the input vector by activating the input neurons. The vector of input activeness is a collection of input signals from a network's neurons. Neuron connection weights are represented as a matrix W, with element w_{ij} representing the connection weight between the i^{th} and j^{th} neurons. The input vector is processed into an output vector during the network's operation, implying that some information processing takes place. The computational power of the network, thus, solves problems with its connections. Connections connect one neuron's input to another's output. Weight coefficients determine the strength of the connections. A bias term can also be included in a neural network (NN), which serves as an offset on a neuron. The bias's purpose is to set a threshold for the activation of neurons. All neurons in the network can be connected to the bias.

Learning in Neural Networks

Learning is the process through which a neural network adapts to a stimulus and finally provides the expected response. It is also a continuous categorization process for input stimuli: when a stimulus arrives at the network, it's either recognized or a new classification is created. In fact, in response to an input stimulus, the network adjusts its parameters, the synaptic weights, so that its actual output response converges to the desired output response. The network has finished the learning phase when the actual output response matches the desired one. Learning equations are mathematical formulas that explain network learning rules. Although the neurons in NNs can be connected in a variety of ways, the learning process is not the same for everyone. Various learning approaches fit different persons, as is well recognized. Different learning strategies fit different NNs in the same way (Kartalopoulos, 1996). Both the input and the actual response, as well as the anticipated response, are available in supervised learning and are utilized to build an error measure. If the actual response differs from the target response, the NN provides an error signal, which is then utilized to determine how the network's weights should be adjusted so that the real output matches the target output (Jain, 1997). Unsupervised learning, unlike supervised learning, does not have a target output. During the training stage, the network gets a large number of diverse input patterns and divides them into categories arbitrarily. When a stimulus is later applied, the network responds with an output response identifying the stimulus's class. If a class for the stimulus cannot be located, a new class is created. Self-organizing learning is a term used to describe this form of learning.

A learning algorithm is a mathematical tool that describes the approach and pace with which NN can effectively attain the steady state of its parameters, weights, and thresholds. It all begins with an error function (energy function) that is stated in weights. The goal is to keep the set of weights as error-free as possible. The network and the weights reach a steady state when the error function is zero or small enough. The error function reduces in value as learning progresses, and the weights are adjusted. Different optimization approaches, such as the delta rule, gradient descent, Boltzman's algorithm, backpropagation learning algorithm, hybrid algorithm and simulation annealing, can be used to achieve the reduction. The error function and optimization method that are chosen are critical because they can increase stability, instability, or find a solution caught in a local minimum.

Adaptive Networks

An adaptive network is a type of multilayer feedforward NN in which each node performs a specific function (node function) on incoming signals and has its own set of parameters. The node function formulas may differ from node to node, and the choice of each node function is determined by the total input-output function that the adaptive network must perform. An adaptive network's links only display the flow direction signals between nodes. The links have no weights attached to them (Jang, 1993). The backpropagation learning rule is the most basic learning rule in adaptive networks. However, because it is slow and prone to being stuck in local minima, Jang presented a hybrid learning rule algorithm to speed up the learning algorithm in 1993, as reported in Figure 3.3.

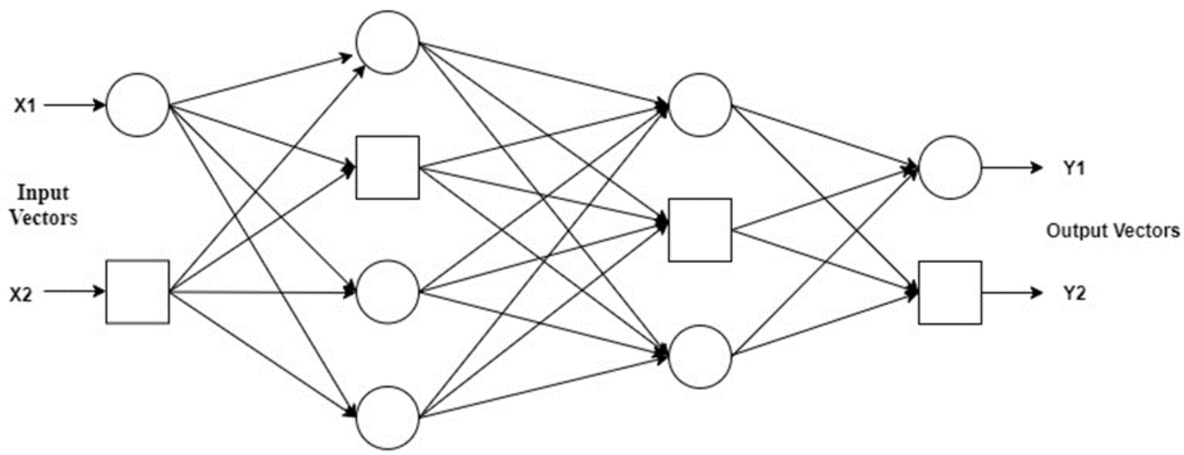

Fig.3.3 Adaptive Network (Jang, 1993)

Backpropagation of Adaptive Networks (Castillo and Melin 2001)

Assume that the adaptive network in Figure 3.3 is made up of N layers. The node in the i^{th} position of the j^{th} layer is (j,i), and the node output is $O_{j,i}$. Because a node's output is determined by its incoming signal and parameter set which can be defined as follows:

$$O_{j,i} = f_{j,i}(O_i^{j-1} \dots \dots .. O_{\#j-1}^{j-1}, a, b, c, \dots ..) \tag{3.3}$$

The parameters for this node are a, b, c, and the node function is f. The total of the square errors can be used to establish an error measure for the p^{th} ($1 \leq p \leq P$) entry of training data where P is the number of training entities, and it is equal to:

$$E_p = \sum_{k=1}^{\#n} (d_k - O_{n,k})^2 \tag{3.4}$$

$O_{n,k}$ is the kth component of the actual output vector created by presentation of the pth input vector, and d_k is the k^{th} component of the p^{th} target vector. As a result, the overall error measure can be written as follows:

$$E = \sum_{p=1}^{p} E_p \tag{3.5}$$

When E_p equals zero, the network can generate the intended output vector in the p^{th} training data pair properly. Reduction of the overall measure is the goal and to do this first error rate $\frac{\partial E_p}{\partial O}$ for p^{th} training data and node output for each one should be calculated. The equation for error rate for output node at layer N can be stated as:

$$\frac{\partial E_p}{\partial O_{i,p}^{N}} = -2(d_{i,p} - O_{i,p}^{N}) \tag{3.6}$$

For internal node, the differential equation for error rate at the i^{th} position of layer j can be derived as:

$$\frac{\partial E_p}{\partial O_{i,p}^{j}} = \sum_{k=1}^{\#j+1} \frac{\partial E_p}{\partial O_{k,p}^{j+1}} \frac{\partial O_{k,p}^{j+1}}{\partial O_{i,p}^{j}} \tag{3.7}$$

Where ($1 \leq j \leq N - 1$). An internal node's error rate at layer j can be described as a linear combination of the layer j+1 error rate. After applying Equation 3.6 and 3.7, all $1 \leq j \leq N$ and $1 \leq i \leq j$ error rates are found. Because the error rates are gathered consecutively from the output layer back to the input layer, the underlying method is called backpropagation. The derivative of the error measure with respect to is defined as the gradient vector α and equals to:

$$\frac{\partial E_p}{\partial \alpha} = \sum_{O^* \epsilon S} \frac{\partial E_p}{\partial O^*} \frac{\partial O^*}{\partial \alpha} \tag{3.8}$$

Here S is the set of nodes whose output depends on α. The derivative of overall measure E with respect to α is written as:

$$\frac{\partial E}{\partial \alpha} = \sum_{p=1}^{p} \frac{\partial E_p}{\partial \alpha} \tag{3.9}$$

The update formula for the generic parameter α is as follows:

$$\Delta\alpha = -\eta \frac{\partial E}{\partial \alpha} \tag{3.10}$$

Where η is the learning rate which can be further expressed as:

$$\eta = \frac{k}{\sqrt{\sum_{\alpha} (\frac{\partial E}{\partial \alpha})^2}} \tag{3.11}$$

where k is "step size," or the length of each transition. The gradient technique should nearly match the gradient path if k is small, but convergence can be sluggish because gradient must be calculated numerous times. If k is big, on the other hand, convergence is slow at first, but the algorithm fluctuates around the optimum. As a result, it is advised that if the error measure experiences four consecutive decreases, k be increased by 10%, and if the error measure experiences two consecutive combinations of one increase and one reduction, k be decreased by 10% (Jang 1993).

Hybrid Learning Rule

For adaptive networks, there are two learning paradigms: offline learning (batch learning) and online learning (pattern learning). The update formula parameter in offline learning is based on Equation 3.9 and the update action occurs only after the entire training data set has been given, i.e., after each epoch. Epoch is actually the number of iterations while training the ANFIS model. The parameters, on the other hand, are updated instantly upon the presentation of each input-output pair in online learning, and the update algorithm is based on Equation 3.8 (Castillo and Melin 2001).

To identify the parameters, the hybrid learning rule combines the gradient method and the least square estimate (LSE). Assume the adaptive network just has one output and that can be expressed as:

$$Output = F(I, S) \tag{3.12}$$

where I denote the input variables and S denotes the parameters. “If there exists a function H such that the composite function H o F is linear for some of the elements of S, these elements can be identified by the least square estimates (Jang, 1993)”. As a result, parameter set S may be split into two sets: S_1 and S_2, with H o F linear in the S_2 elements. H o F is a composite function where the output of one function becomes the input of another function. Applying H to equation 3.12 as follows:

$$Output = H\ o\ F(I, S) \tag{3.13}$$

which is linear in the elements of S_2. A matrix equation is obtained by plugging in the given values of elements of S_1 and P training data which becomes as follows:

$$AX = B \tag{3.14}$$

where X is an unknown vector, whose elements are parameters in S_2, and A is a m x n matrix. This is an over-determined problem since the number of training data pairs is frequently more than the number of linear parameters. There is no accurate solution for Equation 3.14. Jang (1993) developed a sequential LSE approach to deal with this challenge. X is determined iteratively using the sequential formulas used in the literature in this manner that can be expressed as:

$$X_{i+1} = X_i + S_{i+1}a_{i+1}(b_{i+1}^T\text{-}a_{i+1}^T X_i) \tag{3.15}$$

$$S_{i+1} = S_i - \frac{S_i a_i a_{i+1}^T S_i}{1+ S_i a_{i+1} a_{i+1}^T S_i}, i = 0,1, \dots \dots \dots , P-1$$

Where a_i^T is the ith row vector of the matrix A defined in equation 3.14 and b_i^T is the ith element of B and S_i is called as covariance matrix.

A forward pass and a backward pass are included in each epoch of the hybrid learning technique. In forward pass, input data and functional signals are sent forward to calculate each node's output until the matrices A and B in Equation 3.14 are found. The sequential least squares formulas are then used to identify the parameters in S_2. The functional signals continue ahead after identifying parameters in S_2 until the error measure is calculated. The error rates propagate from the output end to the input end in the backward pass, and the gradient method updates the parameters in S_1.

For systems with dynamic features, an online learning method is critical for online parameter identification. When new data pairs become available; a forgetting factor is applied to the original sequential formula to decay the effects of the previous data pairs. This method assigns larger factors to more recent data pairings, accounting for the time-varying properties of the entering data. The sequential formula for online learning is written as follows:

$$X_{i+1} = X_i + S_{i+1}a_{i+1}(b_{i+1}^T\text{-}a_{i+1}^T X_i)$$

(3.16)

$$S_{i+1} = \frac{1}{\lambda}[S_i - \frac{S_i a_i a_{i+1}^T S_i}{\lambda + S_i a_{i+1} a_{i+1}^T S_i}]$$

Where the value of λ is between 0 and 1. The smaller the value is, the more quickly old data decays.

Fuzzy Logic Systems

The outcome of fuzzy reasoning, also known as approximate reasoning, is a conclusion for a collection of fuzzy if-then rules. Input variables are compared with the membership functions (MFs) on the premise part to obtain the membership values of each linguistic label fuzzification. The membership values of each linguistic label are known as fuzzification. The membership values on the premise part are combined through specific fuzzy set operations such as: min, max, or multiplication to get firing strength (weight) of each rule. “The qualified consequent (either fuzzy or crisp) is generated depends on the firing strength. The qualified consequents are aggregated to produce crisp output according to the defined methods such as: centroid of area, bisector of area, mean of maximum, smallest of maximum and largest of maximum (defuzzification) (Jang 1993)”.

Fuzzy systems are made up of a knowledge base and a fuzzy inference engine, which is a type of reasoning process. Figure 3.4 depicts the structure of the fuzzy inference engine. Using fuzzy reasoning methods, a fuzzy inference engine integrates fuzzy if-then rules into a mapping from the system's inputs to its outputs. Fuzzy systems, in other words, are nonlinear mappings with fuzzy if-then rules from the rule base. The local mappings are described by each of these rules. The rule base can be built by a human expert or by automatic generation, which involves extracting rules from numerical input-output data.

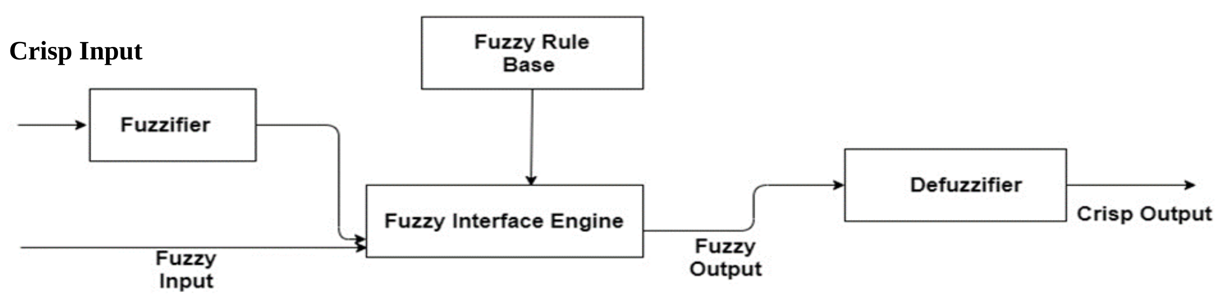

Fig.3.4 Fuzzy Inference Engine

The following is an example of a fuzzy if-then rule (fuzzy rule, fuzzy implication, or fuzzy conditional statement):

If x is A **then** y is B

where A and B linguistic values defined by fuzzy sets. “x is A” is called “antecedent” or “premise”, while “y is B” is called the “consequence” or “conclusion” (Castillo and Melin 2000).

Fuzzy inference systems include the Mamdani and Takagi-Sugeno fuzzy systems. A set of linguistic rules acquired from human operators was initially utilized to regulate a steam engine and boiler combination using the Mamdani fuzzy inference technique (Mamdani and Assilian, 1975). When given two numeric inputs x and y, Figure 3.5. shows how a two-rule Mamdani fuzzy inference system gets the overall output z. Takagi and Sugeno (1985) were the first to introduce the Takagi-Sugeno fuzzy inference system. The Takagi Sugeno model differs in that each rule has a distinct output, and the overall result is calculated as a weighted average of the individual rules' outputs. Figure 3.6 depicts Takagi-Sugeno fuzzy inference system.

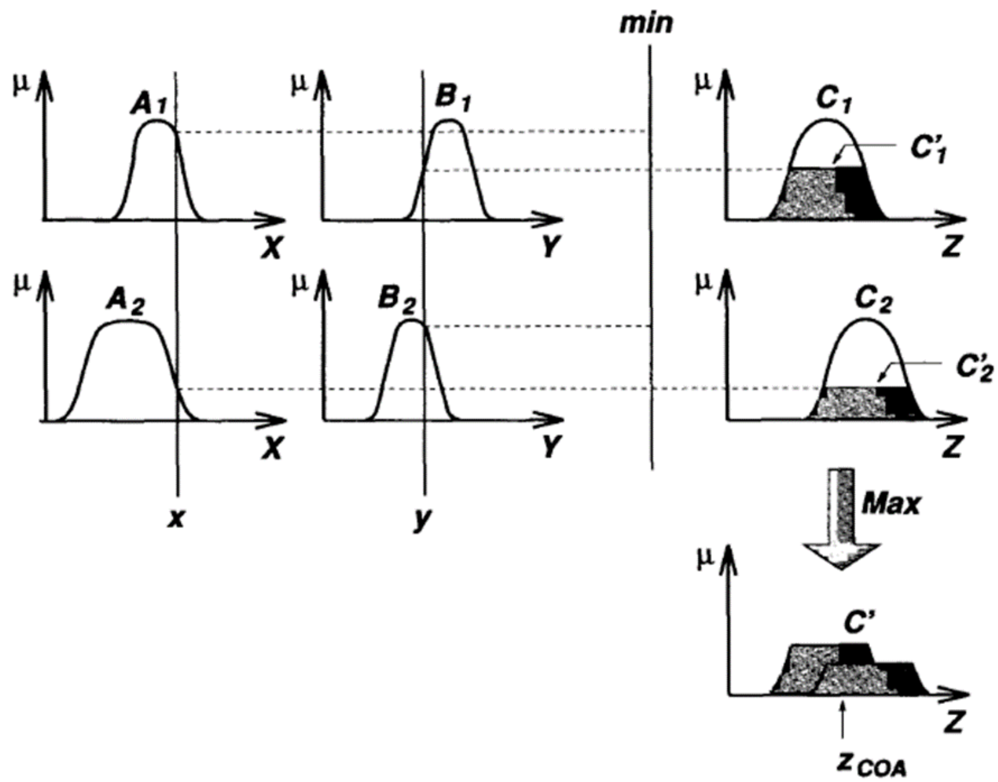

Fig.3.5 Mamdani Fuzzy Inference System (Jang et al., 1997)

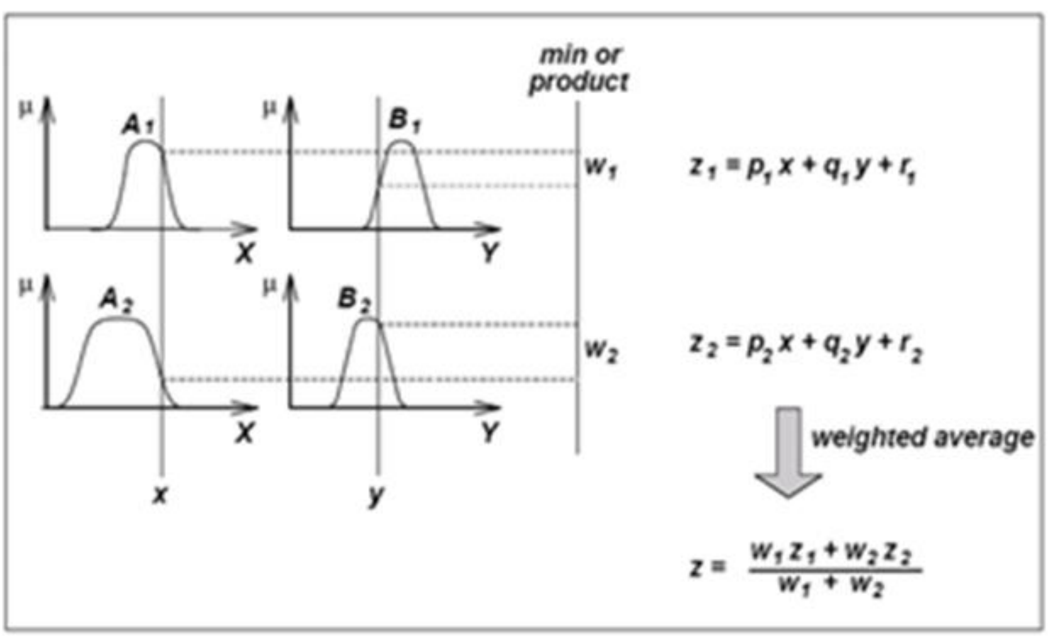

Fig. 3.6 Takagi-Sugeno Fuzzy Inference System (Jang et al., 1997)

ANFIS Architecture

In ANFIS, a Takagi-Sugeno type fuzzy inference system is used. The output of each rule can be a linear combination of input variables plus a constant term or can be only a constant term. The final output is the weighted average of each rule's output. Basic ANFIS architecture that has two inputs x and y, and one output z is shown in Figure 3.7.

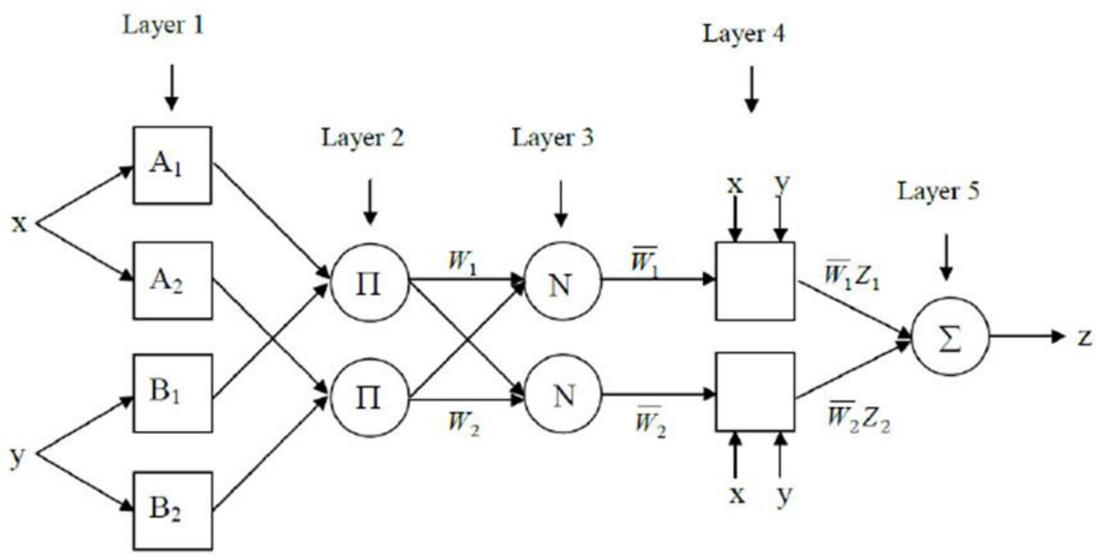

Fig. 3.7 Basic Structure of ANFIS

The rule base contains two Takagi-Sugeno if-then rules as follows:

Rule1: If x is $A_1$and y is B_1, then $f1 = p_1x + q_1y + r_1$

Rule1: If x is A_2 and y is B_2, then $f2 = p2x + q2\ y + r_2$

Where p_1, q_1, r_1, $p2$, $q2$, r_2 are linear and A_1, A_2, B_1, B_2 are nonlinear parameters.

In Figure 3.6, the circular shapes represent fixed nodes and square shapes represent adaptive nodes. The node functions in the same layer are the same as described below:

Layer 1 is the fuzzy membership layer in which the inputs of nodes A1, B1 and A2, B2 are x and y respectively. The linguistic labels A1, A2, B1, B2 are employed in the fuzzy theory to divide the membership functions. Every node i in this layer is square node so they are adaptive. The node function as follows:

$$O_{1,i} = \mu_{Ai}(x) \quad i = 1,2$$
$$O_{1,i} = \mu_{Bi-2}(y) \quad i = 1,2 \tag{3.17}$$

In other words, the membership grade of a fuzzy set A is $O_{1,i}$ and it indicates how well the given input x meets the quantifier A. Any acceptable membership function, such as the triangular or gaussian, bell-shape can be used as membership function for A (or B). When the membership function's parameters vary, the chosen membership function changes as well, resulting in a variety of membership functions for a fuzzy set A. The "premise parameters" are the parameters in this tier. The adaptive-network-based fuzzy inference system uses hybrid learning to simulate and analyze the mapping relation between input and output data in order to identify the ideal membership function distribution. It is primarily based on the Takagi and Sugeno type's fuzzy "if-then" principles. It has two parts: a premise and a result. Figure 3.5 depicts the corresponding ANFIS architecture of Takagi and Sugeno's type. This inference system is made up of five levels. Each layer has a number of nodes, each of which is described by the node function. In this layer, the output signals from nodes in preceding levels are taken as input signals. The output is used as input signals for the next layer after being manipulated by the node function in the current layer.

Every node in layer 2 is fixed node marked by a circle node whose output is the product of all incoming signals:

$$O_{2,i} = t\big(\mu_{Ai}(x), \mu_{Bi}(y)\big) \tag{3.18}$$

$$= \mu_{Ai}(x) x \mu_{Bi}(y)$$

$$= w_i$$

Each node output, w_i ,represents the firing strength of a fuzzy rule.

Every node in layer 3 is a fixed node, denoted by a circle, with the node function computing the ratio of this node's firing strength to the sum of the firing strengths:

$$O_{3,i} = \overline{w_i} = \frac{w_i}{w_i + w_2}, \qquad i = 1,2 \tag{3.19}$$

Every node in layer 4 is adjustable node marked by a square node with a function as:

$$O_{4,i} = \overline{w_i} f_i = \overline{w_i}(p_i x + q_i y + r_i) \tag{3.20}$$

Where $\overline{w_i}$ is a output from layer 3 and {p_i ,q_i ,r_i} is the parameter set of this node. Parameters in this layer are referred to as the consequent parameters.

Every node in layer 5 is a fixed node, marked by a circle node, with the node function to compute the overall output by:

$$O_{5,i} = \sum_i \overline{w_i} f_i = \frac{\sum_i w_i f_i}{\sum_i wi} \tag{3.21}$$

Explicitly, this layer adds the outputs of all the nodes in the previous layer to get the total output of the network.

Experimentation

Work piece and cutting tool material

Turning experiments were conducted using GANESH KSL-5210T CNC Turning Center. The turning machine was equipped with Fanuc 0i-TD series CNC Control, 10 Station Automatic Turret, A2-6 Spindle Nose and a maximum turning diameter of 11 inch. Carbon fiber reinforced plastic (Standard Modulus Carbon) has been used as work piece material. For the experiment, the work pieces were prepared in a dimension of 152.4 mm(length) and 3.81 cm (Outer Diameter). Carbide cutting insert was used as a cutting tool coated with TiCN/AI2O3/TiN. See Figure 3.8.

(a) (b)

Fig. 3.8 (a) Carbide Insert (b) Work piece

The carbide insert schematic diagram and specifications are given below. See Figure 3.9 and Table 1.

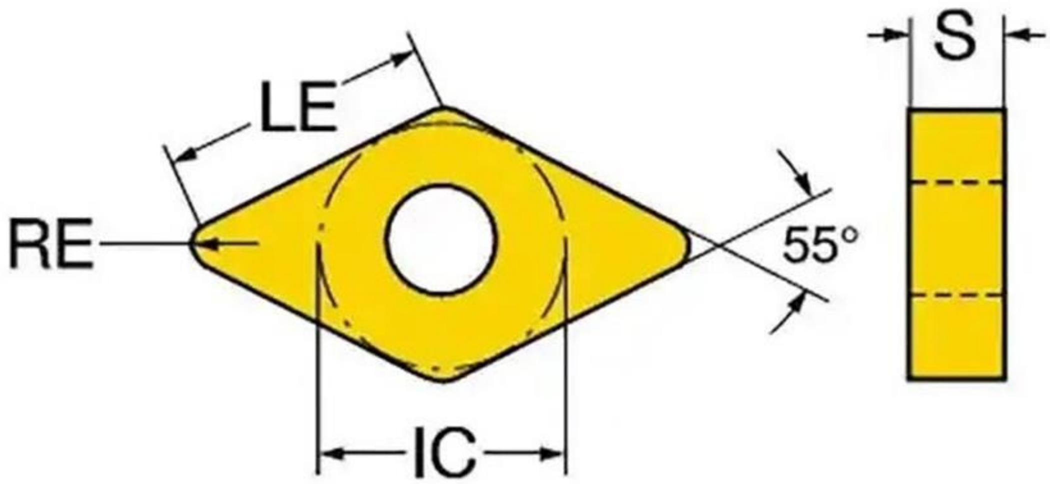

Fig.3.9 Carbide insert schematic diagram (MSC)

Table 1: Specifications for Carbide Insert

Property	**Specifications**
ISO Number	DNMG 15 06 08-QM 2220
Insert Size	442
Material	Carbide
Coating	TiCN/AI2O3/TiN
Included Angle	55
Corner Radius (Inch)	1/32
Inscribed Circle (Inch)	1/2
Cutting Direction	Neutral

Design of Experiment using Takagi-Sugeno Method

In this study, turning experiments of CFRP composite is designed using the Takagi-Sugeno type fuzzy inference system design of experiment. Cutting speed, feed rate, depth of cut, vibration and cutting force are considered as input parameters and tool wear and surface finish are considered as output parameters. Throughout the experiment, workpiece length was kept constant at 152. 4mm. Factors and corresponding levels are found in Table 2. Table 3 further defines neuro-fuzzy algorithms.

Table 2: Factors and Corresponding Levels

Cutting Parameters	**Experiment 1**	**Experiment 2**	**Experiment 3**
Cutting speed (m/min)	125	100	75
Feed rate (mm/rev)	0.05	0.1	0.075
Radial depth of cut (mm)	0.2	0.1	0.15

For each experiment, the constant work piece length (152.4 mm) has been machined sixteen times to the record data for sixteen measurements. After machining the work piece, the value of force, vibration, surface roughness and tool wear have been measured for each measurement.

Table 3: Neuro-Fuzzy Algorithms for Modeling Tool Wear and Surface Finish

Algorithm	**ANFIS**
System	MISO
Clustering	Subtractive
Structure	Fixed
Membership Function Type	Gaussian
Inference System	Takagi-Sugeno
Training Algorithm	Hybrid
Learning Rate	10^{-3}
Error Tolerence	0
Training Data Set	36
Testing Data Set	12

Vibration, Cutting Forces, Surface Finish, and Tool Wear Measurements

Extech 407860 Vibration Meter has been used to measure the vibration and Extech data acquisition software has been used to monitor and analyze the recorded data. 407860 Heavy Duty Vibration Meter has a Velocity range of 7.87 in./s or 200 mm/s; Acceleration range of 656 ft./s or 200 m/s, and displacement range of 0.078 in. or 2 mm.

The cutting forces were measured using a Kistler 9255C dynamometer. A charge amplifier is used to transfer the corresponding force signals, which are then processed using DynoWare software. The dynamometer is comprised of four 3-component force sensors mounted between a baseplate and a top plate under high preload. Each sensor is made up of three pairs of quartz plates, one of which is sensitive to pressure in the z direction and the other two to shear in the x and y directions. The force components are virtually measured without any displacement. The four built-in force sensors' outputs are coupled inside the dynamometer to allow multicomponent force and moment measurements to be done. The 9-conductor flange socket accepts the eight output signals. The four sensors are installed in a ground-isolated configuration. As a result, ground loop issues are virtually avoided. A charge amplifier is used to convey the corresponding force signals from the dynamometer to a specially constructed fixture for keeping the workpiece.

The surface finish value of the machined workpiece surface was measured using a MahrSurf M 300 C profilometer. For calibrating the profilometer, the Ra value was set on 2.4 µm and Rz value was set on 9.3 µm. A 8 mm traversing length was set according to ISO 12085 (MOTIF). Figures 3.10, 3.11 and 3.12 provide photographs and diagrams of the experimental apparatus.

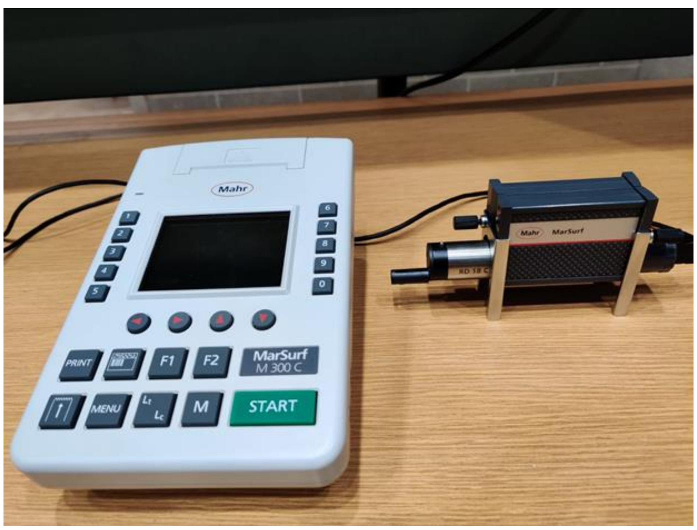

Fig. 3.10 MahrSurf M 300 C Profilometer

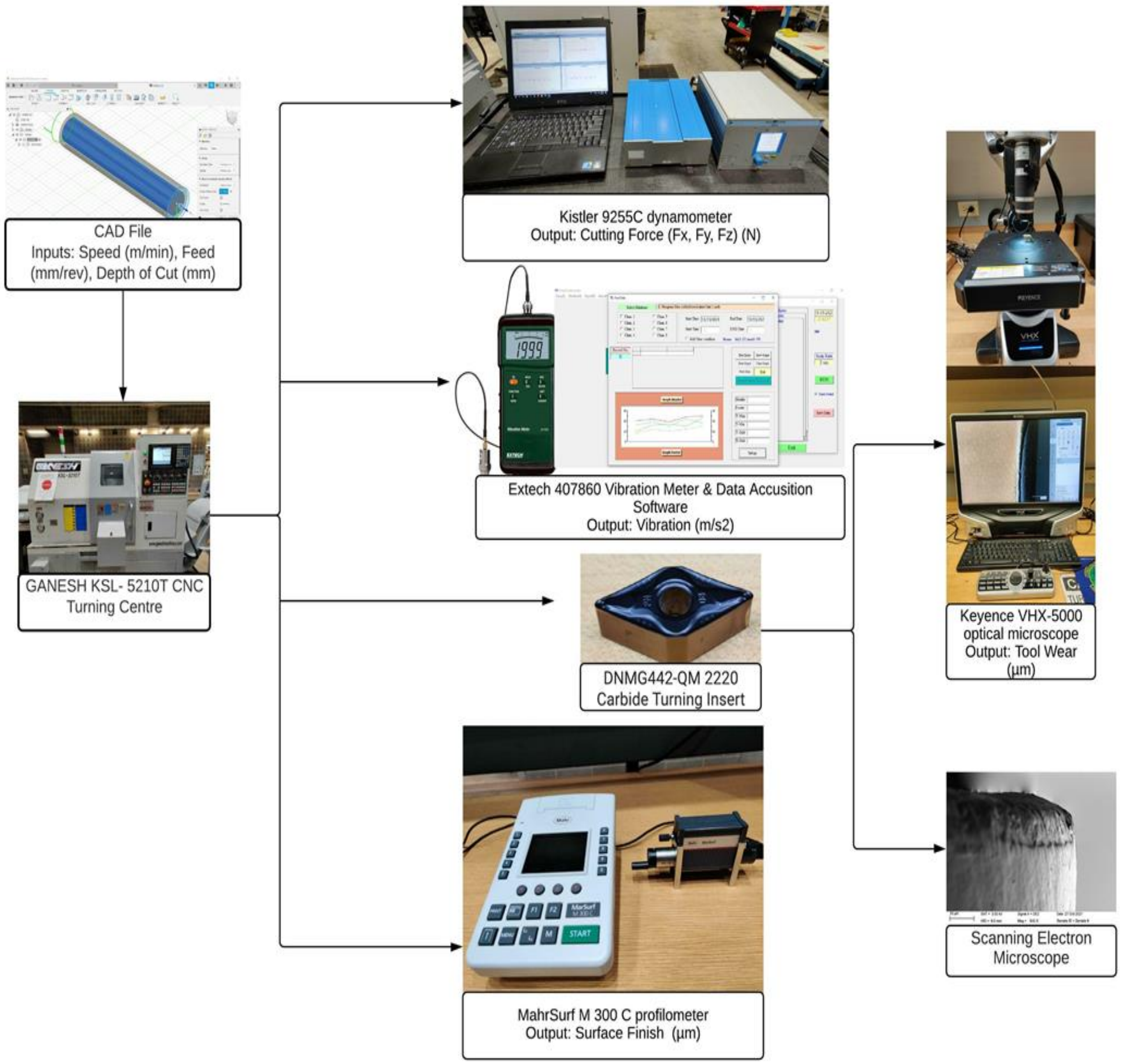

Fig. 3.11 Experimental Apparatus

The overall experimental set up is shown in Figure 3.11. A Keyence VHX-5000 optical microscope shown in Figure 3.12 was used to measure tool wear. 735 µm flank wear corresponds to the maximum tool life.. Micrographs of the surface of the machined samples from the multidirectional laminate were taken using Scanning Electron Microscope (SEM) imaging. These were utilized to determine effects of machining and response parameters on CFRP surface.

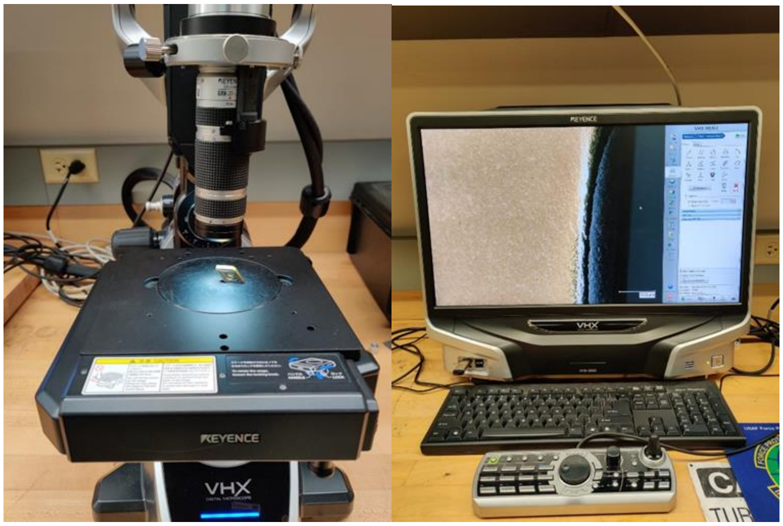

Fig. 3.12 Keyence VHX-5000 Optical Microscope

CHAPTER IV

RESULTS AND DISCUSSION

The ease or difficulty with which materials can be machined is referred to as machinability. Hardness, tensile strength, and ductility are all material properties, but machinability is not one of them. It is an evaluation of the material's response to a machining system, which comprises the cutting tool, machine tool, machining process, and cutting circumstances, in addition to the work material itself. Tool wear or tool life, cutting forces or power consumption, and surface finish are the three basic metrics or criteria used to evaluate machinability. As a result, good machinability entails less tool wear, minimal cutting forces, and a smooth surface finish (Ahmed, 2009). Fibre-reinforced plastics (FRPs) have distinct features that affect machinability in ways that metals do not. The physical properties of the fiber and the matrix, fiber volume percentage, and fiber orientation or architecture are the primary determinants of the attributes of FRP materials. In the first part of this chapter, the relationship between cutting parameters (Speed, Feed, Depth of Cut) and response parameters (Vibration, Cutting Force, Tool Wear and Surface Finish) for continuous turning of CFRP composite and response parameters for continuous turning of CFRP composite are discussed. In the second part, the output for the prediction of tool wear and surface finish using ANFIS modeling is discussed.

Several wear mechanisms may contribute to the total wear of the cutting tool when cutting fiber-reinforced composites. Gross fracture or chipping, abrasion, erosion, micro fracture or microchipping, chemical and electrochemical corrosion, and oxidation are some of the wear mechanisms. While severe fracture causes the cutting edge to fail suddenly or catastrophically in the early phases of cutting, other wear mechanisms cause gradual or cumulative wear. Surface finish and surface integrity in milling and trimming are determined by mechanical and thermal damage to the surface, as well as delamination of the top and/or bottom ply of the laminate structure. Feed rate, cutting speed, and tool wear all have an impact on surface finish (Ahmed, 2009).

In this study, after cutting 152.4 mm, Ra value has been measured from thirteen different places of the CFRP machined surface and an average value has been taken for every measurement shown in Table 4, 5 and 6. For measuring the vibration output, a data sample has been taken in every two second interval throughout the machining time. The response output shown for each experiment in Table 4,5 and 6 are the average values of data samples. Figures 4.1, 4.4, 4.5 and 4.6 were drawn using the data in Tables 4, 5 and 6.

Table 4. Response Table for Speed, v= 125 m/min, Feed, f= 0.05 mm/rev, DOC= 0.2 mm

Measurement No.	**Cutting Force (N)**	**Vibration(m/s^2)**	**Tool wear (μm)**	**Surface Finish (μm)**
1	25.48	3.19	232	1.06
2	25.89	3.35	294	1.08
3	26.31	3.49	335	1.11
4	26.63	3.64	367	1.12
5	26.98	3.81	397	1.14
6	27.27	3.99	427	1.14

Table 4, cont.

Measurement No.	**Cutting Force (N)**	**Vibration(m/s^2)**	**Tool wear (μm)**	**Surface Finish (μm)**
7	27.55	4.16	451	1.15
8	27.86	4.27	460	1.17
9	28.12	4.39	469	1.16
10	28.45	4.52	482	1.17
11	28.78	4.68	501	1.19
12	29.05	4.83	514	1.2
13	29.6	5.01	529	1.22
14	29.91	5.23	543	1.23
15	30.13	5.31	558	1.25
16	30.63	5.51	571	1.26

Table 5. Response Table for Speed, v= 100m/min, Feed, f= 0.1 mm/rev, DOC= 0.1mm

Measurement No.	**Cutting Force (N)**	**Vibration(m/s^2)**	**Tool wear (μm)**	**Surface Finish (μm)**
1	37.31	2.23	310	1.12
2	37.82	2.41	321	1.13
3	38.25	2.57	353	1.15
4	38.66	2.72	389	1.16
5	39.25	2.89	412	1.17

Table 5, cont.

Measurement No.	Cutting Force (N)	Vibration(m/s^2)	Tool wear (µm)	Surface Finish (µm)
6	39.57	3.06	432	1.19
7	39.92	3.28	479	1.21
8	40.36	3.51	508	1.23
9	40.89	3.69	541	1.24
10	41.15	3.82	581	1.25
11	41.67	3.98	605	1.26
12	42.09	4.22	632	1.28
13	42.56	4.47	669	1.29
14	42.86	4.61	698	1.31
15	43.39	4.78	718	1.33
16	43.91	4.91	735	1.34

Table 6. Response Table for Speed, v= 75m/min, Feed, f= 0.075 mm/rev, DOC= 0.15mm

Measurement No.	Cutting Force (N)	Vibration(m/s^2)	Tool wear (µm)	Surface Finish (µm)
1	29.77	1.78	250	1.11
2	30.23	1.92	302	1.13
3	30.65	2.07	345	1.14
4	30.98	2.22	376	1.16

Table 6, cont.

Measurement No.	Cutting Force (N)	Vibration(m/s^2)	Tool wear (µm)	Surface Finish (µm)
5	31.26	2.37	408	1.16
6	31.59	2.51	439	1.17
7	31.89	2.68	463	1.19
8	32.12	2.81	475	1.2
9	32.49	2.97	484	1.2
10	32.81	3.13	497	1.22
11	33.09	3.29	516	1.23
12	33.51	3.44	530	1.24
13	34.01	3.6	543	1.26
14	34.39	3.78	557	1.27
15	34.82	3.86	573	1.27
16	35.26	4.01	589	1.28

Matrix chipping and small pits, fiber breaking, fiber pullout, fiber fuzziness (aramid fibers), cracks, delamination, and spreading of the matrix material are all common damages to the CFRP machined surface. Fiber orientation, feed rate, cutting speed, and fiber composition are all factors that cause surface damage. Surface roughness for CFRP increases with the increase in feed rate (Ahmed, 2009). According to Figure 4.1, cutting parameters with highest feed rate of 0.1 mm/rev provides highest values of surface roughness whereas cutting with feed rate 0.05 mm/rev shows lower values of surface finish. Kim et al. (1992) showed that when compared to the influence of feed rate on CFRP surface finish, cutting speed has a minor impact. Figure 4.2 demonstrates the condition of CFRP surface machined at higher feed rate 0.1 mm/rev. A lot of fractured fibers is visible which indicates the poor surface finish. Figure 4.3 indicates that at lower feed rate of 0.05 mm/rev, there are only a few fractured fibers to attribute the condition of good surface finish at lower feed rate.

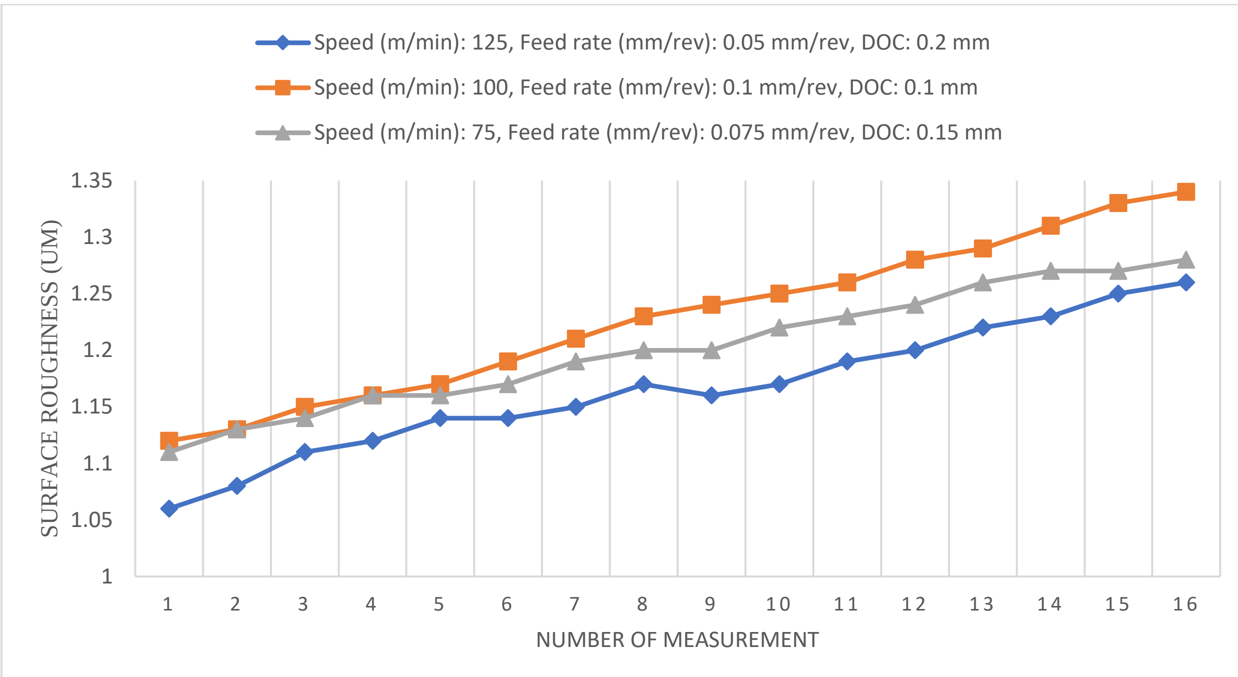

Fig. 4.1 Variation of Surface Roughness with Number of Measurement

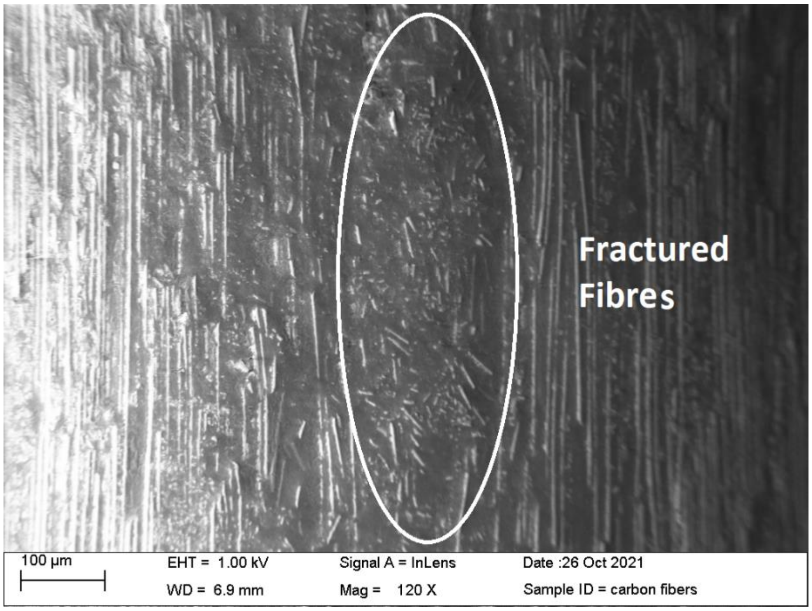

Fig. 4.2 SEM Image at f =0.1 mm/rev (mag. 120X)

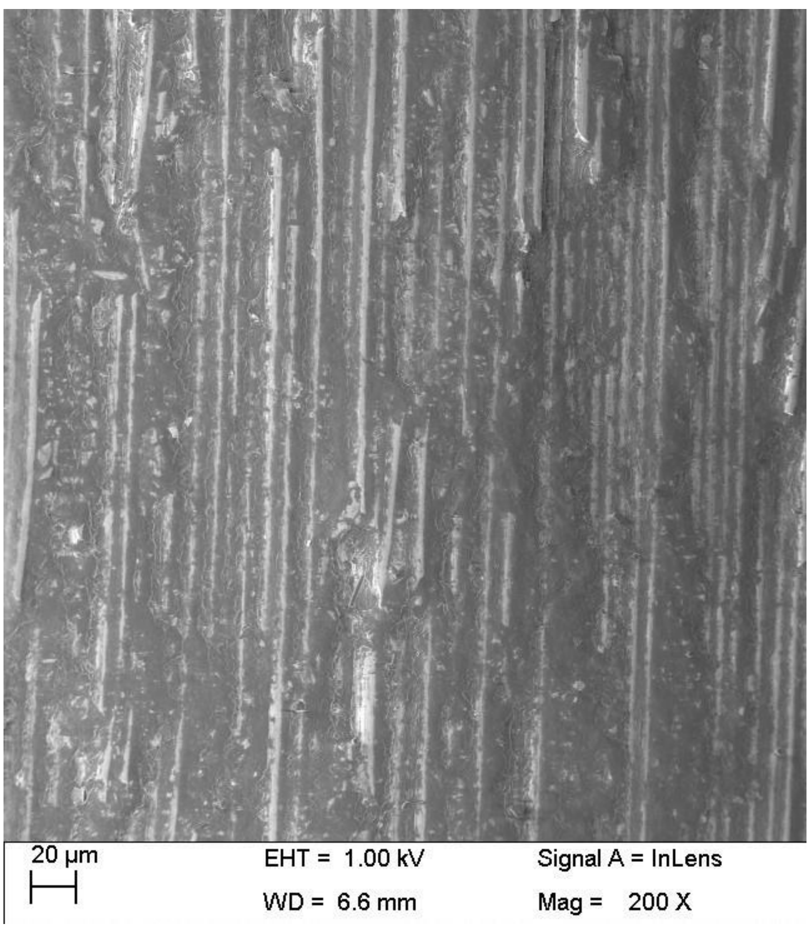

Fig. 4.3 SEM Image at f=0.05 mm/rev (mag. 200X)

The relationship between cutting forces and cutting speed varies depending on the type of FRPs. The cutting force decreases with increase in cutting speed when machining CFRP composite. As the feed rate and depth of cut rise, the cutting forces increase as well (Ahmed, 2009). In Figure 4.4, for highest speed of 125 m/min and lowest feed rate, the lowest cutting force is found. From the speed of 100 m/min and highest feed rate of 0.1 mm/rev, highest cutting force is achieved. Higher cutting force leads to poor surface finish. Due to the magnitude of the cutting forces, the adhesion strength between fiber and matrix can be exceeded, so that fibers either peel (delamination) or are removed by the expansion of matrix parts (Ahmed, 2009).

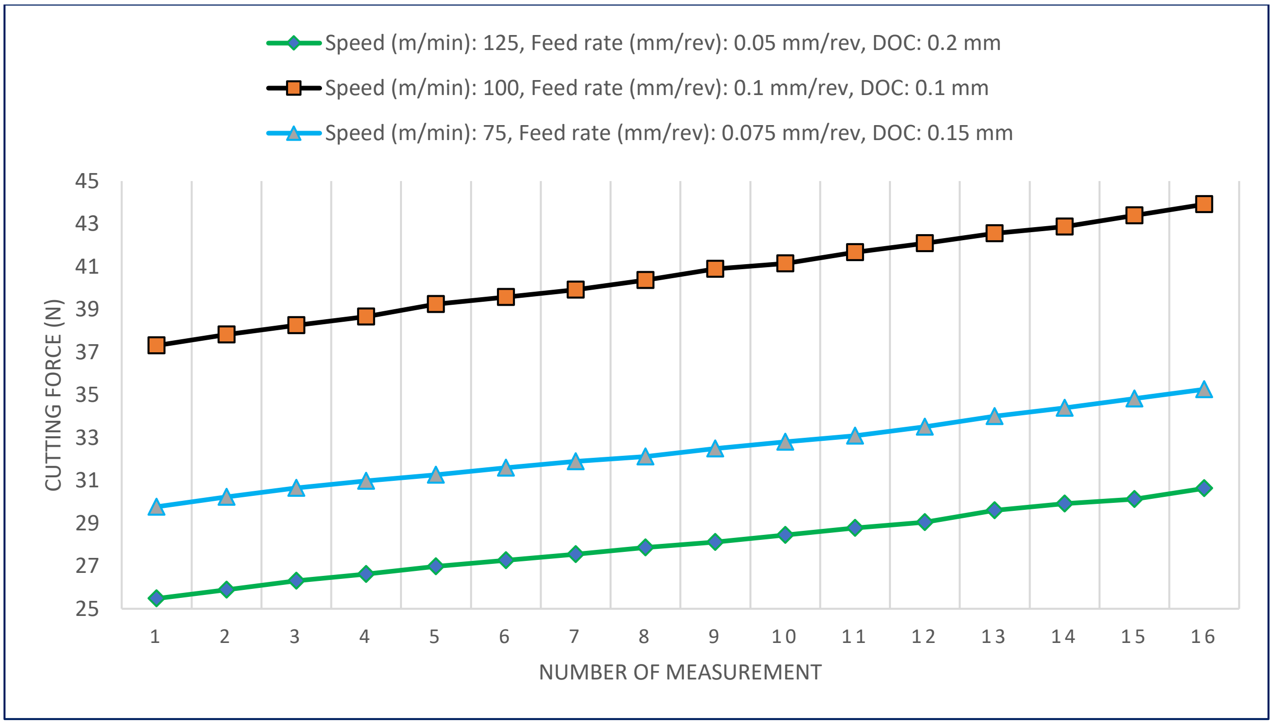

Fig. 4.4 Variation of Cutting Force with Number of Measurement

The value of feed rate and depth of cut showed greater influence on tool vibration. From Figure 4.5, for lowest feed rate (0.05 mm/rev) and highest depth of cut (0.2 mm), the highest amplitude of vibration has been found. Lower feed rate and lowest speed produced minimum vibration. Balasundaram et al. (2020) found similar kind of correlations during investigation on turning parameters on machining time and vibration of carbon fiber reinforced laminates.

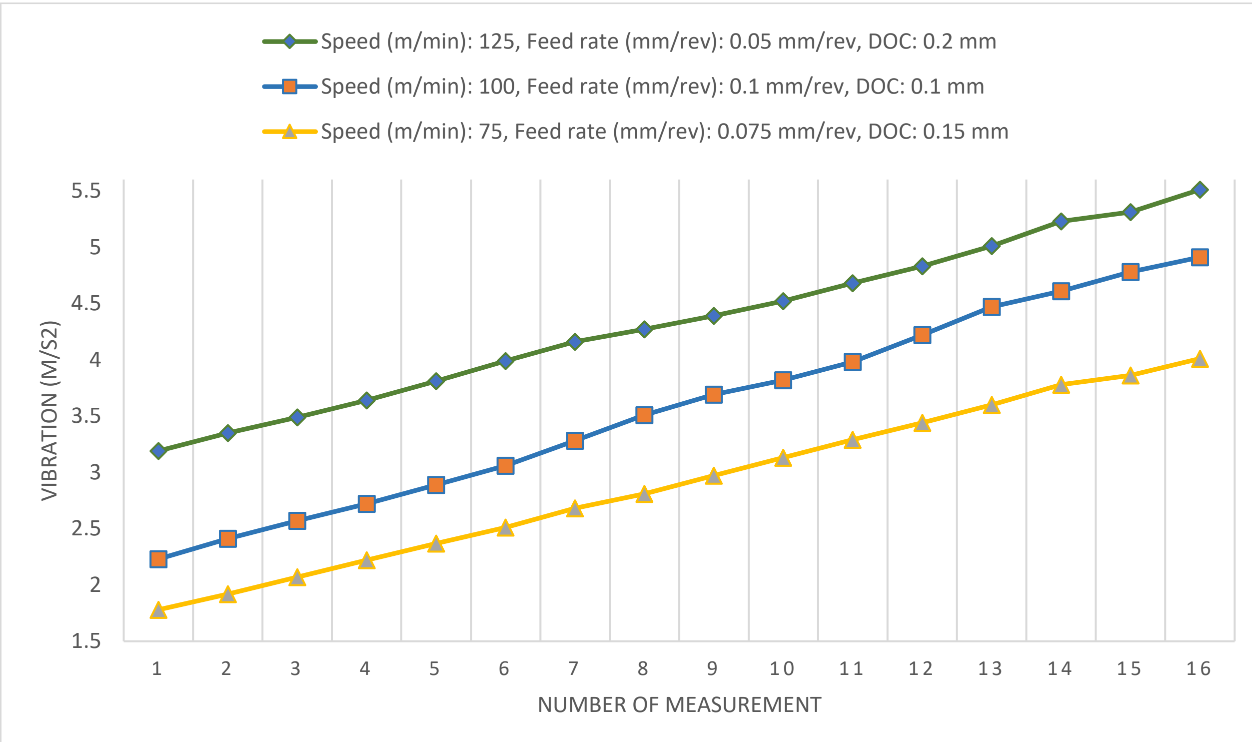

Fig. 4.5 Variation of Vibration with Number of Measurement

When machining CFRP, tool wear is less dependent on cutting speed so faster cutting speeds can be achieved when machining CFRP. This is due to the carbon fibers' superior thermal conductivity and ability to transfer heat away from the cutting zone. As a result, cutting edge temperatures and wear rates are reduced (Ahmed, 2009). Variation of tool wear at different machining conditions has shown in Figure 4.6. The rate of tool wear is found higher for Speed, v= 100 m/min, Feed, f= 0.1 mm/rev, DOC= 0.1 mm whereas for Speed, v= 125 m/min, Feed, f= 0.05 mm/rev, DOC= 0.2 mm, the tool wear is found lower. In the experiment, tool wear is observed to increase as feed rate was increased and depth of cut is decreased. Palanikumar and Paulo (2007) showed in their work that tool wear increased with the increase of cutting speed, feed rate and decrease of depth of cut. Ramulu et al. (1989) showed that tool wear increases with the increase of feed rate. So, results found in this study are consistent with prior research.

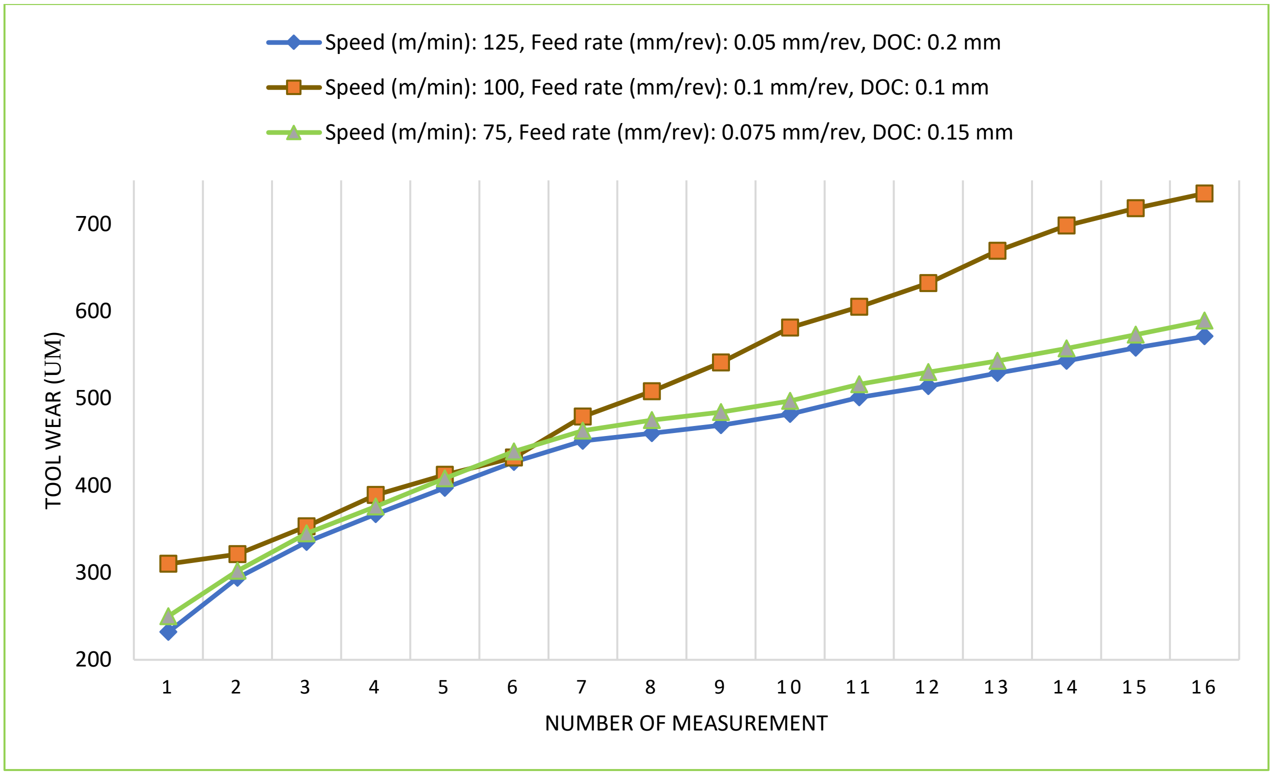

Fig. 4.6 Variation of Tool Wear with Number of Measurement

Figure 4.7 shows the tool wear zone at 195X magnification where abrasion on cutting tool surface is visible. Figure 4.8 illustrates the lower tool wear condition at lower feed rate (0.05 mm/rev) and higher DOC (0.2 mm). However, tool wear has been found higher at higher feed rate (0.1 mm/rev) and lower DOC (0.1 mm) as showed in Figure 4.9 There are some visible presences of CFRP chips on cutting tool which is from the machined material shown in Figure 4.10.

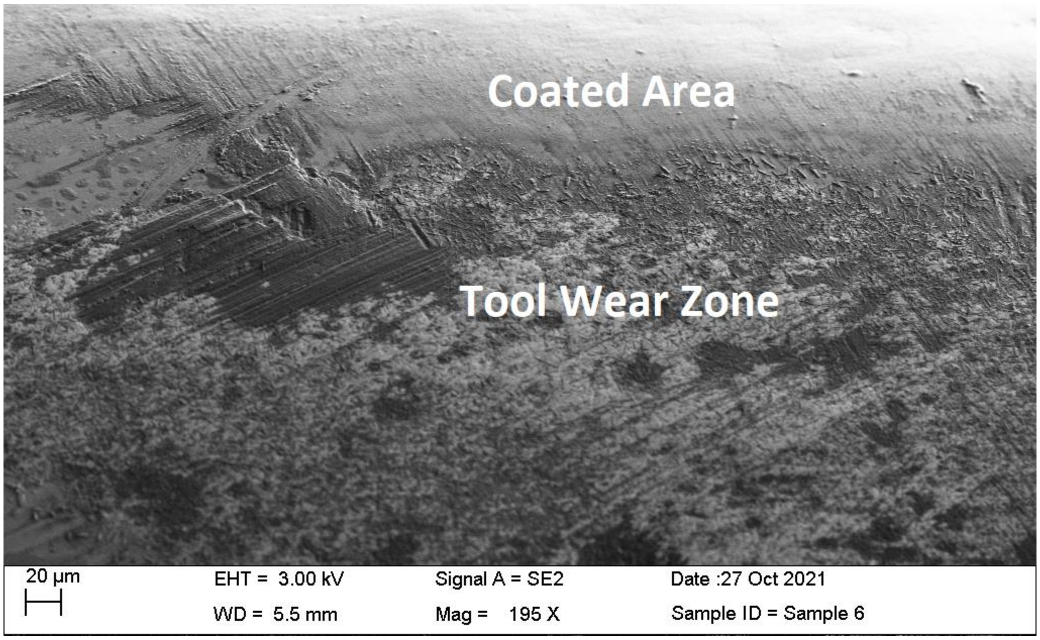

Fig. 4.7 SEM of Tool Wear Zone

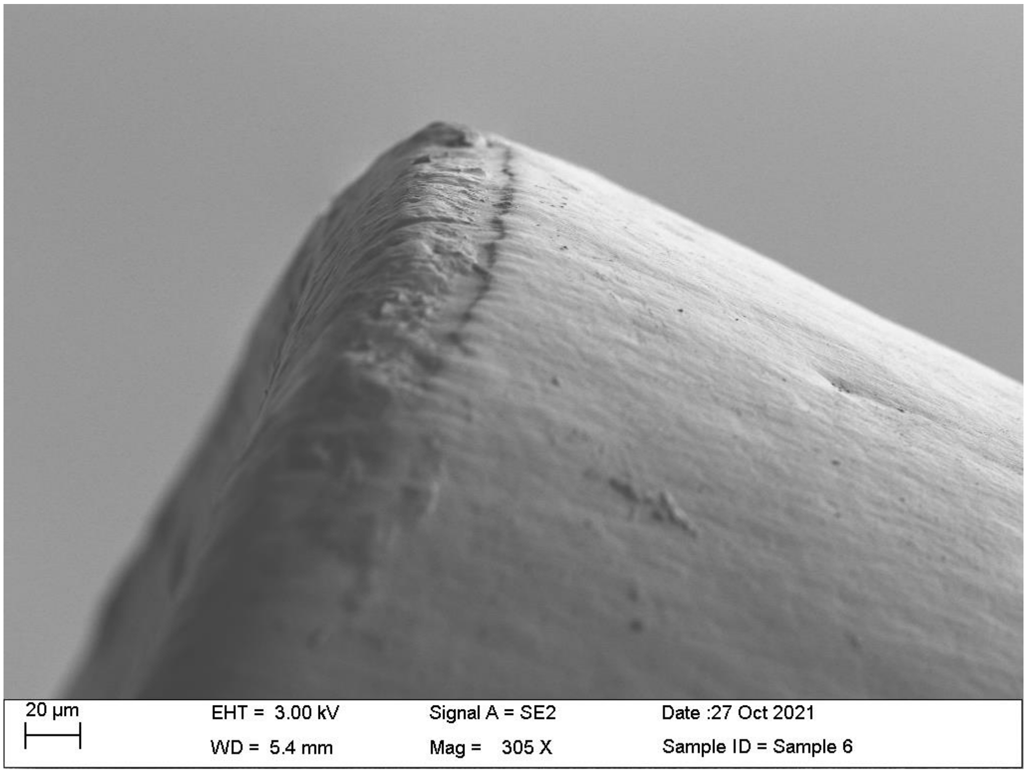

Fig. 4.8 SEM of Cutting Tool after Machining at Speed, v= 125 m/min, Feed, f= 0.05 mm/rev, DOC= 0.2 mm

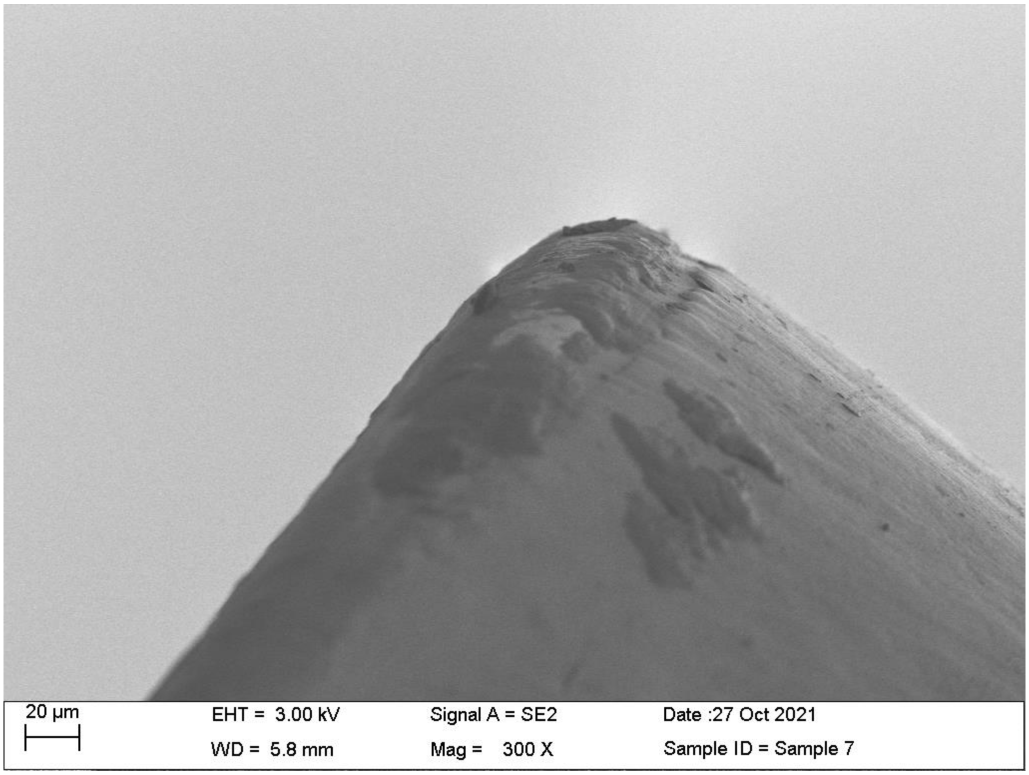

Fig. 4.9 SEM of Cutting Tool after Machining at Speed, v= 100 m/min, Feed, f= 0.1 mm/rev, DOC= 0.1 mm

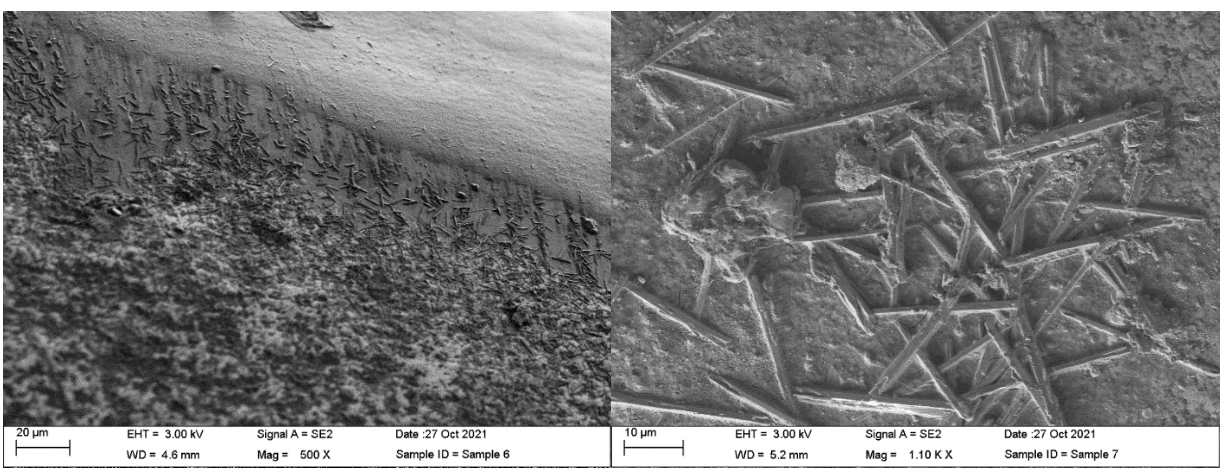

Fig. 4.10 Visible Presence of CFRP on Cutting Tool Surface

ANFIS Model for Tool Wear and Surface Finish Estimation

One of the strategies for analyzing and improving the performance of any system is to use artificial intelligence. The functional combination of various sensors, signal analysis, and artificial intelligence algorithms results in a more promising strategy for meeting today's high-performance needs (Fang, 1995). ANFIS is a fuzzy inference system for adaptive networks that is integrated into the architecture and learning process. A feed forward neural network with supervised learning capabilities is referred to as an adaptive network. ANFIS can be used to optimize membership functions to generate specified input–output pairs, with the added benefit of being able to create fuzzy "if-then" type rules to express these optimized membership functions. In this study, an effort has been made to demonstrate the use the Adaptive Neuro-Fuzzy inference system (ANFIS) for estimation of the tool wear and surface finish during continuous turning of CFRP.

The dataset used for ANFIS modeling is shown in Table 7. Seventy-five percent of all data points has been used for training the model and twenty-five percent has been used for testing the model. The data set has been normalized by dividing the individual maximum values of parameters. When the input properties of neural networks are scaled to the same range, they converge faster. They also benefit from it because it keeps their activations and, as a result, their weights low.

For the estimation of tool wear and surface finish, speed, feed, DOC, force, and vibration has been used as inputs whereas tool wear and surface finish are used as output parameters. Figure 4.11 shows the fuzzy logic designer for tool wear with inputs and outputs and Figure 4.12 presents the model for surface finish.

In this study, MATLAB R2021a is used for ANFIS modeling. Neuro-fuzzy designer, fuzzy logic designer, rule viewer, MATLAB surface plot, membership function editor and rule editor tools have been used to represent the inputs and outputs.

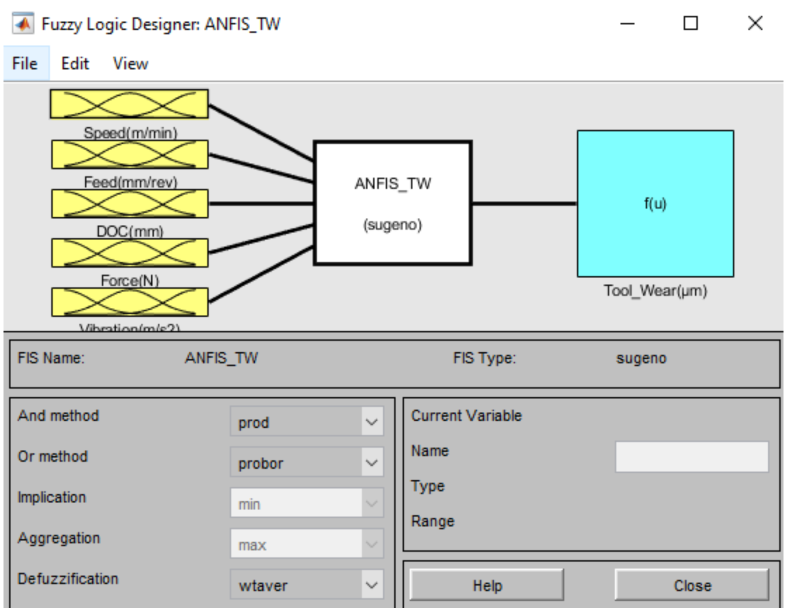

Fig. 4.11 Fuzzy Logic Designer for Tool Wear

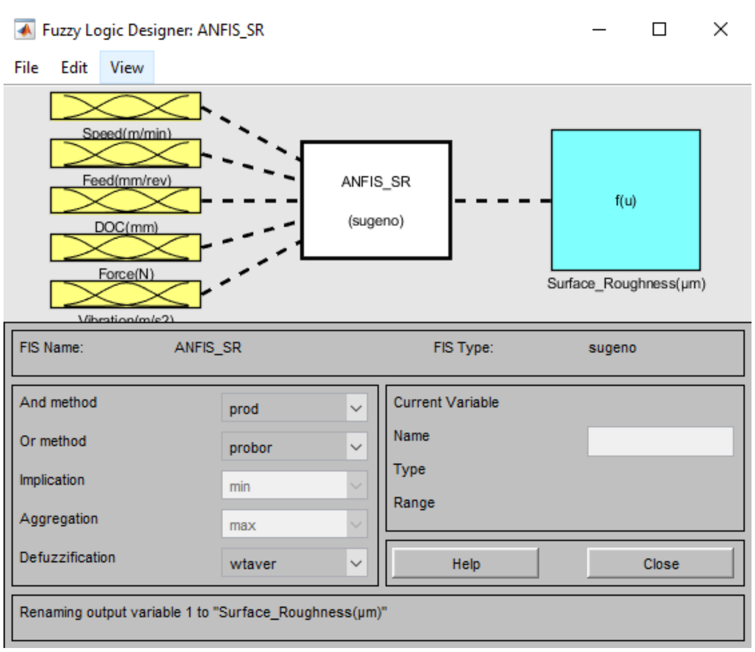

Fig. 4.12 Fuzzy Logic Designer for Surface Finish

Hybrid training has been used to train the data set and the training root mean square error (RMSE) was 0.0052819 for tool wear and RMSE is 0.0025216 for surface finish. The error tolerance of 0 is used and the number of epochs is 200. The conditional statements that make up fuzzy logic are expressed using "if-then rule" statements. Figure 4.13 and 4.14 depicts the model's rules; six rules have been found to be sufficient for matching the data's criteria. A single output membership function corresponds to each rule. Clustering is a technique for extracting natural groupings of data from a huge dataset to create a concise representation of a system's behavior. Clustering is used to overcome the problem of explosion in the number of rules. In this research, subtractive clustering was used to estimate the number of clusters and cluster centers in a set of data.

1. If (Speed(m/min) is in1cluster1) and (Feed(mm/rev) is in2cluster1) and (DOC(mm) is in3cluster1) and (Force(N) is in4cluster1) and (Vibration(m/s2) is in5cluster1) then (Tool_Wear(μm) is out1cluster1) (1)
2. If (Speed(m/min) is in1cluster2) and (Feed(mm/rev) is in2cluster2) and (DOC(mm) is in3cluster2) and (Force(N) is in4cluster2) and (Vibration(m/s2) is in5cluster2) then (Tool_Wear(μm) is out1cluster2) (1)
3. If (Speed(m/min) is in1cluster3) and (Feed(mm/rev) is in2cluster3) and (DOC(mm) is in3cluster3) and (Force(N) is in4cluster3) and (Vibration(m/s2) is in5cluster3) then (Tool_Wear(μm) is out1cluster3) (1)
4. If (Speed(m/min) is in1cluster4) and (Feed(mm/rev) is in2cluster4) and (DOC(mm) is in3cluster4) and (Force(N) is in4cluster4) and (Vibration(m/s2) is in5cluster4) then (Tool_Wear(μm) is out1cluster4) (1)
5. If (Speed(m/min) is in1cluster5) and (Feed(mm/rev) is in2cluster5) and (DOC(mm) is in3cluster5) and (Force(N) is in4cluster5) and (Vibration(m/s2) is in5cluster5) then (Tool_Wear(μm) is out1cluster5) (1)
6. If (Speed(m/min) is in1cluster6) and (Feed(mm/rev) is in2cluster6) and (DOC(mm) is in3cluster6) and (Force(N) is in4cluster6) and (Vibration(m/s2) is in5cluster6) then (Tool_Wear(μm) is out1cluster6) (1)

Fig. 4.13 Rules Used for Tool Wear Model

1. If (Speed(m/min) is in1cluster1) and (Feed(mm/rev) is in2cluster1) and (DOC(mm) is in3cluster1) and (Force(N) is in4cluster1) and (Vibration(m/s2) is in5cluster1) then (Surface_Finish(μm) is out1cluster1) (1)
2. If (Speed(m/min) is in1cluster2) and (Feed(mm/rev) is in2cluster2) and (DOC(mm) is in3cluster2) and (Force(N) is in4cluster2) and (Vibration(m/s2) is in5cluster2) then (Surface_Finish(μm) is out1cluster2) (1)
3. If (Speed(m/min) is in1cluster3) and (Feed(mm/rev) is in2cluster3) and (DOC(mm) is in3cluster3) and (Force(N) is in4cluster3) and (Vibration(m/s2) is in5cluster3) then (Surface_Finish(μm) is out1cluster3) (1)
4. If (Speed(m/min) is in1cluster4) and (Feed(mm/rev) is in2cluster4) and (DOC(mm) is in3cluster4) and (Force(N) is in4cluster4) and (Vibration(m/s2) is in5cluster4) then (Surface_Finish(μm) is out1cluster4) (1)
5. If (Speed(m/min) is in1cluster5) and (Feed(mm/rev) is in2cluster5) and (DOC(mm) is in3cluster5) and (Force(N) is in4cluster5) and (Vibration(m/s2) is in5cluster5) then (Surface_Finish(μm) is out1cluster5) (1)
6. If (Speed(m/min) is in1cluster6) and (Feed(mm/rev) is in2cluster6) and (DOC(mm) is in3cluster6) and (Force(N) is in4cluster6) and (Vibration(m/s2) is in5cluster6) then (Surface_Finish(μm) is out1cluster6) (1)

Fig. 4.14 Rules Used for Surface Finish Model

Table 7. Data set for ANFIS modeling

Speed (m/min)	Feed (mm/rev)	DOC (mm)	Cutting Force (N)	Vibration (m/s2)	Tool wear (μm)	Surface Finish (μm)
125	0.05	0.2	25.48	3.19	232 Tr	1.06 Tr
125	0.05	0.2	25.89	3.35	294 Tr	1.08 Tr
125	0.05	0.2	26.31	3.49	335 Tr	1.11 Tr
125	0.05	0.2	26.63	3.64	367 Tr	1.12 Tr
125	0.05	0.2	26.98	3.81	397 Tr	1.14 Tr
125	0.05	0.2	27.27	3.99	427 Tr	1.14 Tr
125	0.05	0.2	27.55	4.16	451 Tr	1.15 Tr
125	0.05	0.2	27.86	4.27	460 Tr	1.17 Tr
125	0.05	0.2	28.12	4.39	469 Tr	1.16 Tr
125	0.05	0.2	28.45	4.52	482 Tr	1.17 Tr
125	0.05	0.2	28.78	4.68	501 Tr	1.19 Tr
125	0.05	0.2	29.05	4.83	514 Tr	1.2 Tr
125	0.05	0.2	29.6	5.01	529	1.22
125	0.05	0.2	29.91	5.23	543	1.23
125	0.05	0.2	30.13	5.31	558	1.25
125	0.05	0.2	30.63	5.51	571	1.26
100	0.1	0.1	37.31	2.23	310 Tr	1.12 Tr
100	0.1	0.1	37.82	2.41	321 Tr	1.13 Tr

Table 7, cont.

Speed (m/min)	**Feed (mm/rev)**	**DOC (mm)**	**Cutting Force (N)**	**Vibration (m/s2)**	**Tool wear (μm)**	**Surface Finish (μm)**
100	0.1	0.1	38.25	2.57	353 [Tr]	1.15 [Tr]
100	0.1	0.1	38.66	2.72	389 [Tr]	1.16 [Tr]
100	0.1	0.1	39.25	2.89	412 [Tr]	1.17 [Tr]
100	0.1	0.1	39.57	3.06	432 [Tr]	1.19 [Tr]
100	0.1	0.1	39.92	3.28	479 [Tr]	1.21 [Tr]
100	0.1	0.1	40.36	3.51	508 [Tr]	1.23 [Tr]
100	0.1	0.1	40.89	3.69	541 [Tr]	1.24 [Tr]
100	0.1	0.1	41.15	3.82	581 [Tr]	1.25 [Tr]
100	0.1	0.1	41.67	3.98	605 [Tr]	1.26 [Tr]
100	0.1	0.1	42.09	4.22	632 [Tr]	1.28 [Tr]
100	0.1	0.1	42.56	4.47	669	1.29
100	0.1	0.1	42.86	4.61	698	1.31
100	0.1	0.1	43.39	4.78	718	1.33
100	0.1	0.1	43.91	4.91	735	1.34
75	0.075	0.15	29.77	1.78	250 [Tr]	1.11 [Tr]
75	0.075	0.15	30.23	1.92	302 [Tr]	1.13 [Tr]
75	0.075	0.15	30.65	2.07	345 [Tr]	1.14 [Tr]
75	0.075	0.15	30.98	2.22	376 [Tr]	1.16 [Tr]
75	0.075	0.15	31.26	2.37	408 [Tr]	1.16 [Tr]
75	0.075	0.15	31.59	2.51	439 [Tr]	1.17 [Tr]

Table 7, cont.

Speed (m/min)	**Feed (mm/rev)**	**DOC (mm)**	**Cutting Force (N)**	**Vibration (m/s2)**	**Tool wear (μm)**	**Surface Finish (μm)**
75	0.075	0.15	31.89	2.68	463 [Tr]	1.19 [Tr]
75	0.075	0.15	32.12	2.81	475 [Tr]	1.2 [Tr]
75	0.075	0.15	32.49	2.97	484 [Tr]	1.2 [Tr]
75	0.075	0.15	32.81	3.13	497 [Tr]	1.22 [Tr]
75	0.075	0.15	33.09	3.29	516 [Tr]	1.23 [Tr]
75	0.075	0.15	33.51	3.44	530 [Tr]	1.24 [Tr]
75	0.075	0.15	34.01	3.6	543	1.26
75	0.075	0.15	34.39	3.78	557	1.27
75	0.075	0.15	34.82	3.86	573	1.27
75	0.075	0.15	35.26	4.01	589	1.28

[Tr] Training data

Figure 4.15 to 4.19 shows the membership functions of tool wear model and Figure 4.20 to 4.24 shows the membership functions of surface finish for inputs (Speed, Feed, DOC, Force and Vibration) and outputs (Tool Wear and Surface Finish).

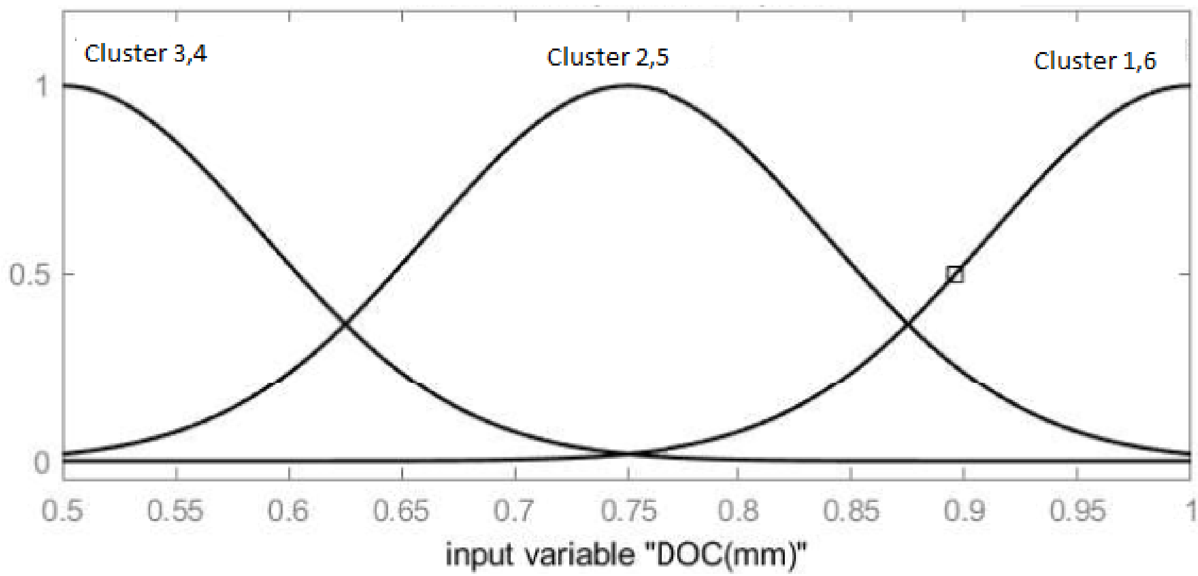

Fig. 4.15 DOC Membership Function for Tool Wear

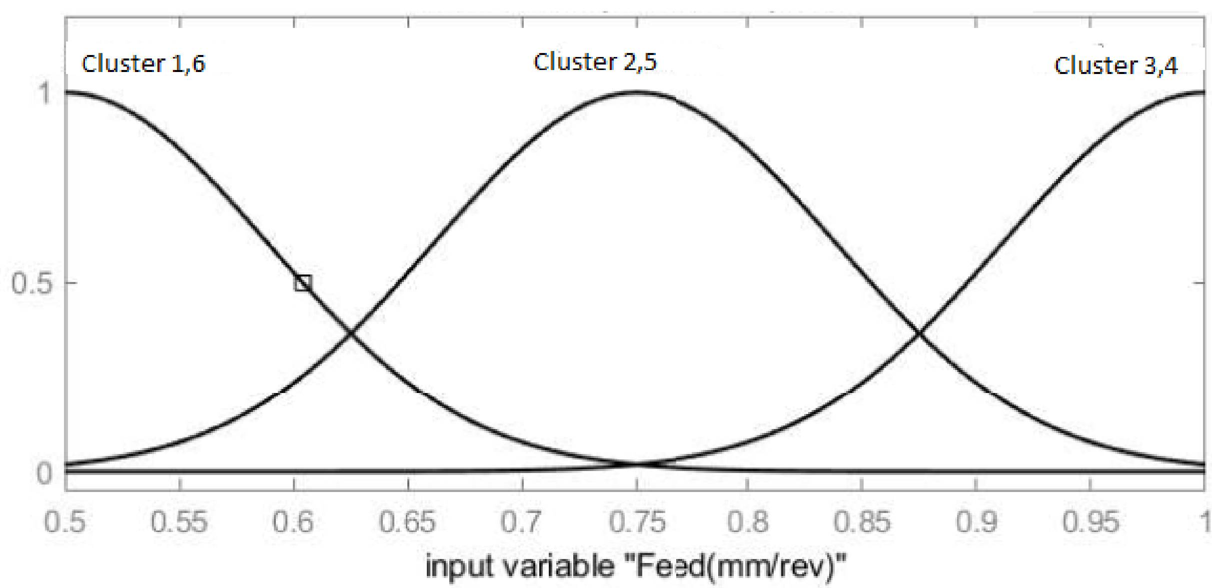

Fig. 4.16 Feed Membership Function for Tool Wear

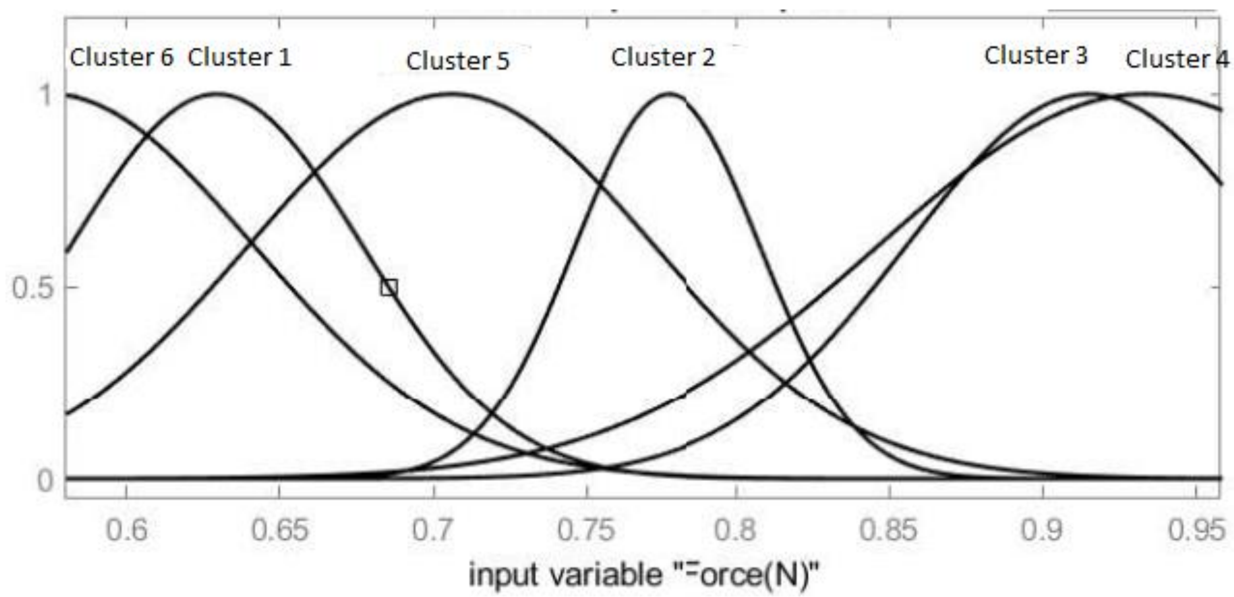

Fig. 4.17 Force Membership Function for Tool Wear

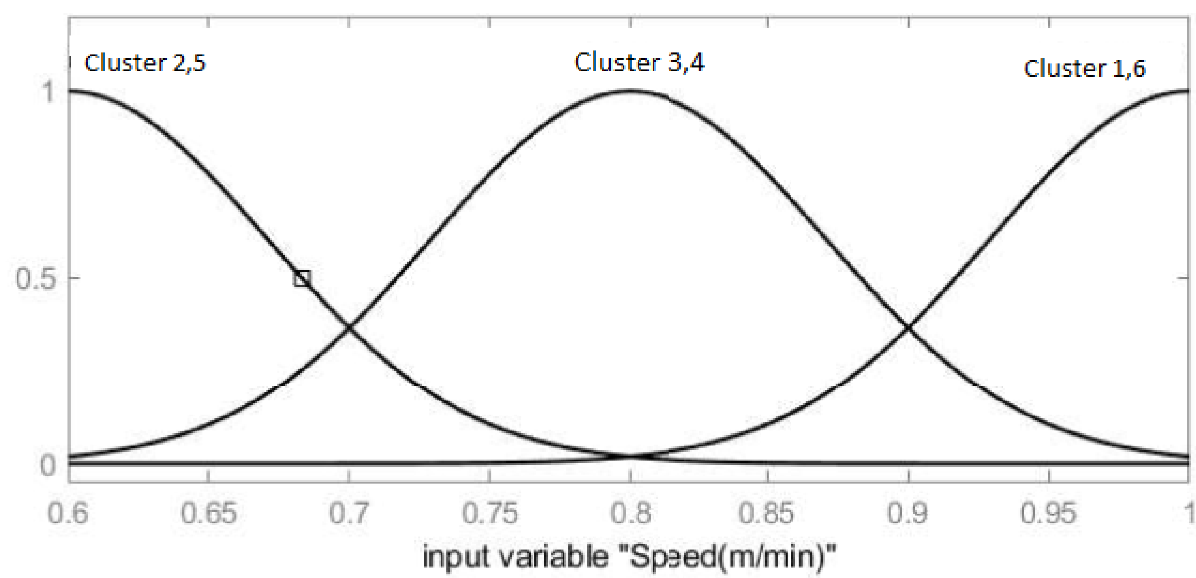

Fig. 4.18 Speed Membership Function for Tool Wear

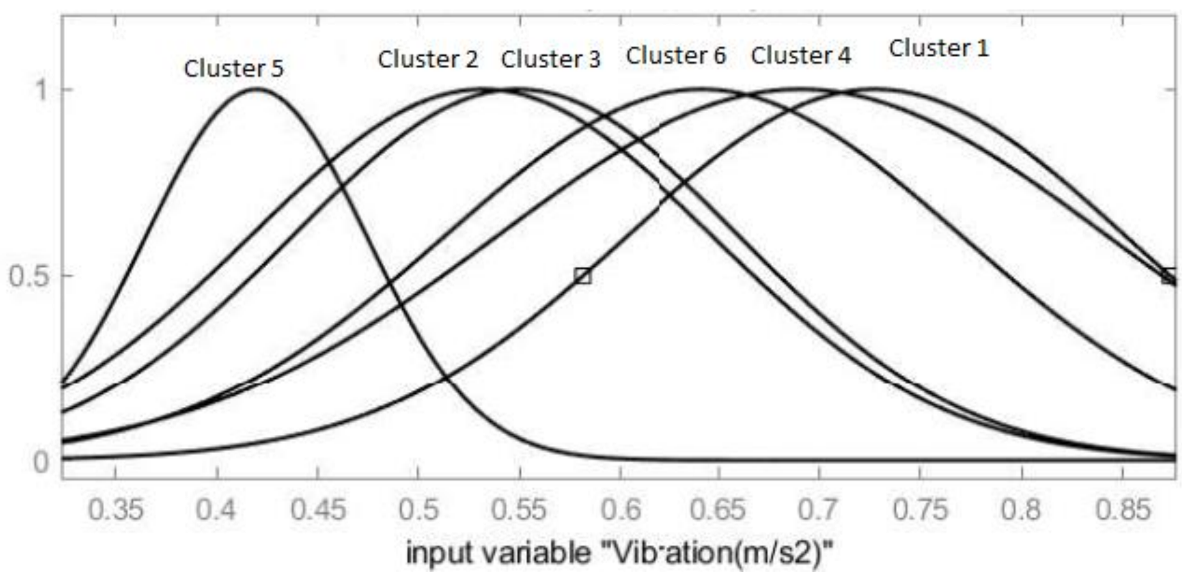

Fig. 4.19 Vibration Membership Function for Tool Wear

The average testing RMSE for tool wear was 0.022673 and for surface finish RMSE was 0.0095623 shown in Figure 4.25 and 4.26. Here six cluster centers were located for force and vibration and for each cluster, a separate membership function and rule is created; whereas, for speed, feed and DOC, three cluster centers were located because of the data set showed in Table 7. According to MATLAB rule viewer showed in Figure 4.27 and 4.28, for speed, feed and DOC, cluster 1 & 6, cluster 2 & 5 and cluster 3 & 4 have same value of MFs centre (c) and MFs width (σ). So, for speed, feed and DOC, cluster 1 & 6, cluster 2 & 5 and cluster 3 & 4 are producing a three cluster center in MF graph.

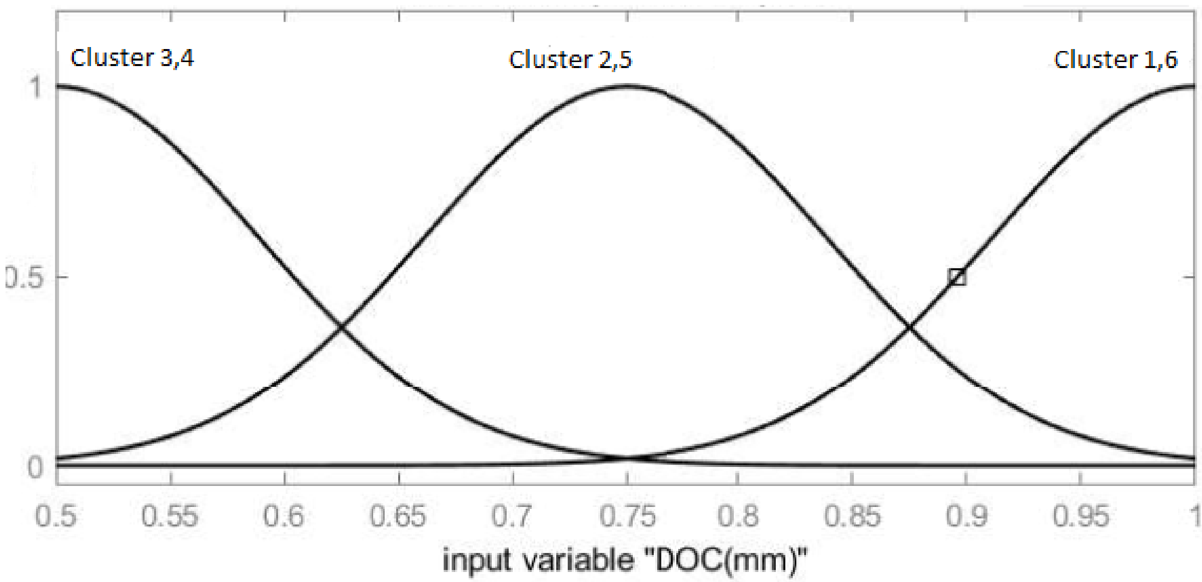

Fig. 4.20 DOC Membership Function for Surface Finish

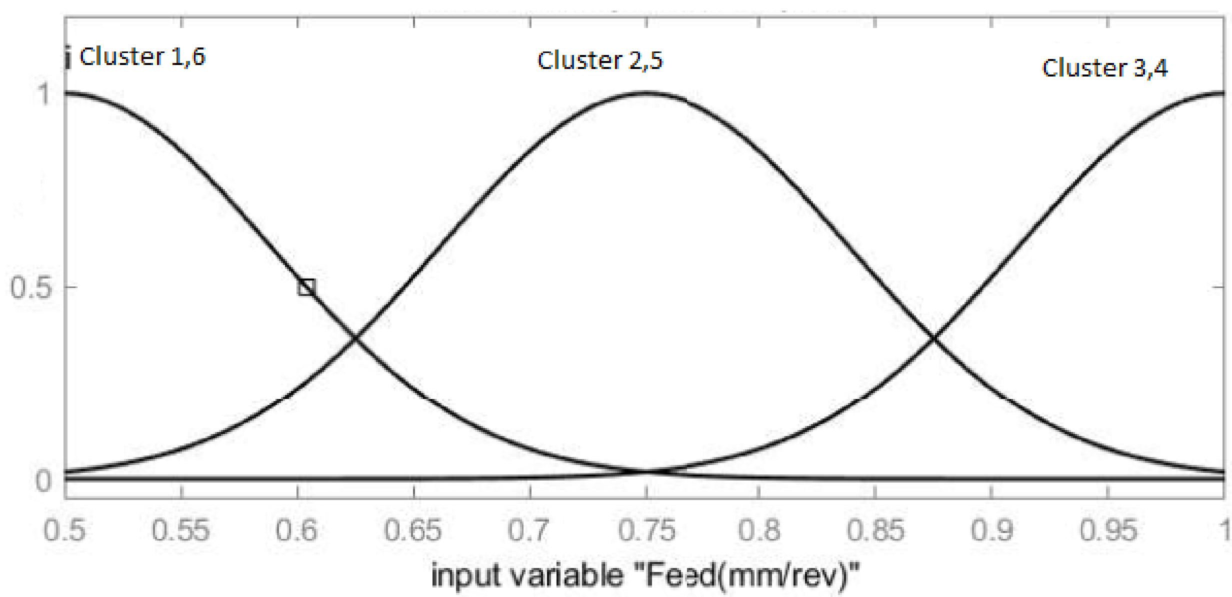

Fig. 4.21 Feed Membership Function for Surface Finish

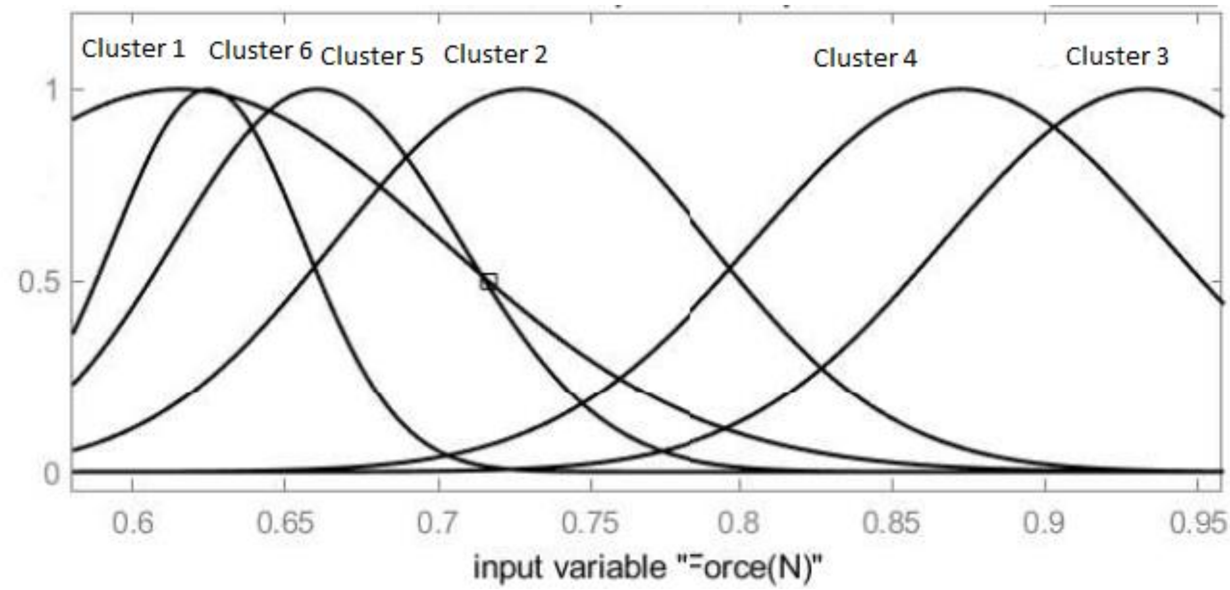

Fig. 4.22 Force Membership Function for Surface Finish

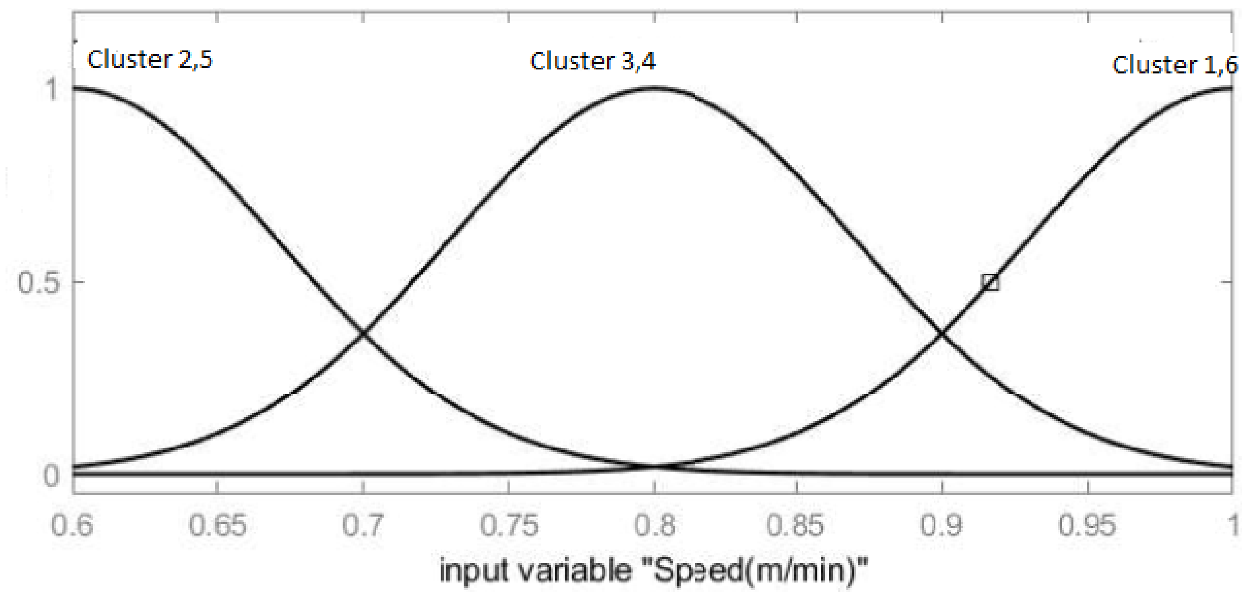

Fig. 4.23 Speed Membership Function for Surface Finish

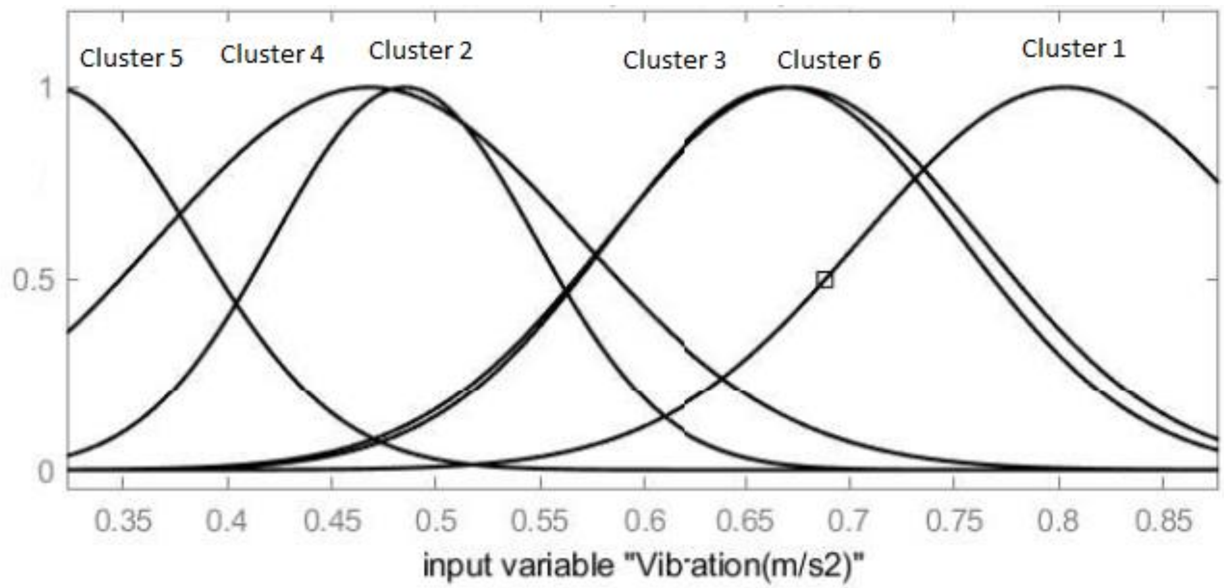

Fig. 4.24 Vibration Membership Function for Surface Finish

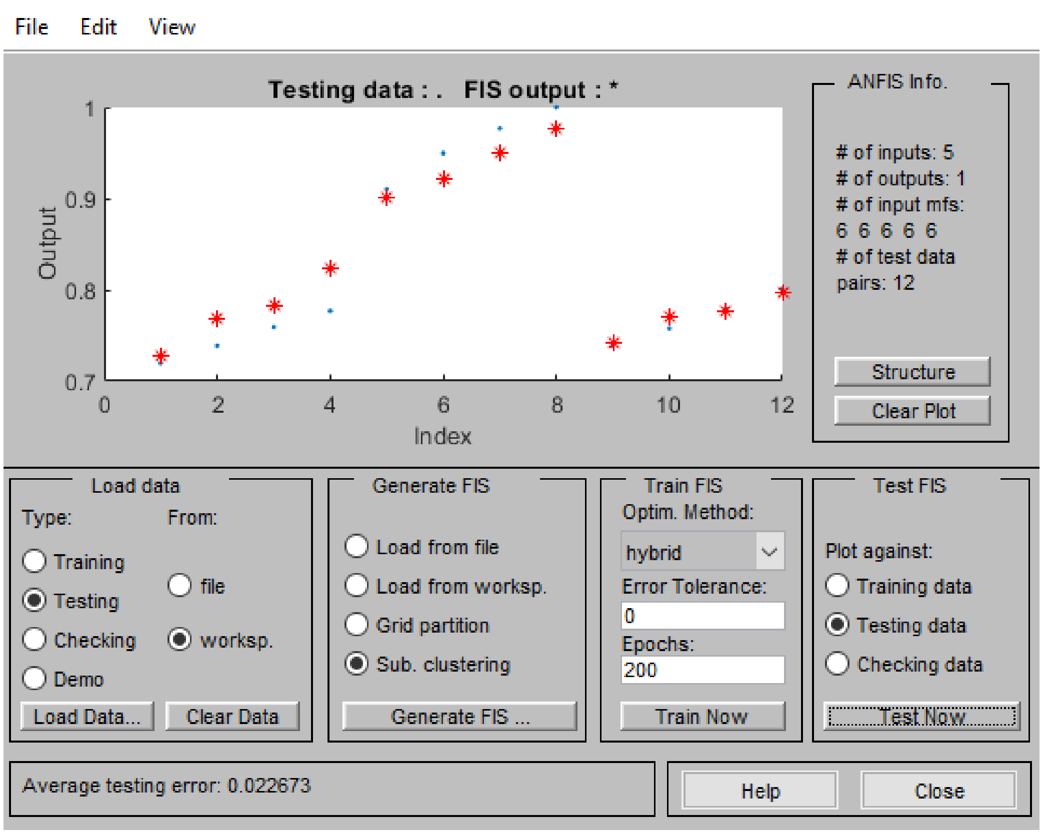

Fig 4.25 Testing Accuracy for Tool Wear

Fig. 4.26 Testing Accuracy for Surface Finish

The MATLAB rule viewers for tool wear model and surface finish model are shown in Figure 4.28 and 4.29.

Fig. 4.27 Rule Viewer for Tool Wear

Fig. 4.28 Rule Viewer for Surface Finish

Table 8 shows the normalized actual and predicted tool wear data for tool wear and Figure 4.29 is the graphical representation of Table 8.

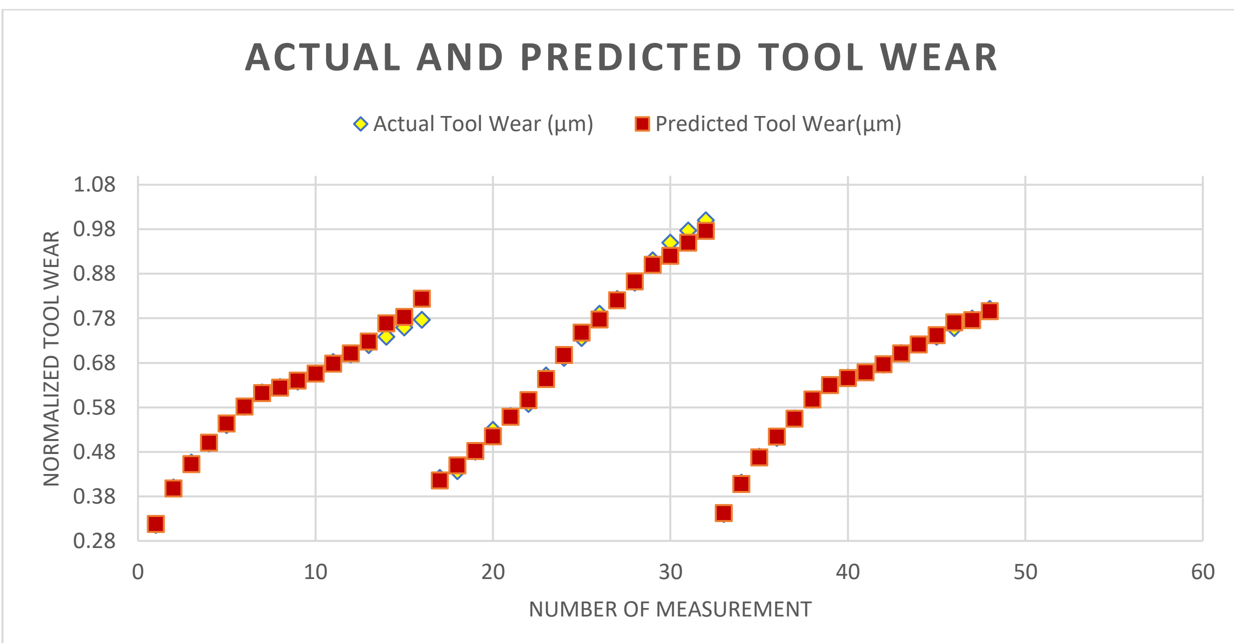

Fig. 4.29 Actual and Predicted Tool Wear with Number of Measurement

Table 8. Normalized Data for Actual and Predicted Tool Wear

Actual Tool wear	**Predicted Tool Wear**	**%Error**
0.315646259	0.317960606	0.733209303
0.4	0.3975812	0.604699963
0.455782313	0.452552749	0.708575862
0.499319728	0.500592165	0.254834059
0.540136054	0.543502139	0.623191898
0.580952381	0.58195599	0.17275235
0.613605442	0.611916778	0.275203549
0.62585034	0.624220469	0.260424993
0.638095238	0.640104515	0.314886668
0.655782313	0.655794487	0.001856486
0.681632653	0.678376574	0.477688312
0.699319728	0.70156593	0.321198219
0.719727891	0.728096641	1.162765854
0.73877551	0.768545707	4.029667463
0.759183673	0.78339435	3.189040692
0.776870748	0.823817871	6.043105944
0.421768707	0.416242625	1.310216399
0.436734694	0.44995438	3.026937575
0.480272109	0.482232942	0.408275401
0.529251701	0.514991066	2.694490138

Table 8, cont.

Actual Tool wear	Predicted Tool Wear	%Error
0.560544218	0.559192854	0.241080663
0.587755102	0.596013881	1.405139552
0.65170068	0.643525157	1.254490469
0.691156463	0.69772344	0.95014336
0.736054422	0.74783233	1.600140948
0.79047619	0.777566379	1.633168914
0.823129252	0.820603866	0.30680303
0.859863946	0.862829342	0.344868078
0.910204082	0.900558636	1.059701395
0.949659864	0.920637923	3.056035355
0.976870748	0.950177917	2.732483464
1	0.97660451	2.339549034
0.340136054	0.342684704	0.749302914
0.410884354	0.407814016	0.747251185
0.469387755	0.467453199	0.412144519
0.511564626	0.514591971	0.591781661
0.555102041	0.554485221	0.111118326
0.597278912	0.597431272	0.025509155
0.629931973	0.629954937	0.003645482
0.646258503	0.645915572	0.05306414
0.658503401	0.658872382	0.056033154

Table 8, cont.

Actual Tool wear	**Predicted Tool Wear**	**%Error**
0.676190476	0.676440313	0.03694771
0.702040816	0.701176526	0.123111053
0.721088435	0.721548351	0.063780748
0.73877551	0.742171703	0.459705695
0.757823129	0.771110377	1.753344118
0.779591837	0.775942298	0.468134525
0.801360544	0.796277187	0.634340828

The overall average error for tool wear model is 1.038%. Out of all data points for tool wear, only four data points cross the 3% individual error mark and highest individual error is 6.043%. The equation used to determine percentage error is shown below:

$$\% \text{ error} = \left|\frac{(Predicted\ Value)-(Actual\ Value)}{(Actual\ Value)}\right| \times 100\% \qquad (4.1)$$

The normalized actual and predicted surface finish data was shown in Table 9 and the graphical representation of Table 9 is Figure 4.30.

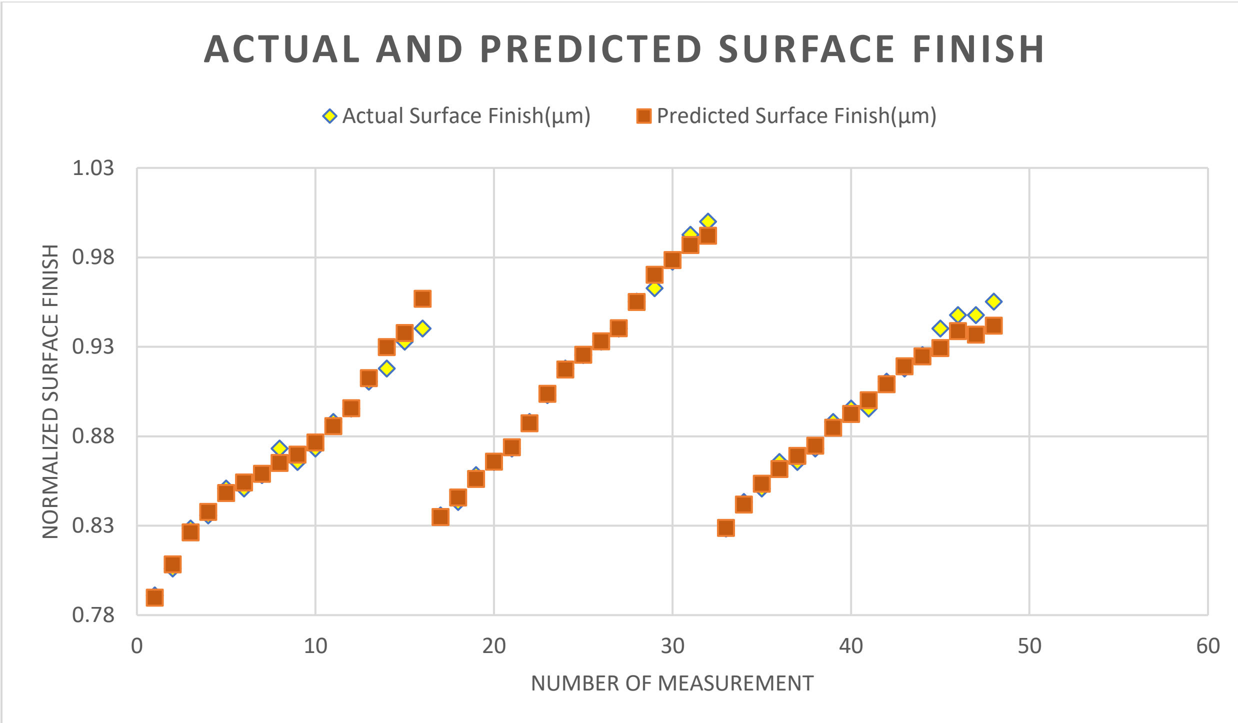

Fig. 4.30 Actual and Predicted Surface Finish with Number of Measurement

Table 9. Normalized Data for Actual and Predicted Surface Finish

Actual Surface Finish	Predicted Surface Finish	Error (%)
0.791045	0.789832	0.15331
0.80597	0.808306	0.289785
0.828358	0.826346	0.24292
0.835821	0.837797	0.236405
0.850746	0.848295	0.28816
0.850746	0.854158	0.400979
0.858209	0.859	0.092166
0.873134	0.865115	0.91847

Table 9, cont.

Actual Surface Finish	Predicted Surface Finish	Error (%)
0.865672	0.869797	0.476523
0.873134	0.876465	0.381492
0.88806	0.885578	0.27947
0.895522	0.895731	0.023239
0.910448	0.912408	0.21529
0.91791	0.929901	1.306283
0.932836	0.937732	0.524904
0.940299	0.956879	1.763316
0.835821	0.834844	0.11692
0.843284	0.845834	0.302401
0.858209	0.856225	0.23122
0.865672	0.865806	0.015571
0.873134	0.873815	0.077985
0.88806	0.887318	0.08355
0.902985	0.90365	0.073625
0.91791	0.917314	0.06496
0.925373	0.925516	0.015392
0.932836	0.93303	0.020784
0.940299	0.940316	0.001823
0.955224	0.955139	0.00892
0.962687	0.970343	0.795329

Table 9, cont.

Actual Surface Finish	Predicted Surface Finish	Error (%)
0.977612	0.978527	0.093552
0.992537	0.986874	0.57064
1	0.992157	0.78426
0.828358	0.828836	0.057703
0.843284	0.841799	0.1761
0.850746	0.853406	0.312605
0.865672	0.861706	0.45815
0.865672	0.869058	0.391235
0.873134	0.874827	0.193896
0.88806	0.884669	0.3818
0.895522	0.892492	0.33839
0.895522	0.900187	0.520862
0.910448	0.909122	0.14564
0.91791	0.919029	0.121833
0.925373	0.924571	0.08673
0.940299	0.929245	1.17556
0.947761	0.938849	0.9403
0.947761	0.936891	1.14697
0.955224	0.941885	1.39646

The overall average error for surface finish model is 0.389%. Only four data points crosses the 1% individual error limit. The maximum individual error is 1.39%.

Figures 4.31 and 4.32 show the interdependency of tool wear and surface finish on speed, feed, DOC, force, and vibration.

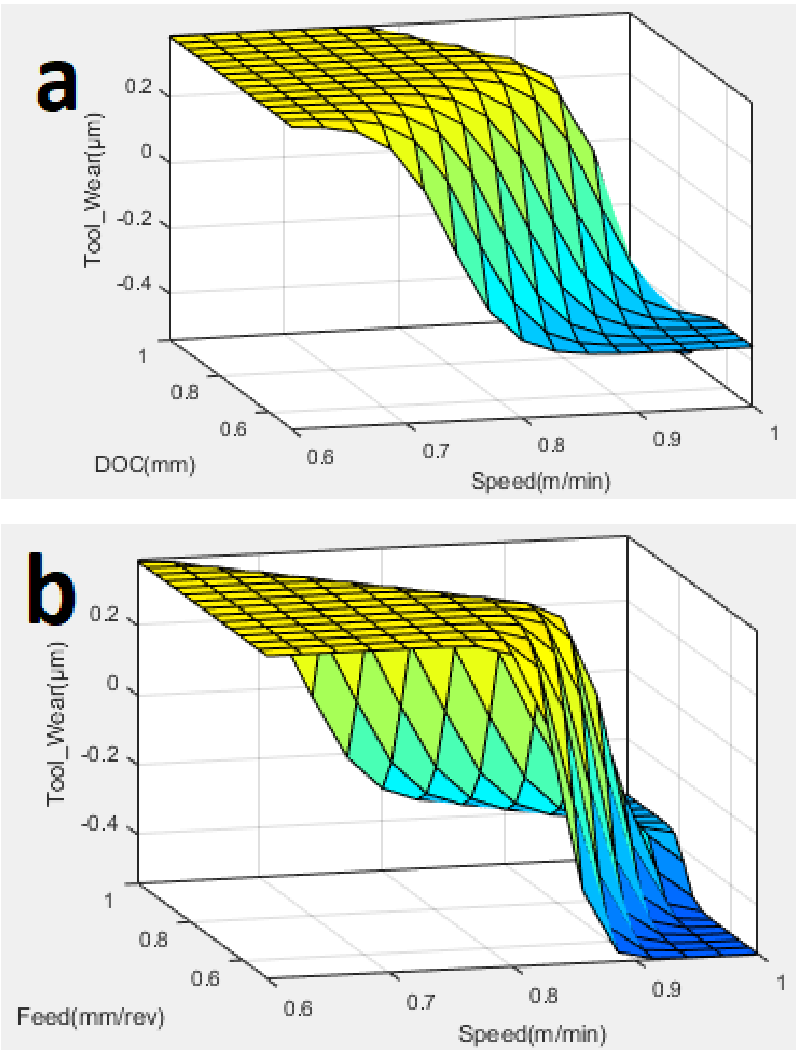

Fig. 4.31 MATLAB Surface Plot Showing Inter Dependency of Tool Wear on a) DOC and Speed; b) Feed and Speed; c) Vibration and Speed; d) Force and Speed; e) Vibration and DOC; f) Vibration and Feed; g) Vibration and Force.

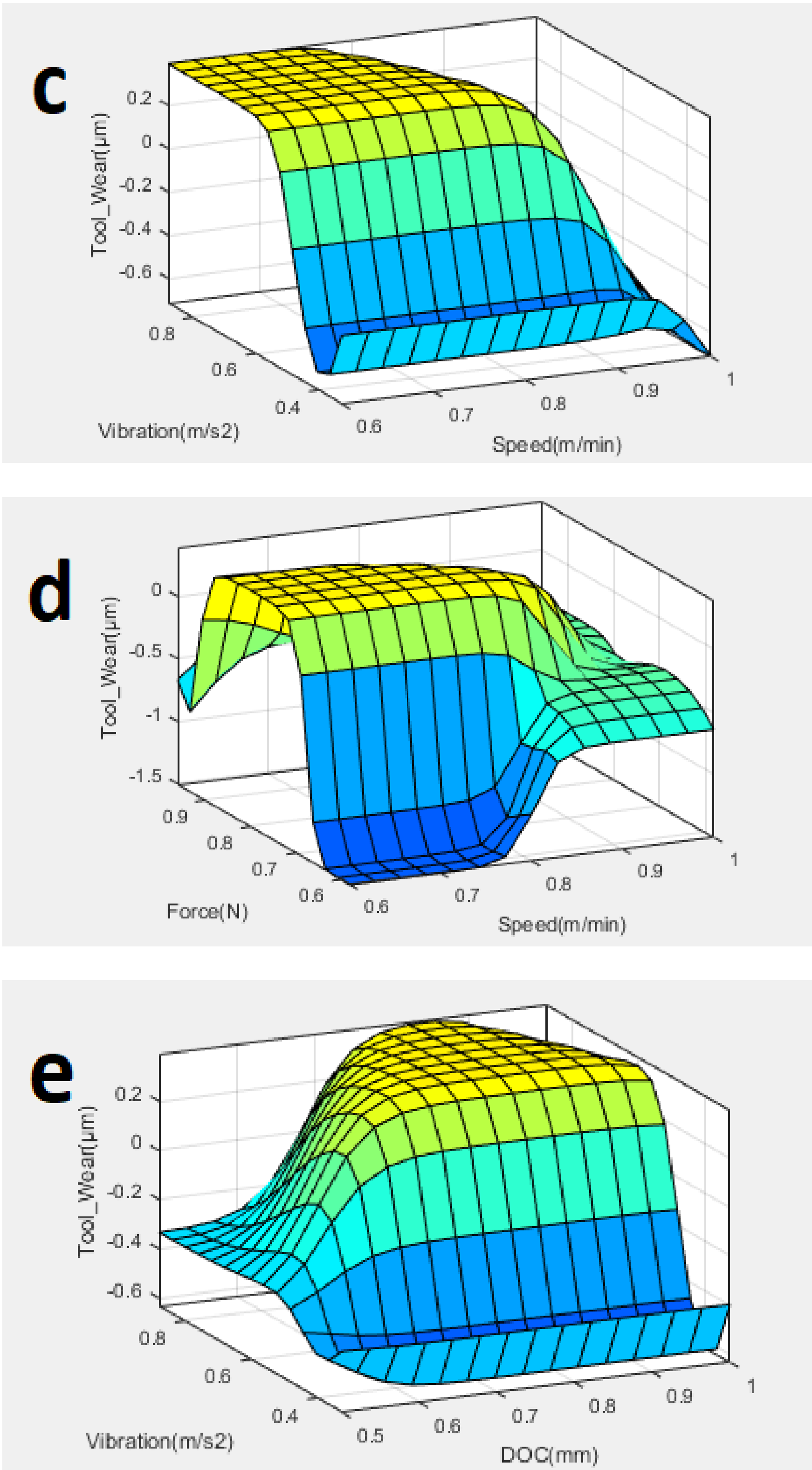
c
Tool_Wear(μm)
0.2
0
-0.2
-0.4
-0.6
0.8
0.6
0.4
Vibration(m/s2)
0.6
0.7
0.8
0.9
1
Speed(m/min)
d
Tool_Wear(μm)
0
-0.5
-1
-1.5
0.9
0.8
0.7
0.6
Force(N)
0.6
0.7
0.8
0.9
1
Speed(m/min)
e
Tool_Wear(μm)
0.2
0
-0.2
-0.4
-0.6
0.8
0.6
0.4
Vibration(m/s2)
0.5
0.6
0.7
0.8
0.9
1
DOC(mm)

Fig. 4.31, cont.

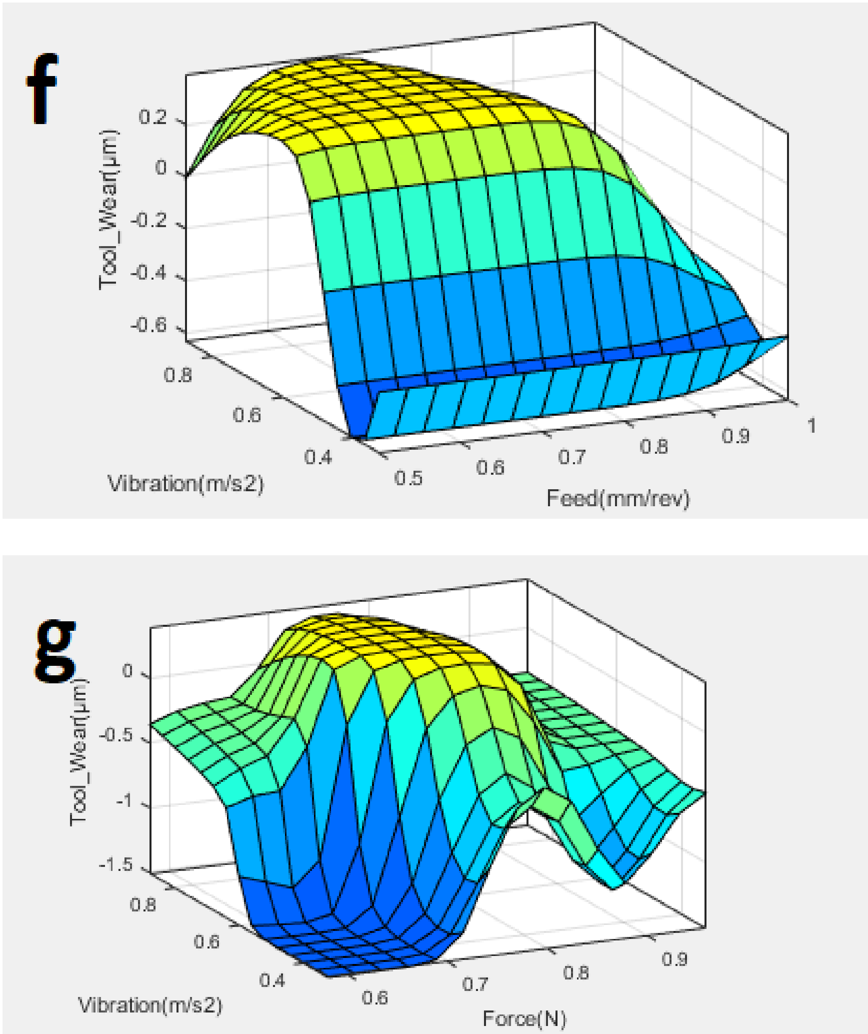
f
Tool_Wear(μm)
0.2
0
-0.2
-0.4
-0.6
0.8
0.6
0.4
Vibration(m/s2)
0.5
0.6
0.7
0.8
0.9
1
Feed(mm/rev)
g
Tool_Wear(μm)
0
-0.5
-1
-1.5
0.8
0.6
0.4
Vibration(m/s2)
0.6
0.7
0.8
0.9
Force(N)

Fig. 4.31, cont.

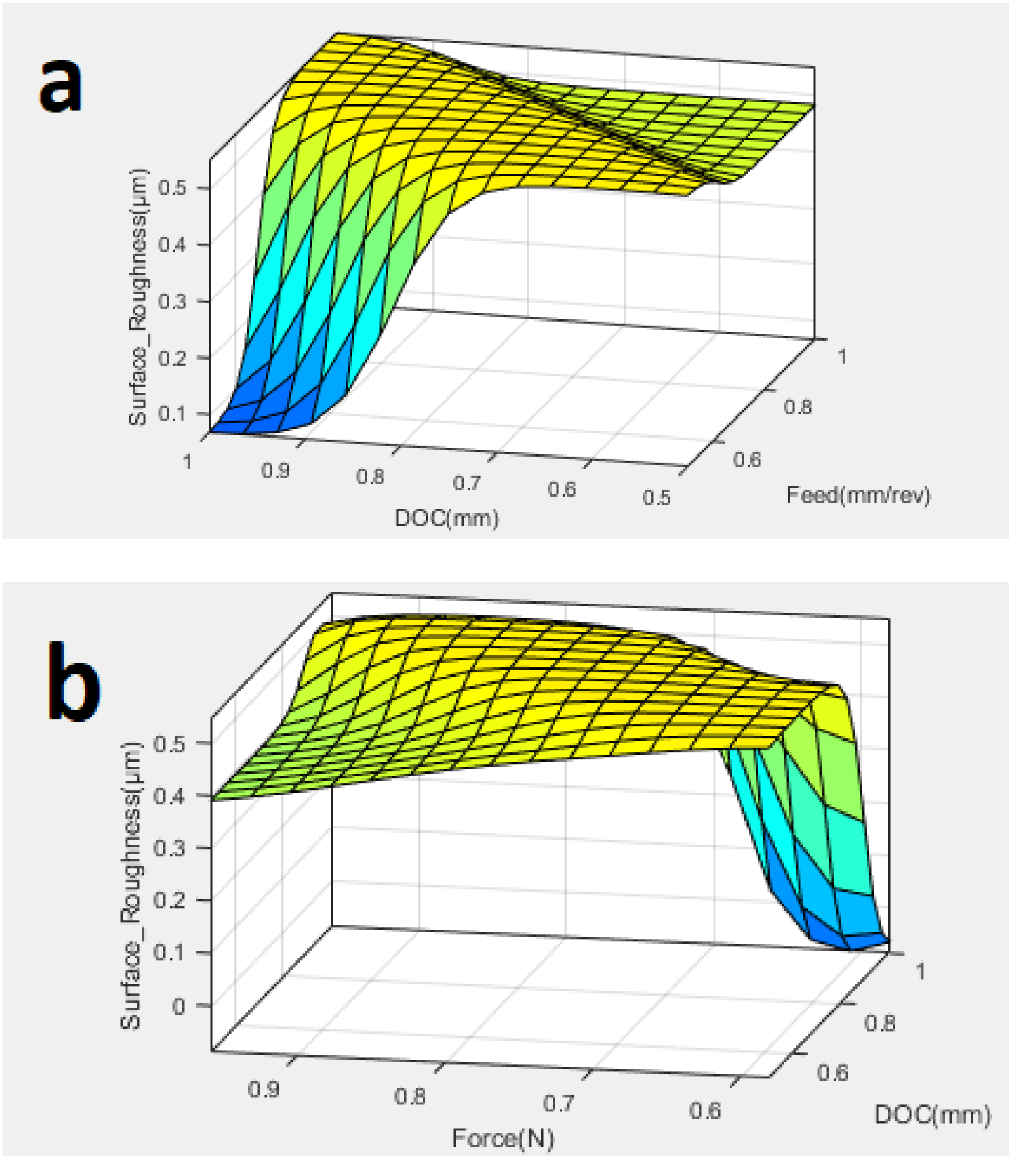

Fig. 4.32 MATLAB Surface Plot Showing Inter Dependency of Surface Finish on a) DOC and Feed; b) Force and DOC; c) DOC and Speed; d) Vibration and DOC; e) Feed and Speed; f) Vibration and Feed; g) Force and Feed; h) Force and Speed; i) Force and Vibration; j) Vibration and Speed.

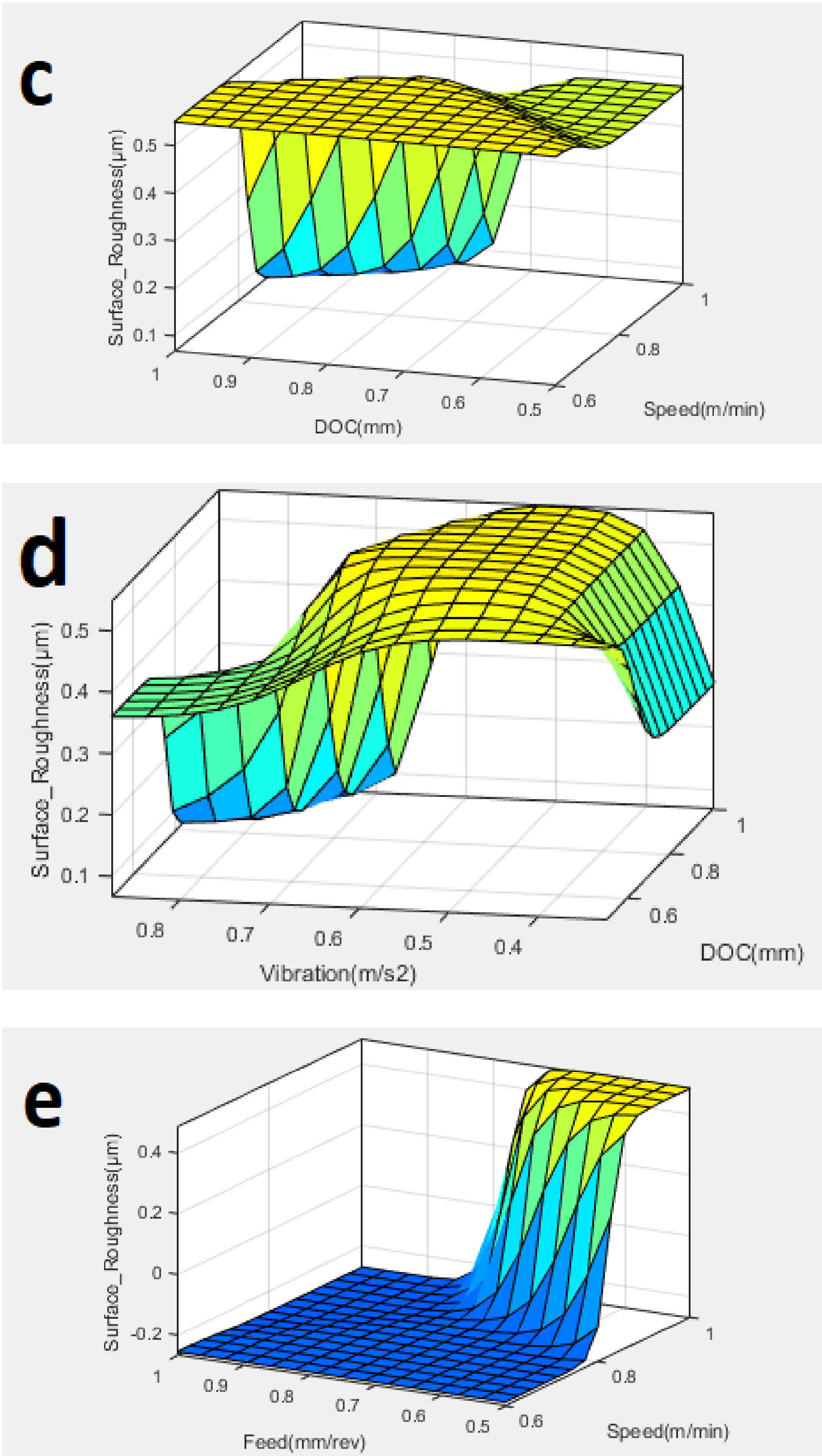
c
Surface_Roughness(μm)
0.5
0.4
0.3
0.2
0.1
1
0.9
0.8
0.7
0.6
0.5
DOC(mm)
0.6
0.8
1
Speed(m/min)
d
Surface_Roughness(μm)
0.5
0.4
0.3
0.2
0.1
0.8
0.7
0.6
0.5
0.4
Vibration(m/s2)
0.6
0.8
1
DOC(mm)
e
Surface_Roughness(μm)
0.4
0.2
0
-0.2
1
0.9
0.8
0.7
0.6
0.5
Feed(mm/rev)
0.6
0.8
1
Speed(m/min)

Fig. 4.32, cont.

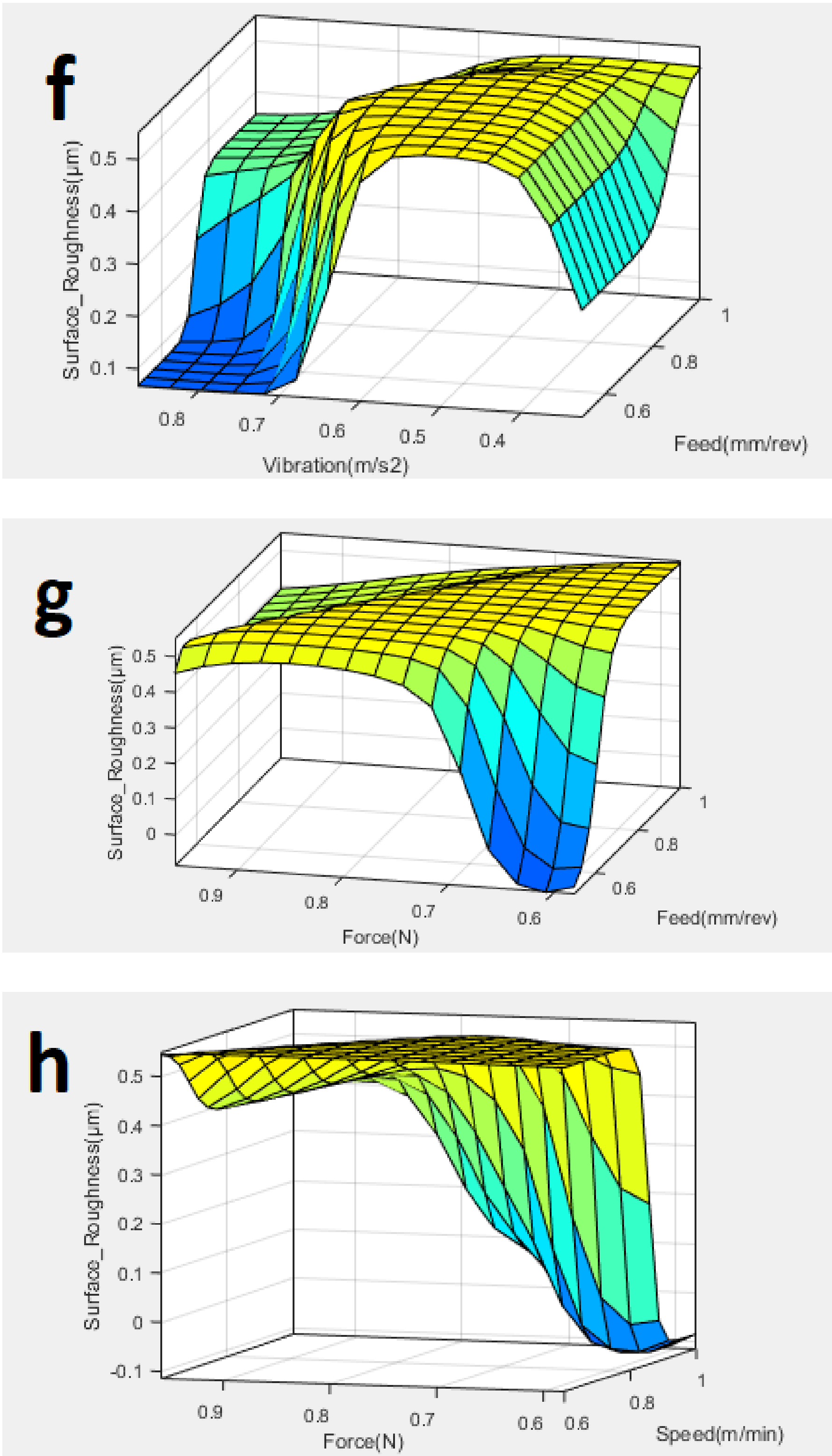
f
Surface_Roughness(µm)
0.5
0.4
0.3
0.2
0.1
0.8
0.7
0.6
0.5
0.4
Vibration(m/s2)
1
0.8
0.6
Feed(mm/rev)
g
Surface_Roughness(µm)
0.5
0.4
0.3
0.2
0.1
0
0.9
0.8
0.7
0.6
Force(N)
1
0.8
0.6
Feed(mm/rev)
h
Surface_Roughness(µm)
0.5
0.4
0.3
0.2
0.1
0
-0.1
0.9
0.8
0.7
0.6
Force(N)
1
0.8
0.6
Speed(m/min)

Fig. 4.32, cont.

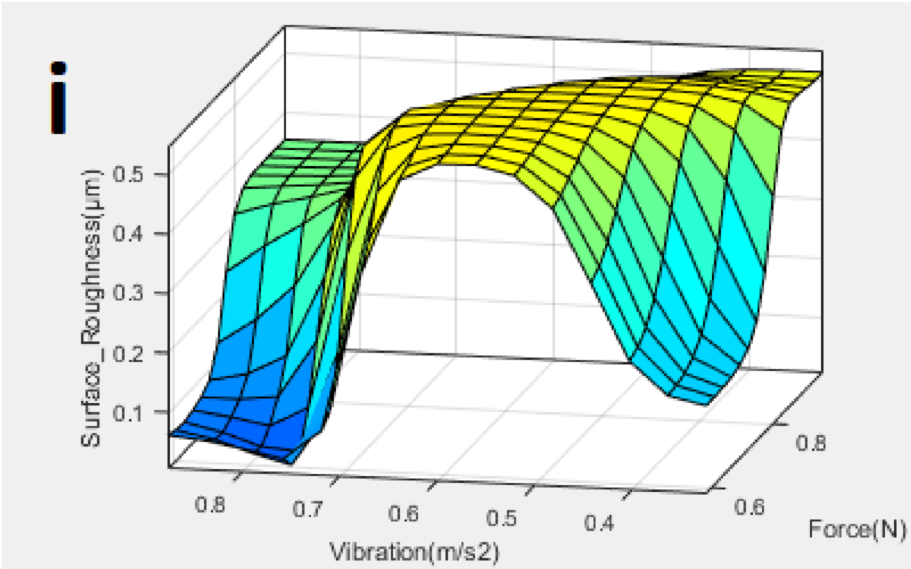
i
Surface_Roughness(μm)
0.5
0.4
0.3
0.2
0.1
0.8
0.7
0.6
0.5
0.4
Vibration(m/s2)
0.8
0.6
Force(N)

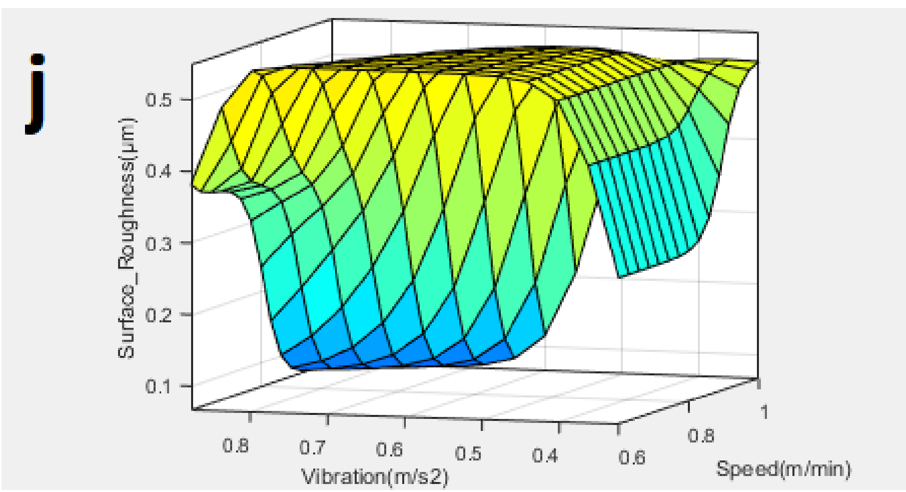
j
Surface_Roughness(μm)
0.5
0.4
0.3
0.2
0.1
0.8
0.7
0.6
0.5
0.4
Vibration(m/s2)
0.6
0.8
1
Speed(m/min)

Fig. 4.32, cont.

CHAPTER V

ANALYSIS ON DESIGN OF EXPERIMENTS

In this experiment, a total of 48 data point has been used. A regression analysis test has been performed in Minitab. Due to problem with multi-collinearity in the dataset, regression analysis could not establish any relation of DOC with tool wear, surface finish, speed, feed, cutting force and vibration. The Minitab Regression output is shown in Figure 5.1.

Regression Analysis: Tool w...

WORKSHEET 1

Regression Analysis: Tool wear (μm) versus Speed, Feed, DOC, Cutting Froce (N), Vibration(m/s2)

The following terms cannot be estimated and were removed:
DOC

Fig. 5.1 Minitab Regression Output

A correlation analysis of five inputs has also been performed for the regression model. The results of the correlation analysis are shown in Figure 5.2.

Correlations

	Speed	Feed	DOC	Cutting Froce (N)
Feed	-0.500			
DOC	0.500	-1.000		
Cutting Froce (N)	-0.327	0.936	-0.936	
Vibration(m/s2)	0.614	-0.327	0.327	0.024

Fig.5.2 Correlation Analysis

From the correlation analysis, the correlation coefficient between feed and DOC has been found to have a value of -1. This is a perfect negative correlation and implies that the variables feed, and DOC are not independent, and cannot both be included in statistical models which has been shown in a matrix plot in Figure 5.3.

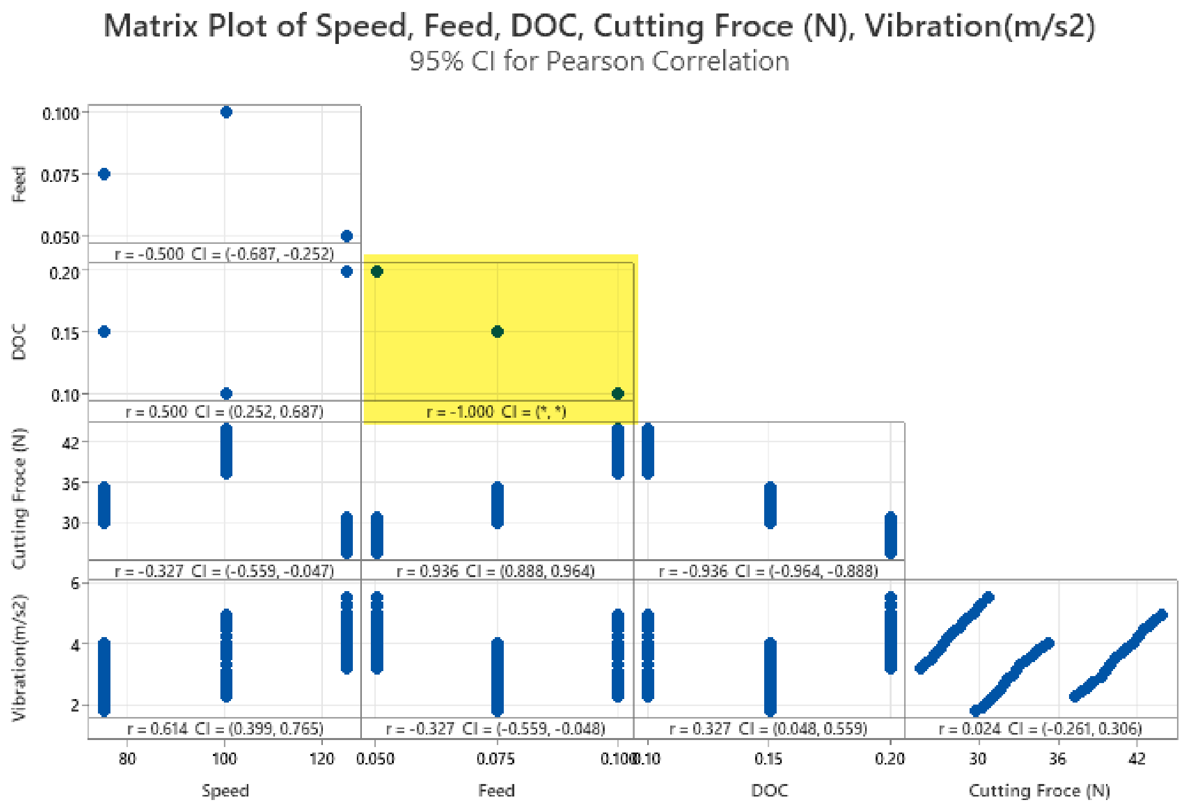

Fig.5.3 Matrix Plot of Input Variables

According to the matrix plot, if the value of DOC or speed is known, the value of the other variables can automatically be known.

A regression model has been developed without DOC values to find out the meaningful correlation between parameters. The regression model for cutting force is found statistically significant. The coefficients for speed and feed (rate) are both positive which makes sense. See Figure 5.4.

Regression Equation

Cutting Force = 7.91 + 0.0505 Speed + 276.5 Feed

Coefficients

Term	Coef	SE Coef	T-Value	P-Value	VIF
Constant	7.91	2.21	3.57	0.001	
Speed	0.0505	0.0145	3.49	0.001	1.33
Feed	276.5	14.5	19.13	0.000	1.33

Fig. 5.4 Regression Model for Cutting Force

A large amount of noise has been found during regression analysis of vibration model with R^2 value of 37.74% which makes the model a poor one. The coefficient for speed is found positive whereas the coefficient of feed rate is found negative which means as the feed rate is increased, less vibrations are observed.

Regression Equation

Vibration = 0.894 + 0.02804 Speed - 1.27 Feed

Coefficients

Term	Coef	SE Coef	T-Value	P-Value	VIF
Constant	0.894	0.971	0.92	0.362	
Speed	0.02804	0.00634	4.42	0.000	1.33
Feed	-1.27	6.34	-0.20	0.843	1.33

Fig. 5.5 Regression Model for Cutting Force

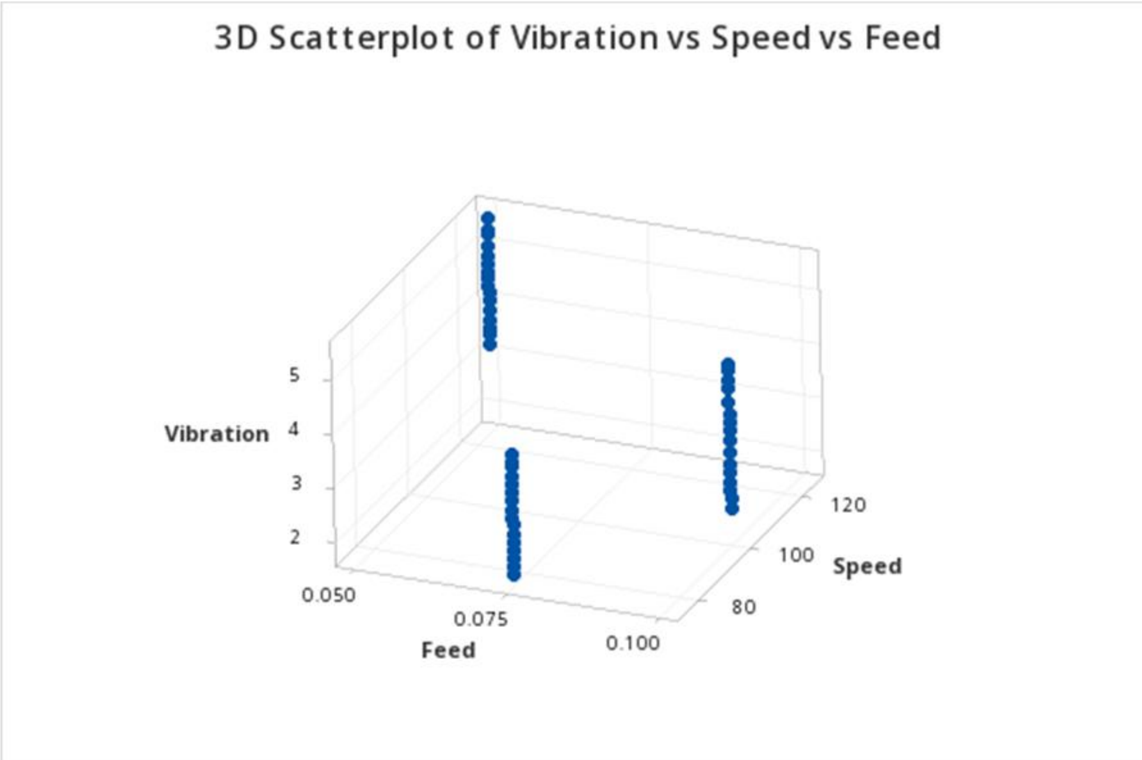

Fig. 5.6 Scatterplot of Vibration Model

The experimental dataset of 48 data points has been found insufficient to predict the tool wear and surface roughness effectively using ANFIS methodology. Further, it is not possible to build statistical models from this data. For this experiment, with the 48 data points appropriate modeling has failed.

CHAPTER VI

CONCLUSIONS

The relationship between the cutting parameters (Speed, Feed, DOC) and response parameters (Vibration, Surface Finish, Cutting Force and Tool Wear) has been investigated during turnng of CFRP composite. The ANFIS methodology has been used to predict the tool wear and surface finish with minimal error percentage. Based on the study's experimental findings, the following conclusions can be drawn:

- The experimental dataset of 48 data points has been found insufficient to predict the tool wear and surface roughness effectively using ANFIS methodology.
- During Minitab analysis, problem with multi-collinearity in the dataset has been found and regression analysis could not establish any relation of depth of cut with tool wear, surface finish, cutting speed, feed rate, cutting force and vibration.
- The value of DOC has been found to have a value of -1 during correlation analysis in Minitab of five inputs (depth of cut, cutting speed, feed rate, cutting force and vibration). This is a perfect negative correlation and implies that the variables feed, and DOC are not independent, and cannot both be included in statistical models.
- A large amount of noise has been found during regression analysis of vibration model with R^2 value of 37.74% which makes the model to be considered as a poor one.

- According to the scatterplot in Minitab, it has been found that if the value of depth of cut or cutting speed is known, the value of other variables are also known autometically.

In consideration of above conclusions, It is not possible to build statistical models from this data. The DOE approach for this experiment fails.

Due to resource and time constraints, it was not possible to conduct the experiment again to get a meaningful data for this thesis. Future work can retake the data to get sufficient amount of data points with the same experimental setup and a proper DOE approach. This experiment is conducted with two MISO model. A multiple input multiple output (MIMO) modeling can also be done in future for similar kinds of problems.

The result of this experiment is not a proper representation of what it should be because of the failure to conform to a correct DOE approach. Hence, this thesis does not contain publishable content.

REFERENCES

Achiche, S., Balazinski, M., Baron, L., & Jemielniak, K. (2002). Tool wear monitoring using genetically generated fuzzy knowledge bases. *Engineering Applications of Artificial Intelligence*, 15(3-4), 303-314. doi:10.1016/s0952-1976(02)00071-4

Ahmad, J. (2009). Machining of Polymer Composites. doi:10.1007/978-0-387-68619-6

Altintas, Y., 1988, "In-process detection of tool breakages using time series monitoring of cutting forces," *International Journal of Machine Tools and Manufacture*, 28(2): 157-172.

Altintas, Y., 2000, *Manufacturing Automation: Metal Cutting Mechanics, Machine Tool Vibration, and CNC Design*, Cambridge University Press, New York

Altintas, Y., and Yellowley, I., 1989, "In process detection of tool failure in milling using cutting force models Transactions," ASME Transactions, *Journal of Engineering for Industry*, 111: 149-157.

Azmi, A. (2015). Monitoring of tool wear using measured machining forces and neuro-fuzzy modelling approaches during machining of GFRP composites. *Advances in Engineering Software*, 82, 53-64. doi:10.1016/j.advengsoft.2014.12.010

Azmi, A. I., Lin, R. J., & Bhattacharyya, D. (2013). Tool wear prediction models during end milling of glass fibre-reinforced polymer composites. *The International Journal of Advanced Manufacturing Technology*, 67(1-4), 701-718. doi:10.1007/s00170-012-4516-2

Balasundaram, R., Rajkumar, G., & Srinivasan, D. (2020). Investigation on turning parameters on machining time and vibration of carbon fibre reinforced laminates. *International Journal of Manufacturing Technology and Management*, 34(1), 78. doi:10.1504/ijmtm.2020.10027160

Brezocnik, M., Kavocic, M., and Ficko, M.,2004., “Prediction of surface finish withgenetic programming” *Journal of Material Processing Technology,* 2

Byrne, G., Dornfield, D., Inasaki, I., Ketteler, G., Lonig, W., and Teti, R. (1995). “Tool Condition Monitoring (TCM) – the Status of Research and Industrial Applications.” Annals of CIRP (44) 2, p.

Castillo, O., Melin, P., (2001), “Soft Computing for Control Nonlinear Dynamical System”, Physica-Verlag Heidelberg, New York

Chen, C. C., Chiang, K. T., Chou, C. C., Liao, Y. C. (2011). The use of D-optimal design for modeling and analyzing the vibration and surface finish in the precision turning with a diamond cutting tool, *International Journal of Advanced Manufacturing Technology* 54 465-478.

Chen, J. C. and Savage. M. (2001) A Fuzzy-Net-Based Multilevel In-process Surface Finish Recognition System in Milling Operations, *The International Journal of Advanced Manufacturing Technology* 17 670-676.

Chen, W., (1997). Some experimental investigations in the drilling of carbon fiber-reinforced plastic (CFRP) composite laminates. *International Journal of Machine Tools and Manufacture*, 37(8), 1097-1108. doi:10.1016/s0890-6955(96)00095-8

Choudhary, A., Harding, J., Tiwari, M. (2009). Data mining in manufacturing: A review based on the kind of knowledge, *Journal of Intelligent Manufacturing* 20(5) 501-521.

Choudhury, S., Jain, V., and Rao, C. R. (1999). On-line monitoring of tool wear in turning using a neural network. *International Journal of Machine Tools and Manufacture*, 39(3), 489-504. doi:10.1016/s0890-6955(98)00032-7

Cook, R. D., Malkus, D. S., and Plesha, and M. E., 1989, *Concepts and Applications of Finite Element Analysis*, 3rd edn. Wiley, New York, NY

Cus, F., and Zuperl, U.,2006, "Approach to optimization of cutting conditions by using artificial neural networks," *Journal of Material Processing Technology*, 173, 281–290.

Dan, L., and Mathew, J., 1990, "Tool wear and failure monitoring techniques for turning – a review" *Int J Mach Tools Manuf*; 30:579–98.

Denai, M. A., Palis, F., and Zeghbib, A., 2007, "Modeling and control of non-linear systems using soft computing techniques," *Applied Soft Computing Journal, 7*(3), 728–738

Dilma, D.E., and Lister, P.M., 2000, "On-line metal cutting tool condition monitoring I: force and vibration analyses," *International Journal of Machine Tools and Manufacture*, 40: 739-768.

Du, R., Elbestawi, M.A., and Wu, S.M., 1995, "Automated monitoring of manufacturing processes," *Journal of Manufacturing Science and Engineering*, 117(2), 121-132.

Dweiri, F., Al-Jarrah, M., & Al-Wedyan, H.,2003, Fuzzy surface finish modeling of CNC down milling of Alumic-79. *Journal of Materials Processing Technology*, 133(3), 266-275. doi:10.1016/s0924-0136(02)00847-6

El-Wardany, T.I., Gao, D. and Elbestawi, M.A., 1996, "Tool condition monitoring in drilling using vibration signature analysis," *International Journal of Machine Tools and Manufacture,* 36: 687-768.

Fang, X. (1995). Expert system-supported fuzzy diagnosis of finish-turning process states. International *Journal of Machine Tools and Manufacture*, 35(6), 913-924. doi:10.1016/0890-6955(94)e0033-f

Gajate, A., Haber. R., Toro, R. D., Vega, P., and Bustillo, A., 2012, "Tool wear monitoring using neuro-fuzzy techniques: a comparative study in a turning process," *Journal of Intelligent Manufacturing*, 23:869–882

Gill, S. S., Singh, R., Singh, J., & Singh, H. (2012). Adaptive neuro-fuzzy inference system modeling of cryogenically treated AISI M2 HSS turning tool for estimation of flank wear. *Expert Systems with Applications*, 39(4), 4171-4180. doi:10.1016/j.eswa.2011.09.117

Gua, J., Barber, G., Tungc, S., and Gub R.J., 1999, "Tool life and wear mechanism of uncoated and coated milling inserts," *Wear* 225–229 1999 273–284

Haber, R. E., and Alique, A. (2003). Intelligent process supervision for predicting tool wear in machining processes. Mechatronics, 13(8-9), 825-849. doi:10.1016/s0957-4158(03)00005-9

Hadi, Y., and Ahmed, S. G. (2006) Assessment of Surface Finish Model for Turning Process. Knowledge Enterprise: Intelligent Strategies In Product Design, *Manufacturing, and Management, in International Federation for Information Processing (IFIP)* 207 152-158.

Iqbal, A., He, N., Dar, N. U., & Li, L. (2007). Comparison of fuzzy expert system based strategies of offline and online estimation of flank wear in hard milling process. *Expert Systems with Applications*, 33(1), 61-66. doi:10.1016/j.eswa.2006.04.003

Jain, C.H., (1997), " Soft computing techniques in knowledge based intelligent engineering systems: approaches and applications", Physica-Verlag Heidelberg, New York

Jang, J. (1993). ANFIS: Adaptive-network-based fuzzy inference system. IEEE Transactions on Systems, Man, and Cybernetics, 23(3), 665-685. doi:10.1109/21.256541

Jang, J., Sun, C., & Mizutani, E. (1997). Neuro-Fuzzy and Soft Computing-A Computational Approach to Learning and Machine Intelligence

Kartalopoulos, V.S., (1996), "Understanding Neural Networks and Fuzzy Logic: Basic Concepts and its Applications", IEEE Press, New York

Kim, K.S., Lee, D.G., Kwak, Y.K., Namgung, S. 1992, Machinability of carbon fiber-epoxy composite. Journal of Materials Processing Technology 32, 553–570

Ko, T. J., & Cho, D. W. (1994). Tool Wear Monitoring in Diamond Turning by Fuzzy Pattern Recognition. *Journal of Engineering for Industry*, 116(2), 225-232. doi:10.1115/1.2901934

Kuo, R. (2000). Multi-sensor integration for on-line tool wear estimation through artificial neural networks and fuzzy neural network. *Engineering Applications of Artificial Intelligence*, 13(3), 249-261. doi:10.1016/s0952-1976(00)00008-7

Mamdani, E.H., Assilian, S., (1975), "An Experiment in Linguistic Synthesis with a Fuzzy Logic Controller", *International Journal of Man-Machine Studies,* Vol. 7, pp. 1-13

Masory, O. (1991). Monitoring machining processes using multi-sensor readings fused by artificial neural network. *Journal of Materials Processing Technology*, 28(1-2), 231-240. doi:10.1016/0924-0136(91)90222-z

Mesina, O. S., & Langari, R. (2001). A Neuro-Fuzzy System for Tool Condition Monitoring in Metal Cutting. *Journal of Manufacturing Science and Engineering*, 123(2), 312-318. doi:10.1115/1.1363599

Ming, L., Xiaohong, Y., & Shuzi, Y. (1999). Tool Wear Length Estimation with a Self-Learning Fuzzy Inference Algorithm in Finish Milling. *The International Journal of Advanced Manufacturing Technology*, 15(8), 537-545. doi:10.1007/s001700050099

Mohan N. S., Ramachandra A., Kulkarni S. M. (2005). Influence of process parameters on cutting force and torque during drilling of glass–fiber polyester reinforced composites. *Composite Structures* 71:407–413

MSC, https://www.mscdirect.com/product/details/32596041?item=32596041

Niu, Y. M., Wong, Y. S., Hong, G. S., & Liu, T. I. (1998). Multi-Category Classification of Tool Conditions Using Wavelet Packets and ART2 Network. *Journal of Manufacturing Science and Engineering*, 120(4), 807-816. doi:10.1115/1.2830224

Nouri, M., Fussell, B.K., Jerard, R.B., Gao, L., and Linder, E., 2012, Estimation of cutting force model coefficients to track tool wear in milling using Bayesian analysis," *ASME Proceedings, Manufacturing Science and Engineering Conference.*

Pal, S., Heyns, P. S., Freyer, B. H., Theron, N. J., and Pal, S. K. (2011). Tool wear monitoring and selection of optimum cutting conditions with progressive tool wear effect and input uncertainties. *Journal of Intelligent Manufacturing*, 22(4), 491-504. doi:10.1007/s10845-009-0310-x

Palanikumar K. (2007), Modeling and analysis for surface finish in machining glass fibre reinforced plastics using response surface methodology. Mater Des 28:2611–2618

Palanikumar, K., Paulo Davim, J. (2007), Mathematical model to predict tool wear on the machining of glass fibre reinforced plastic composites. *Materials and Design* 28(7), 2008–2014.

Purushothaman, S. (2010). Tool wear monitoring using artificial neural network based on extended Kalman filter weight updation with transformed input patterns. *Journal of Intelligent Manufacturing*, 21(6), 717-730. doi:10.1007/s10845-009-0249-y

Rahman, M., Zhou, Q., & Hong, G. S. (1995). On-line cutting state recognition in turning Using a neural network. The International Journal of Advanced Manufacturing Technology, 10(2), 87-92. doi:10.1007/bf01179276

Rajasekaran, T., Palanikumar, K., Vinayagam B. K. (2011). Application of fuzzy logic for modeling surface finish in turning CFRP composites using CBN tool, *Production Process* 5(2) 191-199

Ramulu, M., Faridnia, M., Garbini, J.L., Jorgensen, J.E. (1989), Machining of graphite/epoxy materials with polycrystalline diamond (PCD) tools, in Ramulu, M., Hashish, M. (eds), *Machining Characteristics of Advanced Materials*. ASME, New York, NY, MD-Vol. 16, pp. 33–40.

Rangwala, S., and Dornfeld, D. (1990). Sensor Integration Using Neural Networks for Intelligent Tool Condition Monitoring. *Journal of Engineering for Industry*, 112(3), 219-228. doi:10.1115/1.2899578

Recognition System in Milling Operations, *The International Journal of Advanced Manufacturing Technology* 17 (2001) 670-676.

Rehorn, A. G., Jiang, J., and Orban, P. E. (2005) “State-of-the-Art Methods and Results in Tool Condition Monitoring: A Review,” *International Journal of Advanced Manufacturing Technology*, 26, pp. 693-710.

Roberts, T., 2007, Rapid Growth Forecast for Carbon Fibre Market, Reinforced Plastics, 51/2: 10–13

Saglam, H., and Unuvar, A., 2003, “Tool condition monitoring in milling on cutting forces by a neural network,” *International Journal of Production Research*, 41(7): 1519-1532.

Savković, B., Kovač, P., Gerić, K., Sekulić, M., Rokosz, K. (2013). Application of neural network for determination of cutting force changes versus instantaneous angle in face milling, *Journal of Production Engineering* 16(2) 25-28.

Sharma, V. S., Dogra, M., and Suri, N. M., 2008b, Advances in the turning process for productivity improvement—A review. *Proceedings of the Institution of Mechanical Engineers*, Part B: *Journal of Engineering Manufacture*, 222(11), 1417–1442.

Shaw, M.L., 2005, *Metal Cutting Principles*, Oxford University Press, New York

Sheikh-Ahmad, J.Y., 2009, Machining of Polymer Composites, Springer Verlag, Abu Dhabi.

Sick, B. (2002). On-Line and Indirect Tool Wear Monitoring In Turning With Artificial Neural Networks: A Review Of More Than A Decade Of Research. *Mechanical Systems and Signal Processing*, 16(4), 487-546. doi:10.1006/mssp.2001.1460

Sivarao, Castillo, Taufik., 2000, Machining Quality Predictions: Comparative Analysis of Neural Network and Fuzzy Logic, *International Journal of Electrical & Computer Sciences IJECS* 9 451-456.

Srinivasa Pai, P., and Ramakrishna Rao, P.K. (2002). “Acoustic emission analysis for tool wear monitoring in face milling,” *International Journal of Production Research*, 40(5): 1081-1093.

Tool-life testing with single-point turning tools, ISO 3685:1993

Umaras, E., Barari, A., and Tsuzuki, M., 2019, “Intelligent Design Tolerance Allocation for Optimum Adaptability to Manufacturing Using a Monte Carlo Approach,” *IFAC PapersOnLine,* 52-10 165–170.

Uros, Z., Franc, C., & Edi, K. (2009). Adaptive network-based inference system for estimation of flank wear in end-milling. *Journal of Materials Processing Technology*, 209(3), 1504-1511. doi:10.1016/j.jmatprotec.2008.04.002

Wang, X., Wang, W., Huang, Y., Nguyen, N., and Krishnakumar, K. (2008). Design of neural network-based estimator for tool wear modeling in hard turning. Journal of Intelligent Manufacturing, 19(4), 383-396. doi:10.1007/s10845-008-0090-8

Warnecke, G., and Kluge, R.(1998). Control of tolerances in turning by predictive control with neural networks. Journal of Intelligent Manufacturing, 9, 281–287

Yoshio, O., Naoya, O., Chikako, K., Shinya, I., Susumu, O., Hiroyuki, M., et al., 2007, “Development of new CVD-coating ‘‘super FF coat’’ and its application to cutting tools,” *SEI Technical Review,* 64, 68–73

Zain, A.M., Haron, H., and Sharif, S., 2010, “Prediction of surface finish in the end milling machining using Artificial Neural Network,” *Expert Systems with Applications*, 37, 1755–176

BIOGRAPHICAL SKETCH

Md Mofakkirul Islam acquired his bachelor's degree in Mechanical Engineering from Bangladesh University of Engineering and Technology in 2017 and joined the department of Manufacturing and Industrial Engineering at the University of Texas Rio Grande Valley in 2020 for pursuing a Master's Degree. He worked as a research assistant at the Advanced Machining Lab under Dr. Alley Butler and Dr. Anil Srivastava and completed his Master of Science in Engineering in Manufacturing Engineering in May 2022. His research interests are focused on advanced machining, additive manufacturing, neural network, and high entropy alloys. During his Master's, he was awarded the Graduate Research Assistantship award for all two years. For pursuing a future assignment, he is pursuing employment on the Optional Practical Training (OPT) program. He can be reached at mofakkirul.islam@gmail.com.